eNOS DERIVED OXIDATIVE STRESS AND ITS ROLE IN THE REGULATION OF BLOOD PRESSURE

INAUGURAL-DISSERTATION

ZUR ERLANGUNG DES DOKTORGRADES
DER MATHEMATISCH-NATURWISSENSCHAFTLICHEN FAKULTÄT
DER HEINRICH-HEINE-UNIVERSITÄT DÜSSELDORF

VORGELEGT VON

STEPHANIE HAN-WHEI PICK, GEB. KUMPF
AUS ESSEN

DÜSSELDORF, APRIL 2018

aus dem Institut für Pharmakologie und Klinische Pharmakologie
der Heinrich-Heine-Universität Düsseldorf

Gedruckt mit der Genehmigung der
Mathematisch-Naturwissenschaftlichen Fakultät der
Heinrich-Heine-Universität Düsseldorf

Berichterstatter:

1. Prof. Dr. Georg Kojda

2. Prof. Dr. Matthias Kassack

Tag der mündlichen Prüfung: 25.06.2018

Meiner Familie

TABLE OF CONTENTS

ABBREVIATIONS

Akt	protein kinase B
Ala	alanine
AMP	adenosine monophosphate
AMPK	AMP activated protein kinase
ATP	adenosine triphosphate
BH_4	(6*R*)-5,6,7,8-tetrahydro-L-bioterin
bp	base pairs
BW	body weight
C101A-eNOS	bovine eNOS destabilized by a replacement of cysteine 101 to alanine
C101A-eNOS-tg	transgenic mouse with an endothelial-specific overexpression of a destabilized eNOS variant
C101A-eNOS-tgn	transgenic negative littermate of C101A-eNOS-tg
$CaCl_2$	calcium chloride
cDNA	complementary DNA
cGMP	cyclic guanosine monophosphate
CO_2	carbon dioxide
Cys	cysteine
DNA	deoxyribonucleic acid
ecSOD	extracellular superoxide dismutase
EDRF	endothelium-derived relaxing factor
EDTA	ethylenediaminetetraacetic acid

EGTA	ethylene glycol tetraacetic acid
eNOS	endothelial nitric oxide synthase
eNOS-KO	eNOS deficient mouse (knock-out)
eNOS-tg	transgenic mouse with an endothelial-specific overexpression of native eNOS
eNOS-tgn	transgenic negative littermate of eNOS-tg
FAD	flavin adenine dinucleotide
FAM	fluoresceinamidite
FMN	flavin adenine mononucleotide
GMP	guanosine monophosphate
GTP	guanosine triphosphate
HEK 293	human embryonic kidney cells 293
HEPES	4-(2-hydroxyethyl)-1-piperazineethanesulfonic acid
IP_3	1,4,5-inositoltriphosphate
IRAG	IP_3-receptor associated cGMP kinase substrate
K_2HPO_4	dipotassium hydrogen phosphate
kb	kilo base pairs
KCl	potassium chloride
kDa	kilodalton
L-NA	Nω-nitro-L-arginine (N5-(nitroamidino)-L-2,5-diaminopentanoic acid)
L-NAME	methyl ester of L-NA
$MgSO_4$	magnesium sulfate

mRNA	messenger RNA
NADPH	nicotinamide adenine dinucleotide phosphate (reduced form)
Na_2HPO_4	disodium hydrogen phosphate
NaCl	sodium chloride
$NaHCO_3$	sodium hydrogen carbonate
NO	nitric oxide
NOS	nitric oxide synthase
$O_2^{-\bullet}$	superoxide anion radical
PBS	phosphate buffered saline
PBSGA	phosphate buffered saline containing glucose and albumine
PBST	phosphate buffered saline containing Tween-20®
PCR	polymerase chain reaction
PECAM-1	platelet endothelial cell adhesion molecule 1
pH	negative decadic logarithm of the hydronium ion activity
PKG	proteinkinase G
PMSF	phenylmethanesulfonyl fluoride
RNA	ribonucleic acid
ROS	reactive oxygen species
Ser	serine
SERCA	sarcoplasmatic reticulum adenosine triphosphatase
sGC	soluble guanylyl cyclase
SOD	superoxide dismutase

SDS	sodium dodecyl sulfate
SNAP	S-nitroso-N-acetyl-D,L-penicillamine
TAE	Tris-acetate-EDTA
TE	Tris-EDTA
Tempol®	4-hydroxy-2,2,6,6,-tetramethylpiperidine-1-oxyl
Thr	threonine
TierSchG	Tierschutzgesetz (German law on animal welfare)
Tris	tris-(hydroxymethyl)-aminomethane
Tyr	tyrosine
VASP	vasoactive stimulated protein

1. INTRODUCTION

Cardiovascular diseases with hypertension as a significant risk factor are the major contributors to global morbidity and mortality. The prevalence of hypertension appears to be around 30-45% of the population overall and escalates with an increase in age [1]. Environmental and genetical factors seem to play a role in the development of hypertension, but also several secondary factors like chronic kidney diseases, diseases of the thyroid gland, pheochromocytoma, sleep apnea, pharmacotherapy (e.g. corticosteroids), or aortic coarctation can cause hypertension which makes its genesis multifactorial. In only about 10% of the cases a cause can be identified (secondary hypertension), but in more than 90% no etiology can be found and this is referred to as essential hypertension [2]. *Vascular oxidative stress is considered* to be *a pathophysiological factor* that promotes *cardiovascular diseases* like *coronary artery disease, heart failure, diabetes, and hypertension* [3,4]. *It has been suggested, that the impairment of endothelial function at the level of resistance vessels may precede the development of cardiovascular disease and, therefore,* be *an additional risk factor* [5]. *For example, endothelial dysfunction at this level of vessels* has been *identified in normotensive young adults with a family history of hypertension* [6]. *Another clinical study* showed *that the magnitude of the impairment of endothelium function, as measured by flow-dependent vasodilation in the right forearm, may predict the onset of essential hypertension in postmenopausal women* [7]. Though, this study assessed *the dilator response of the brachial artery to increased flow. However, as a recent thorough review* pointed out [8], *hypertension* is *also likely* to induce *endothelial dysfunction associated with increased vascular oxidative stress. Therefore, the authors concluded, that the interconnection between endothelial dysfunction and essential hypertension is two-sided, that is, both may worsen and/or improve the other.*

1.1. ENDOGENOUS NITRIC OXIDE

In 1980, Robert F. Furchgott discovered that blood vessels relax only in response to the vasodilator acetylcholine if the endothelial layer is intact [9]. He postulated that the

This work was published in

Suvorava T*, Pick S*, and Kojda G. (* equal contribution)
Selective impairment of blood pressure reduction by endothelial nitric oxide synthase dimer destabilization in mice.
J Hypertens 2017;35(1):76-88. journals.lww.com/jhypertension/

endothelium must be releasing a substance, which is responsible for this effect. This endothelium-derived relaxing factor (EDRF) was independently identified in 1987 by Louis Ignarro, Robert Furchgott and Salvador Moncada to be nitric oxide (NO) [10]. Two years later, the responsible enzyme was discovered to be the endothelial nitric oxide synthase (eNOS) [11].

1.2. ENDOTHELIAL NO-SYNTHASE

Within the endothelial layer, which lines the inner wall of the vasculature and forms the junction between blood and tissue, eNOS synthesizes NO. In this redox reaction L-arginine is specifically transformed into L-citrulline [12], depending on nicotinamide adenosine diphosphate (NADPH) and essential cofactors like heme, flavin adenine dinucleotide (FAD), flavin adenine mononucleotide (FMN), Ca^{2+}/calmodulin, and (6*R*)-5,6,7,8-tetrahydro-L-biopterin (BH_4) (see fig. 1.1) [13].

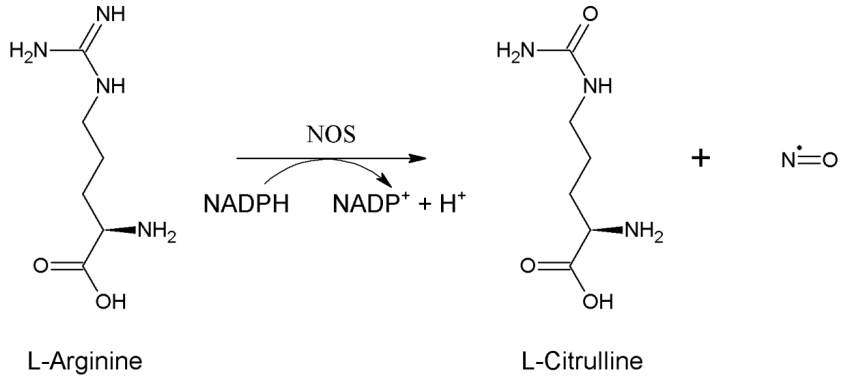

Fig. 1.1: *Scheme on the catalyzed reaction by nitric oxide synthases: L-Arginine is transformed into L-citrulline, and nitric oxide is formed.*

In mammals, three isozymes of NO synthases (NOS) have been identified: inducible NOS (iNOS), neuronal NOS (nNOS) and endothelial NOS (eNOS). All NOS are enzymes with a reductase domain at the carboxy-terminus and an oxygenase domain at the amino-terminus [14]. After binding of NADPH to the reductase domain [15], electrons are transferred via the cofactors FAD and FMN to molecular oxygen, bound to the iron atom

This work was published in

Suvorava T*, Pick S*, and Kojda G. (* equal contribution)
Selective impairment of blood pressure reduction by endothelial nitric oxide synthase dimer destabilization in mice.
J Hypertens 2017;35(1):76-88. journals.lww.com/jhypertension/

word-for-word citations within the running text stand out in italic type

in the heme center in the oxygenase domain. Binding of oxygen to the heme iron is enabled by the reduction of Fe^{3+} to Fe^{2+}. The electron flux itself depends on the binding of calmodulin [16]. Molecular oxygen is activated by reduction and reacts with the guanidine group of the substrate L-arginine. The intermediate N^{ω}-hydroxy-L-arginine is formed. In a second reaction cycle this interstate product serves as the substrate and is transferred into L-citrulline under separation of nitrogen from the guanidine group. Thus, NO is released [17].

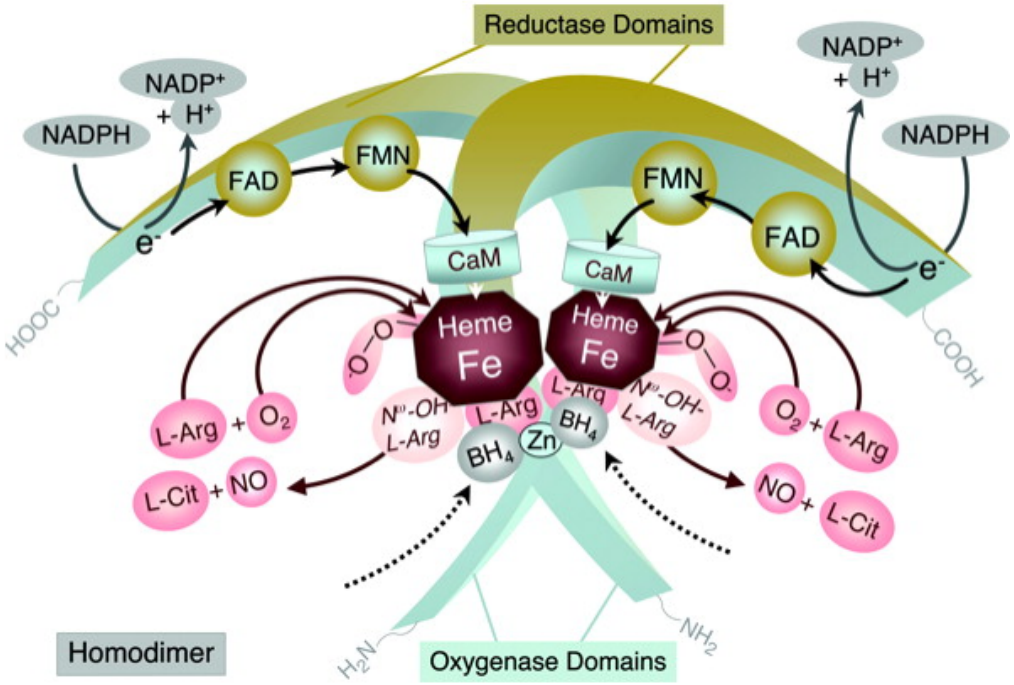

Fig. 1.2: *Scheme on the enzymatic reaction catalyzed by eNOS under normal conditions [18].*

The functional homodimer is stabilized by a zinc-cluster. As fig. 1.3 shows, the central zinc ion is coordinated in its tetrahedral conformation with pairs of symmetrically oriented cysteine residues: cysteines 96 and 101 of each monomer [19].

Within the endothelial cell, eNOS is locked in caveolae. After the influx of Ca^{2+}, eNOS is released [20]. Ca^{2+} binds to calmodulin and this construct to eNOS [21]. This activates

This work was published in

Suvorava T*, Pick S*, and Kojda G. (* equal contribution)
Selective impairment of blood pressure reduction by endothelial nitric oxide synthase dimer destabilization in mice.
J Hypertens 2017;35(1):76-88. journals.lww.com/jhypertension/

word-for-word citations within the running text stand out in italic type

the electron flux on eNOS, and NO can be released. If caveolin-1 binds to the reductase domain of eNOS, the electron flux is interrupted, and eNOS is inactivated and locked back in caveolae [22]. This step seems to be crucial as in mice with a caveolin-1 small interfering ribonucleic acid (siRNA)-induced knockdown plasma NO concentrations are 2.5 fold higher [23] and, in murine lung vascular endothelial cells with a caveolin-1 knockout, the deficiency leads to a 4-fold increase in NO production [24], both indicating a permanent eNOS activation. A recent study on endothelial-specific caveolin-1 knockout mice revealed increased eNOS expression, an enhancement of the NO-cGMP pathway, suppression of endothelium-dependent hyperpolarization-mediated responses in resistance vessels, coronary microcirculatory dysfunction and cardiac hypertrophy, and enhanced nitrative stress [25].

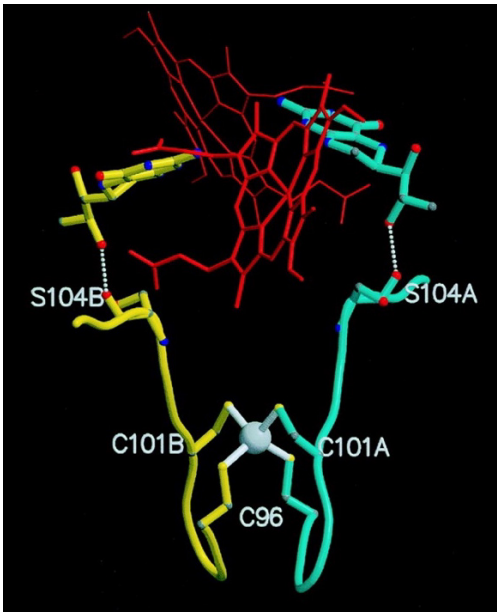

Fig. 1.3: *The ZnS_4 metal center and its relationship with tetrahydrobiopterin (red) [19]. The central zinc ion (grey) coordinates the dimerization two eNOS monomers (yellow and green) via the binding cysteines 96 and 101.*

An essential cofactor of eNOS is BH_4. It is one of the most potent naturally occurring reducing agents and is highly sensitive to oxidation by peroxynitrite [18] and modestly by superoxide anion radical ($O_2^{-\bullet}$) [26]. A lack of BH_4, as occurring in states of oxidative stress, is likely to be a cause for so-called eNOS-'uncoupling' [26]. Crucial for its binding within the oxygenase domain and, thus, the coupling of eNOS is the ability to coordinate two monomers via a Zn-finger [19]. If eNOS acts in the 'uncoupled' state, monomers can

This work was published in

Suvorava T*, Pick S*, and Kojda G. (* equal contribution)
Selective impairment of blood pressure reduction by endothelial nitric oxide synthase dimer destabilization in mice.
J Hypertens 2017;35(1):76-88. journals.lww.com/jhypertension/

word-for-word citations within the running text stand out in italic type

still bind calmodulin. But no binding of BH_4 or L-arginine is possible and eNOS cannot produce NO [14]. Rather, the electrons leak from their transport within the reductase domain or directly from the oxy-iron complex and are transferred to molecular oxygen, which is reduced to $O_2^{-\bullet}$ [27]. Studies have shown, that in these states, adding BH_4 or enhancing its regeneration by ascorbic acid can rescue the dimerization and, thus, the function of eNOS and shifts the reaction from producing $O_2^{-\bullet}$ back towards that of NO [18].

The expression eNOS 'uncoupling', as widely used in the literature, may mislead the reader, as it is not meant, that an isolated monomer can be active. Still two monomers have to be sterically associated in order to enhance oxidative stress by either an increased degradation of NO by its reaction with $O_2^{-\bullet}$, or a conversion of eNOS from an enzyme generating NO to one that produces $O_2^{-\bullet}$ [14]. In this work, the expression 'uncoupled' is used as in the literature for physiologically occurring states and solely employed in quotation marks to point out on this miswording. To distinguish the state of the genetically modified C101A-eNOS variant used in this study, this is referred to as 'destabilized' (see chapter 1.5).

eNOS is transcriptionally upregulated by certain growth factors (vascular endothelial growth factor, transforming growth factor beta 1) and hormons (insulin, estrogen). Another important stimulus is shear stress caused by the laminar flow of blood along endothelial cells. Additionally, oxygen radicals, e.g. hydrogen peroxide, and hypoxia as well as pharmaceutical drugs (statins) can enhance eNOS expression [28].

The activity of the enzyme is regulated by Ca^{2+}-activated calmodulin, which enforces eNOS to synthesize NO in a pulsatile manner [14]. eNOS can be phosphorylated on several serine (Ser), threonine (Thr), and tyrosine (Tyr) residues. Phosphorylation at Ser1177 activates eNOS by stimulating the electron flow within the reductase domain and increasing Ca^{2+} sensitivity. This can be elicited by shear stress and the activation of protein kinase A [14]. The serine residue at 1177 in humans corresponds to Ser1176 in murine and Ser1179 in bovine species. With elevated intracellular Ca^{2+} concentrations,

This work was published in

Suvorava T*, Pick S*, and Kojda G. (* equal contribution)
Selective impairment of blood pressure reduction by endothelial nitric oxide synthase dimer destabilization in mice.
J Hypertens 2017;35(1):76-88. journals.lww.com/jhypertension/

word-for-word citations within the running text stand out in italic type

dephosphorylation at Thr495 comes along with an increase of eNOS activity and the binding of calmodulin [14]. The phosphorylation by proline-rich tyrosine kinase 2 on Tyr657 directly inhibits eNOS [29]. In vitro studies have shown that this phosphorylation results in a complete loss of the ability of eNOS to generate L-citrulline, NO or $O_2^{-\bullet}$ [29,30].

1.3. eNOS Signaling

After its formation, the endogenous transmitter NO is able to diffuse freely across membranes and has several effects. The most prominent is vasodilation [20], but it also has an antiaggregatory effect on thrombocytes [31], an antiadhesive on leucocytes [32], and it is supposed to be antiproliferative [33] and antioxidative [34-36].

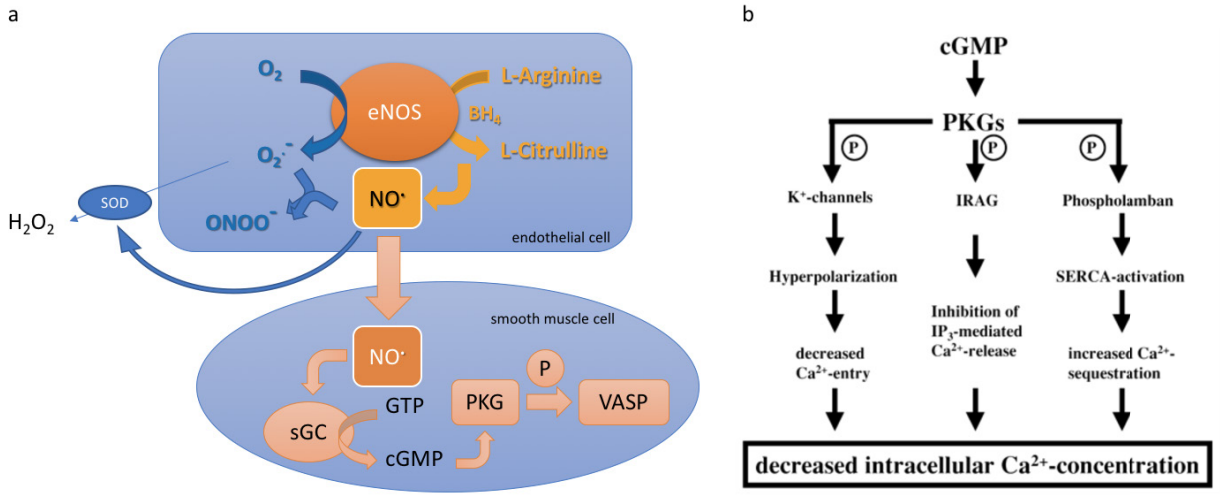

Fig. 1.4: *eNOS and NO/cGMP-signaling pathway: (a) After release of NO by endothelial cells the NO/cGMP-pathway is induced in smooth muscle cells. Here, upon activation of sGC, cGMP is formed, which stimulates cGMP-dependent protein kinases (PKG). One of the enzymes being phosphorylated and thus serving as a marker for eNOS activation is VASP. (b) Vasodilation is triggered by phosphorylation of three important proteins resulting in a decrease of the intracellular Ca^{2+} concentration [36].*

This work was published in

Suvorava T*, Pick S*, and Kojda G. (* equal contribution)
Selective impairment of blood pressure reduction by endothelial nitric oxide synthase dimer destabilization in mice.
J Hypertens 2017;35(1):76-88. journals.lww.com/jhypertension/

word-for-word citations within the running text stand out in italic type

All these effects including vasodilation are mostly mediated by activation of soluble guanylyl cyclase (sGC). This activation leads to formation of cyclic guanosine monophosphate (cGMP) from guanosine triphosphate (GTP), which, in turn, activates cGMP-dependent proteinkinase G (PKG) (see fig. 1.4). This PKGs then phosphorylate different enzymes yielding in the effects mentioned above. cGMP is deactivated by phosphodiesterase V under formation of guanosine monophosphate (GMP). In addition to the classical NO-sGC-cGMP signaling, NO can also exert its regulatory effects via post-translational protein modification and changes in function through S-nitrosylation of cysteine thiols [37].

1.4. Endothelium-Dependent Vasodilation

One of the effects of released NO upon activation of eNOS is vasodilation. The activation of PKG by cGMP seems to play a central role here: Phosphorylation of either phospholamban, 1,4,5-inositoltriphosphate receptor associated cGMP kinase substrate (IRAG) or potassium channels result in decreased intracellular Ca^{2+} concentration. In dephosphorylated states, phospholamban monomers inhibit sarcoplasmatic reticulum adenosine triphosphatase (SERCA) by binding to its cytoplasmic and membrane domains which causes a Ca^{2+} pump aggregation. Upon phosphorylation by PKG, phospholamban pentamers are formed and the inhibition of SERCA is reversed. This results in an increased sequestration of intracellular Ca^{2+} and in turn diminishes the influx of extracellular Ca^{2+} into the sarcoplasmatic reticulum. By phosphorylation of IRAG, 1,4,5-inositoltriphosphate (IP_3)-mediated Ca^{2+}-release is inhibited. And, by activation of Ca^{2+}-dependent potassium channels, the increase of outward K^+ current is increased which leads to a cell membrane hyperpolarization. Besides, a cGMP-independent effect of NO on potassium channels in smooth muscle cells has been described, too [38]. Taken together, all these mechanisms result in a decrease of intracellular calcium concentrations and a diminishing effect of depolarizing signals, which lead to an impairment of actin/myosin-interactions within smooth muscle cells and finally result in vasodilation. Other effects of vascular NO generation include antiaggregatory,

This work was published in

Suvorava T*, Pick S*, and Kojda G. (* equal contribution)
Selective impairment of blood pressure reduction by endothelial nitric oxide synthase dimer destabilization in mice.
J Hypertens 2017;35(1):76-88. journals.lww.com/jhypertension/

word-for-word citations within the running text stand out in italic type

antiadhesive, antioxidative and antiapoptotic effects, all of which confer vasoprotection and endothelial dysfunction [36].

1.5. Oxidative Stress

We know that rats with hereditary hypertension have increased $O_2^{-\bullet}$ levels and show an impaired endothelium-dependent relaxation [39]. Already more than 30 years ago, it was postulated that $O_2^{-\bullet}$ seems to be involved in the breakdown of EDRF [40]. The imbalance of $O_2^{-\bullet}$ and NO is associated with endothelial dysfunction. There are indications, that, in this situation, eNOS activity could be reduced, which may partly be dependent on the NO-cGMP-pathway [40].

In resistance vessels, endothelium-dependent vasorelaxation to acetylcholine is different from that of conductance vessels like *aorta or coronary arteries. Resistance vessels possess many options to compensate for a loss of NO produced by eNOS by other endothelium-dependent vasodilators like prostaglandins, by neuronal NOS expression or by endothelium-derived hyperpolarizing factor* [41-44].

Certainly, increased vascular oxidative stress is linked to a conversion of eNOS activity, leading to an 'uncoupled' state in which eNOS produces more $O_2^{-\bullet}$ and less NO. In addition to the deficiency of the cofactor BH_4, mechanisms underlying this process include the depletion of L-arginine, the accumulation of endogenous asymmetrical dimethylarginine, and eNOS-S-glutathionylation [14]. In detail, the catalytic domains of eNOS consist of a flavin-containing NADPH-binding reductase and a heme-binding oxygenase, which is the binding site for the substrate L-arginine and the redox labile cofactor BH_4 [45]. *There are several sources of $O_2^{-\bullet}$ in vascular smooth muscle and endothelial cells* [46].

1.6. eNOS and Blood Pressure

The specific role of endothelial oxidative stress in the regulation of blood pressure before overt hypertension occurs – that is, under otherwise healthy conditions – remains

This work was published in

Suvorava T*, Pick S*, and Kojda G. (* equal contribution)
Selective impairment of blood pressure reduction by endothelial nitric oxide synthase dimer destabilization in mice.
J Hypertens 2017;35(1):76-88. journals.lww.com/jhypertension/

uncertain. One study showed that increased $O_2^{-\bullet}$ generation, induced by a very strong eight-fold endothelial-specific overexpression of bovine eNOS and presumably caused by a shortage of the essential cofactor BH_4, does reduce blood pressure, and concomitant overexpression of guanosine triphosphate cyclohydrolase 1 to increase the endothelial generation of BH_4 in a double transgenic strain did change $O_2^{-\bullet}$ levels but had no effect on blood pressure [47]. *However, in both transgenic mouse models, there is clear evidence of an impairment of vascular NO signaling, which* may also have an *impact on blood pressure. For example, the magnitude of hypotension observed in another mouse model characterized by endothelial-specific overexpression of eNOS, that is, a reduction of systolic blood pressure of about 15 mmHg, is already achievable by a 3.3-fold overexpression of bovine eNOS. In this model, no impairment of NO signaling, and no increase of vascular oxidative stress is evident* [37,48].

eNOS significantly contributes to the regulation of blood pressure as, in four different strains of eNOS-deficient mice (eNOS-KO) [49-52], hypertension is the most evident phenotype. It is generally assumed that the lack of vasodilation by endothelial NO, more precisely, the lack of endothelium-dependent NO-induced vasodilation, is an important underlying cause [49,50] for hypertension in eNOS-KO. Obviously, other physiologic systems cannot compensate the absence of eNOS in these animals. Similarly, after treatment with NOS inhibitors like L-N^G-monomethyl arginine or L-NA, rabbits [53], mice [49,54], and humans [53,55] develop hypertension. Among all three NOS isoform, eNOS appears to play the key role in blood pressure regulation, as nNOS-deficient mice are normotensive [56], and triple e/i/nNOS-knockouts have similar hypertension to that in single eNOS- and double e/nNOS-deficient animals [57].

1.7. AIM OF THE STUDY

The aim of this study is to investigate the influence of eNOS dimer stability on the regulation of blood pressure. In the states in which eNOS is 'uncoupled', one mechanism is that the balance between NO and $O_2^{-\bullet}$ shifts towards $O_2^{-\bullet}$ [26]. *It remains to be*

This work was published in

Suvorava T*, Pick S*, and Kojda G. (* equal contribution)
Selective impairment of blood pressure reduction by endothelial nitric oxide synthase dimer destabilization in mice.
J Hypertens 2017;35(1):76-88. journals.lww.com/jhypertension/

word-for-word citations within the running text stand out in italic type

elucidated whether a partial impairment of the catalytic function of eNOS and, thus, the generation of endothelial oxidative stress in otherwise healthy conditions might support the development of hypertensive disease states like essential hypertension.

A mutant eNOS was generated in this work group *in which one of the two essential cysteines that are required for the coordination with the central Zn-ion, correct dimer formation and normal activity* [19] *is replaced by alanine [bovine eNOS destabilized by the replacement of cysteine* (Cys) *101 to alanine* (Ala) *(C101A-eNOS)]. The expression of this mutant eNOS in human embryonic kidney cells* 293 (HEK 293) *resulted in a substantial reduction of* L-*citrulline formation in cell homogenates and similar data are obtained following the investigation of purified C101A-eNOS. At the same time,* $O_2^{-\bullet}$ *generation detected by electron spin resonance was strongly increased* [58]. *This mutant eNOS was used to generate a novel transgenic mouse model [mice with endothelium-specific overexpression of destabilized C101A-eNOS (C101A-eNOS-tg)] characterized by endothelial-specific overexpression of C101A-eNOS on a C57BL/6 background. In this novel transgenic mouse strain, largely increased vascular oxidative stress* can be observed *but no impairment of vascular NO signaling, suggesting that this transgenic model might help to clarify whether oxidative stress induced by the impairment of the catalytic function of eNOS may have an impact on blood pressure. To accomplish this, another newly generated mouse model characterized by an about 2.4-fold increase in endothelial-specific overexpression of normal bovine eNOS, is used for comparison purpose* (eNOS-tg).

This work was published in

Suvorava T*, Pick S*, and Kojda G. (* equal contribution)
Selective impairment of blood pressure reduction by endothelial nitric oxide synthase dimer destabilization in mice.
J Hypertens 2017;35(1):76-88. journals.lww.com/jhypertension/

word-for-word citations within the running text stand out in italic type

2. MATERIALS AND METHODS

2.1. SUBSTANCES AND SOLUTIONS

All substances and solvents are either purchased from Sigma-Aldrich Laborchemikalien GmbH (Seelze, Germany), Merck KGaA (Darmstadt, Germany), or Carl Roth GmbH + Co. KG (Karlsruhe, Germany). They are of the best quality available. For the preparation of buffers and solutions demineralized and freshly distilled water is used.

LYSIS BUFFER FOR MOUSE TAIL BIOPSIES

50 mM Tris, 100 mM EDTA, 100 mM NaCl, 1% SDS, pH 8.0

TE BUFFER

10 mM Tris, 1 mM EDTA, pH 8.0

TAE BUFFER

40 mM Tris, 0.1% acetic acid, 10 mM EDTA, pH 8.0

AGAROSE GELS

Agarose gels are prepared by boiling 2% agarose in TAE buffer for dissolution. GelRed™ (10,000x stock; Biotium Inc., Hayward, CA, USA) is added before pouring the gel. The probes and additionally a 100 bp DNA ladder (Fermentas, Thermo Fisher Scientific, Schwerte, Germany) are mixed 1:1 with a blue staining solution (aqueous solution containing 30% glycerol and 0.005% bromphenol blue). Gel electrophoresis is performed in a Bio-Rad chamber (Bio-Rad, Munich, Germany) at 90 V for about 30 min in TAE buffer, serving as a running buffer. Evaluation is carried out under UV light (254 nm).

This work was published in

Suvorava T*, Pick S*, and Kojda G. (* equal contribution)
Selective impairment of blood pressure reduction by endothelial nitric oxide synthase dimer destabilization in mice.
J Hypertens 2017;35(1):76-88. journals.lww.com/jhypertension/

MATERIALS AND METHODS

KREBS-HEPES BUFFER

99.0 mM NaCl, 4.69 mM KCl, 1.87 mM $CaCl_2$, 1.20 mM $MgSO_4$, 25.0 mM $NaHCO_3$, 1.03 mM K_2HPO_4, 20.0 mM Na-Hepes, 11.1 mM D-glucose, pH 7.4

KREBS-HENSELEIT BUFFER (MODIFIED)

118.07 mM NaCl, 4.70 mM KCl, 1.60 mM $CaCl_2$, 1.18 mM $MgSO_4$, 25.0 mM $NaHCO_3$, 1.18 mM K_2HPO_4, 5.55 mM D-glucose, pH 7.4

LYSIS BUFFER FOR ORGAN TISSUE

5 mM Tris, 1 mM EDTA, 1 mM EGTA, 2.5 mM sodium pyrophosphate, 1 mM β-glycerol phosphate,
1 mM sodium orthovanadate, 5 mM sodium fluoride, 1 mM PMSF, protease inhibitors (10 µg/ml of each antipain, aprotinin, benzamidine and leupeptin)

BRADFORD REAGENT

0.02% Coomassie Blue G 250, 5% (v/v) ethanol, 10% (v/v) phosphoric acid

WESTERN BLOT SAMPLE BUFFER

50 mM Tris, 2% SDS, 10% glycerol, 0.005% bromphenol blue, 15% β-mercaptoethanol

WESTERN BLOT RUNNING GEL BUFFER (4x)

1.5 M Tris, 0.4% SDS, pH 8.8

WESTERN BLOT STACKING GEL BUFFER (4x)

250 mM Tris, 0.2% SDS, pH 6.8

This work was published in

Suvorava T*, Pick S*, and Kojda G. (* equal contribution)
Selective impairment of blood pressure reduction by endothelial nitric oxide synthase dimer destabilization in mice.
J Hypertens 2017;35(1):76-88. journals.lww.com/jhypertension/

WESTERN BLOT TANK BUFFER

25 mM Tris, 200 mM glycine, 0.1% SDS

WESTERN BLOT BLOTTING BUFFER

25 mM Tris, 200 mM glycine, 20% (v/v) methanol

PBS

1.059 mM KH_2PO_4, 0.155 M NaCl, 2.966 mM Na_2HPO_4, pH 7.4

PBST

1.059 mM KH_2PO_4, 0.155 M NaCl, 2.966 mM Na_2HPO_4, 1% (v/v) Tween 20, pH 7.4

STRIPPING BUFFER

25 mM glycine, 1% SDS, pH 2.0

PBSGA

5% bovine serum albumine, 10% D-glucose, 0.137 M NaCl, 2.683 mM KCl, 3.560 mM KH_2PO_4, 0.010 M Na_2HPO_4, pH 7.4

2.2. LABORATORY ANIMALS

The animal experiments described in this study are conducted following §8 TierSchG [in its judgement of 18th May 2006 (last modified on 9th December 2010)] and have been approved by the district government of Düsseldorf ("Bezirksregierung Düsseldorf," AZ 8.87-51.04.20.09.383, AZ 84-02.04.2013.A213). The mice are kept and bred under standardized conditions (room temperature 20°C, relative humidity 55 ± 5%, 12-hrs day-night rhythm with the use of artificial light) in the animal facility

This work was published in

Suvorava T*, Pick S*, and Kojda G. (* equal contribution)
Selective impairment of blood pressure reduction by endothelial nitric oxide synthase dimer destabilization in mice.
J Hypertens 2017;35(1):76-88. journals.lww.com/jhypertension/

("Tierversuchsanlage") of Heinrich-Heine-University, Düsseldorf. The mice receive germ-free drinking water (pH 3) ad libitum and are kept under veterinary supervision.

2.2.1. TRANSGENIC ANIMALS

In order to investigate the effect of eNOS derived oxidative stress, a transgenic mouse model established at the local institute ("Institute of Pharmacology und Clinical Pharmacology") is used. As this model has an endothelial specific overexpression of a destabilized eNOS variant (C101A-eNOS-tg) a transgenic model with an endothelial specific overexpression of native eNOS (eNOS-tg) is used for comparison.

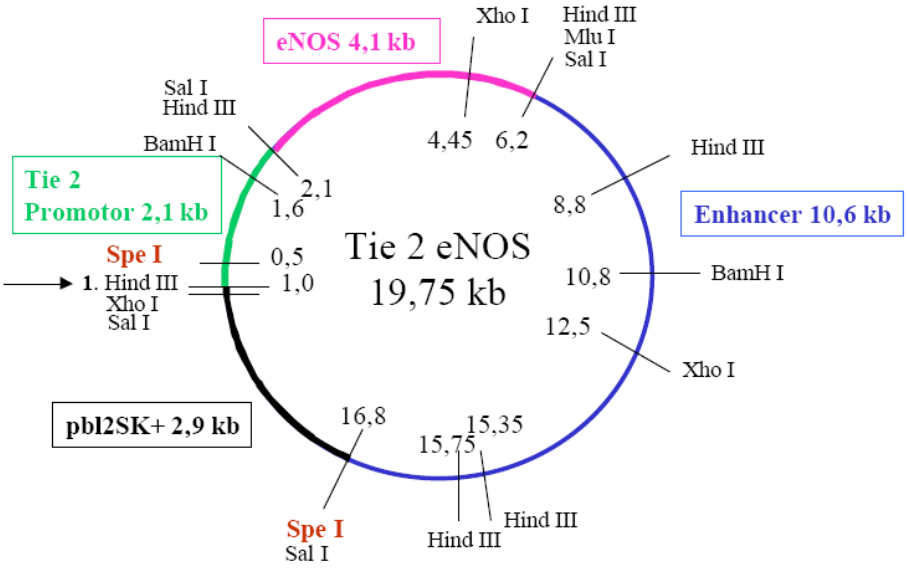

Fig. 2.1: *Schematic illustration of the plasmid serving for the generation of mouse models overexpressing eNOS provided by the local working group (eNOS-tg and C101A-eNOS-tg). Bovine eNOS, which could be either native or destabilized, has been cloned in between the murine Tie-2-promoter and a Tie-2-enhancer fragment. In this figure, the restriction sites are also shown. A linearization was achieved by Spe I in order to restrict the construct from vector parts [59].*

Both strains were generated using bovine eNOS complementary deoxyribonucleic acid (cDNA) (4.1 kb). This cDNA was cloned in between the murine Tie-2 promoter (2.1 kb)

This work was published in

Suvorava T*, Pick S*, and Kojda G. (* equal contribution)
Selective impairment of blood pressure reduction by endothelial nitric oxide synthase dimer destabilization in mice.
J Hypertens 2017;35(1):76-88. journals.lww.com/jhypertension/

word-for-word citations within the running text stand out in italic type

and a Tie-2 intron fragment, which served as a Tie-2 enhancer in order to achieve the expression within the vasculature. Destabilization was accomplished by replacing Cys 101 by Ala, using primer overlap extension polymerase chain reaction (PCR) [59].

Transgenic positive mice (eNOS-tg and C101A-eNOS-tg) were backcrossed at least seven times to C57BL/6-mice in order to achieve the genetic background of this particular strain. Those eNOS-tg mice used in this study are backcrossed with C57BL/6 mice in the 17^{th}-23^{rd} generation and those C101A-eNOS-tg mice in the 15^{th}-20^{th} generation. Thus, transgenic negative littermates can be considered as C57BL/6 and are used as the controls for all experiments. All mice used in this study are of male gender and 3-6 months old.

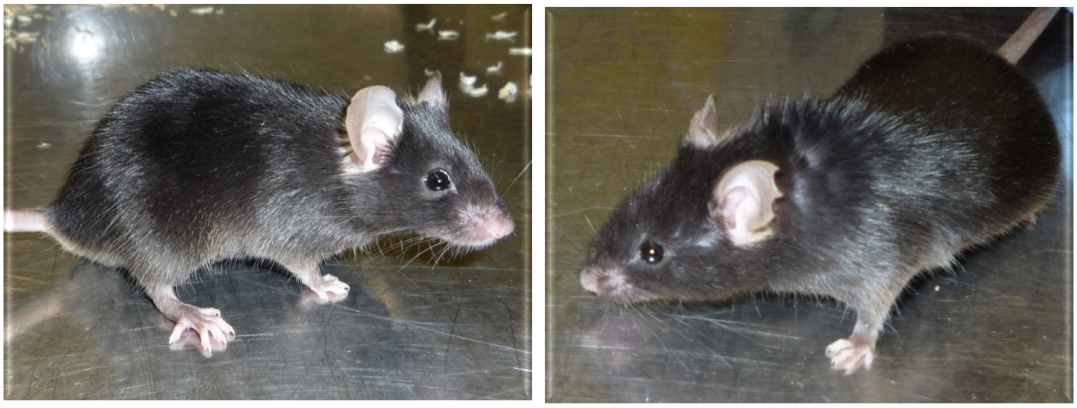

Fig. 2.2: *Both animal strains (**eNOS-tg** and **C101A-eNOS-tg**) produced vital and healthy offsprings of normal size, weight and litter size.*

2.2.2. GENOTYPING OF TRANSGENIC ANIMALS

Genomic deoxyribonucleic acid (DNA) is prepared from tail biopsies, which are excised from the mice at the age of three weeks and provided by the local animal facility.

750 µl of lysis buffer, including Proteinase K (final concentration 0.5 µl/ml; Qiagen, Hilden, Germany), are added to the tips of the tails and these are then incubated for 16 hours over night at 55°C. After complete lysis of all proteins, 250 µl of concentrated

This work was published in

Suvorava T*, Pick S*, and Kojda G. (* equal contribution)
Selective impairment of blood pressure reduction by endothelial nitric oxide synthase dimer destabilization in mice.
J Hypertens 2017;35(1):76-88. journals.lww.com/jhypertension/

NaCl solution (6 M) are added. The probe is mixed thoroughly and then incubated at room temperature for 5 minutes before centrifugation at 16,000xg for 10 minutes. 600 µl of cold ethanol (96%, -20°C) are added to the supernatant and after incubation for 10 minutes centrifugated for 30 minutes at 16,000xg and 4°C. The pellet is washed with cold ethanol (70%) by centrifuging it again at 16,000xg and 4°C for 5 minutes. The pellet is then dried and dissolved over night at room temperature in 100 µl of TE-buffer. In random samples, the obtained concentration is determined at a wavelength of 260 nm with a BioPhotometer (Eppendorf, Hamburg, Germany).

Genotyping is then carried out by using PCR. The primers are chosen in a manner that only transgenic positive animals could give a signal, as the detected sequence is not present in wild-type mice. Thus, the sense primer binds within the Tie-2-promoter and the antisense primer within the bovine eNOS-DNA to give a product of 351 bp. As the antisense primer does not bind within the genetically modified region of C101A-eNOS-tg, the same primers could be used for the detection of the transgene in both investigated animal strains.

sense primer: 5'-GGG AAG TCG CAA AGT TGT GAG-3'
antisense primer: 5'-GCT CCC AGT TCT TCA CGC GAG-3'

To ensure breeding correctness in the long term, a transgene-specific PCR is done at regular intervals to distinguish between mutated and wild-type bovine eNOS by specific primers giving a product of 310 bp for C101A-eNOS or one of 326 bp for wild-type eNOS.

C101A-eNOS-specific:

sense primer: 5'-TTG AAG AGT GTG GGC CAG GA-3'
antisense primer: 5'-ACA CCA GGG AGC CCA GGG C-3'

wild-type bovine eNOS-specific:

sense primer: 5'-CAG CGA CAT GGG CAA GA-3'
antisense primer: 5'-ACA CCA GGG AGC CCA GGC A-3'

This work was published in

Suvorava T*, Pick S*, and Kojda G. (* equal contribution)
Selective impairment of blood pressure reduction by endothelial nitric oxide synthase dimer destabilization in mice.
J Hypertens 2017;35(1):76-88. journals.lww.com/jhypertension/

The PCRs themselves are performed with 1 µg of genomic DNA using “Mastermix 2.5x” (Eppendorf, Hamburg, Germany) and 0.4 µl of each of the primers (synthesis by MWG, Ebersberg, Germany).

PCR conditions:	step 1	95°C, 3 min	
	step 2	95°C, 1 min 10 sec	
	step 3	54°C, 1 min 15 sec	
	step 4	72°C, 2 min 7 sec	35 repeats of steps 2-4
	step 5	4°C, hold	

For visualization of the PCR products an agarose gel electrophoresis with a 2% gel is used. Therefor, the complete reaction volume was applied on the gel. DNA of probes characterized earlier serve as positive and negative controls during all the experiments perfomed.

2.2.3. PHYSICAL EXERCISE TRAINING

In order to determine the effects of physical activity on the expression of ROS in-vivo, C101A-eNOS-tg mice as well as their transgenic negative littermates are trained in acoordance with a voluntary training protocol [60]. Mice at the age of two months are singularized for six weeks. After randomization, one group of each strain remain in the small cages of singularization (360 cm²), whereas the other group is placed in special cages (510 cm²) with integrated running wheels (diameter: 0.025 m, Tecniplast, Hohenpeißenberg, Germany). The mice are allowed to enter and use the wheel ad libitum. The efficacy of training is controlled by recording the running distance every day. Voluntary training is performed for four weeks. To ensure training efficacy not only running distances per 24 hours are determined but also exercise parameters (heart weight/body weight, soleus weight/body weight, soleus weight/tibia length) are calculated [60].

This work was published in

Suvorava T*, Pick S*, and Kojda G. (* equal contribution)
Selective impairment of blood pressure reduction by endothelial nitric oxide synthase dimer destabilization in mice.
J Hypertens 2017;35(1):76-88. journals.lww.com/jhypertension/

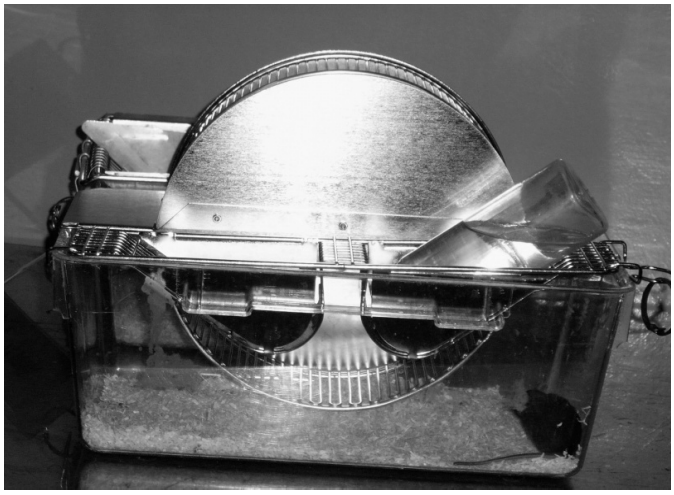

Fig. 2.3: *Physical exercise equipment for voluntary training.*

2.2.4. BLOOD PRESSURE AND HEART RATE

Blood pressure and heart rate are determined in awake male mice using tail-cuff method [61]. Here, the mouse tail is passed through a cuff and by a light source above and a photoresistor below the tail, the blood flow is evaluated photo electrically by recording oscillating waveforms using an automated system (BP-2000 Blood Pressure Analysis System, Visitech Systems, Apex, USA) and its software ("Blood Pressure Analysis," Visitech Systems, Apex, USA). The waveform amplitude is reduced as a result of the increasing pressure in consequence of cuff inflation. The systolic blood pressure is defined as the cuff inflation pressure at which the amplitude falls below 10% of the original amplitude for 10 waveform cycles.

Measurements are performed every day at the same time during the active phase of the mice. After an adaptation period of seven days measurements are performed for a period of 10 days with three cycles and 10 measurements per cycle. Then mice receive oral treatment of Tempol® (see 2.2.5) for two weeks. To ensure that the observed effects are a result of the treatment a wash-out phase of three weeks is subsequently affiliated. Measurements are carried out during the entire duration of treatment and washing out.

This work was published in

Suvorava T*, Pick S*, and Kojda G. (* equal contribution)
Selective impairment of blood pressure reduction by endothelial nitric oxide synthase dimer destabilization in mice.
J Hypertens 2017;35(1):76-88. journals.lww.com/jhypertension/

word-for-word citations within the running text stand out in italic type

Fig. 2.4: *Equipment for measuring blood pressure and heart rate using tail-cuff method. Four mice are sitting in a black box each, their tails are visible.*

2.2.5. TREATMENT WITH TEMPOL®

A group of each C101A-eNOS-tg and their transgenic negative littermates are treated with the antioxidant Tempol® (for chemical structure see fig. 2.5). It is applied orally for three weeks by dissolving Tempol® in the drinking water at a concentration of 1 mmol/L. Assuming that mice usually drink 2 ml per day and have a body weight of about 25 g, this corresponds to a dosage of 80 µmol/kg BW/day [62]. The drinking water is replaced every day.

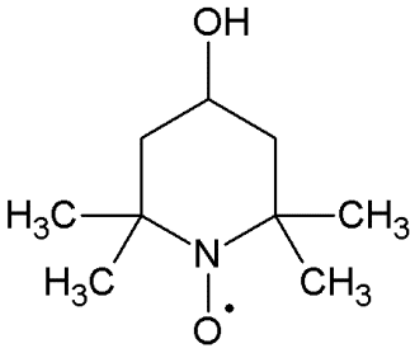

Fig. 2.5: *Chemical structure of the SOD-mimetic Tempol®.*

2.2.6. PREPARATION AND ORGAN REMOVAL

The mice are euthanized by inhalation of CO_2 and fixed on a preparation table. After removing the fur, the thorax is opened by discission of the rib cage. Heart and lungs are removed after puncture of the ventricle to rinse out the blood. They are then

This work was published in

Suvorava T*, Pick S*, and Kojda G. (* equal contribution)
Selective impairment of blood pressure reduction by endothelial nitric oxide synthase dimer destabilization in mice.
J Hypertens 2017;35(1):76-88. journals.lww.com/jhypertension/

word-for-word citations within the running text stand out in italic type

placed into Krebs-Hepes buffer. The abdominal cavity is further opened and the complete intestine is shifted to one side in order to expose the aorta, which is then dissected from the aortic arch until bifurcation. After being transferred into Krebs-Hepes buffer, it is trimmed from any adhering fat and connective tissue. The remaining blood is rinsed out by washing the lumen with the buffer. Aortic preparation is carried out carefully without stretching or clenching in order not to damage the endothelial layer. Rings of 5 mm are applicable for functional organ bath experiments or measurements of $O_2^{-\bullet}$. Finally, skeletal muscle tissue is removed from the upper leg of the mice. Pieces of organs used for the lucigenin assay are immediately excised and transferred into pre-gassed and pre-warmed Krebs-Henseleit buffer. All remaining organs are shock frozen in liquid nitrogen and then kept at -80°C until they are used for preparation of ribonucleid acid (RNA) or protein.

2.3. FUNCTIONAL STUDIES ON ISOLATED MOUSE AORTA

2.3.1. EQUIPMENT AND CALIBRATION

Aortic vascular reactivity is determined using organ bath equipment. The apparatus consists of four water jacketed glass vessels with a total volume of 20 ml. For experiments, exact 10 ml of Krebs-Henseleit buffer are used per vessel and aeration with carbogen gas (95% oxygen, 5% carbon dioxide; Linde Gas Therapeutics, Unterschleißheim, Germany) is accomplished through sintered-glass filters. Using a circulating water bath with constant temperature (NB-22; Haake, Karlsruhe, Germany), the buffer can be held on 37°C. A likewise double-walled but 1.5 L containing vessel served as a reservoir for the pre-warmed and pre-gassed buffer.

Aortic constriction is registered via force sensors (Straham, USA) which are connected to intensifiers (DCB-4B, ifd). These intensifiers transfer the signals to the recorder (SE-120; ABB, Mannheim, Germany).

This work was published in

Suvorava T*, Pick S*, and Kojda G. (* equal contribution)
Selective impairment of blood pressure reduction by endothelial nitric oxide synthase dimer destabilization in mice.
J Hypertens 2017;35(1):76-88. journals.lww.com/jhypertension/

word-for-word citations within the running text stand out in italic type

For calibration and standardization of experimental conditions the apparatus has to be calibrated with standard weightings before every single trial. The baseline value is set to the weight of 1 g, which corresponds to a resting tension of 9.81 mN.

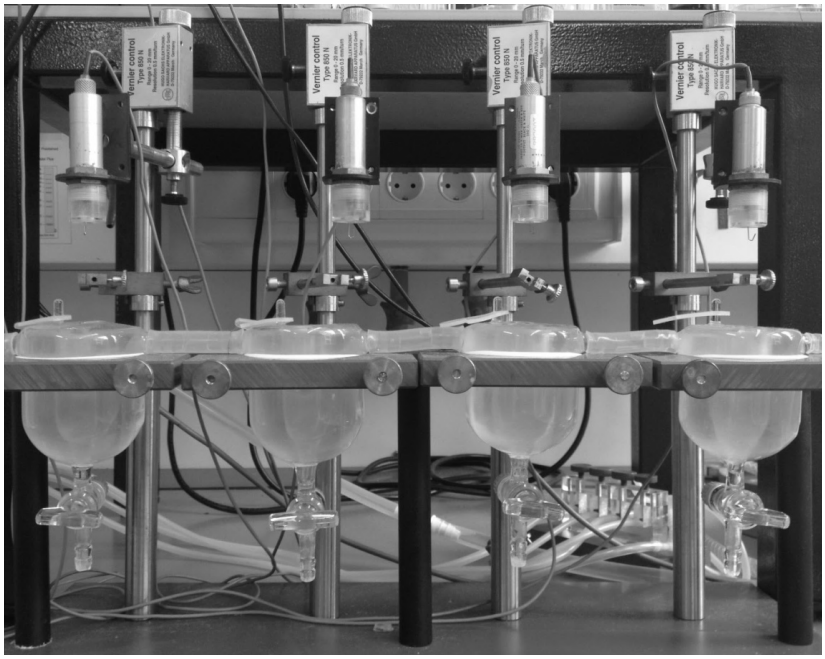

Fig. 2.6: *Organ bath apparatus with four double-walled vessels, each equipped with a force sensor, which are then connected to intensifiers.*

After calibration, aortic rings are placed between two triangles of stainless steel made of wires with a diameter of 0.1 mm. The lower element is fixed, whereas the upper element is connected to the force sensor by a polyester filament.

For every single mouse, two aortic rings are investigated. The buffer contains 10 µM diclofenac.

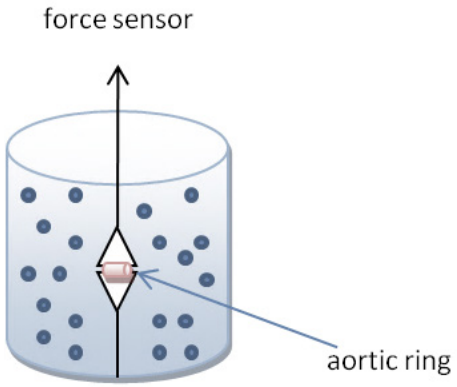

Fig. 2.7: *Schematic illustration of an organ bath vessel showing the aortic ring placed on triangles in gassed Krebs-Henseleit buffer.*

This work was published in

Suvorava T*, Pick S*, and Kojda G. (* equal contribution)
Selective impairment of blood pressure reduction by endothelial nitric oxide synthase dimer destabilization in mice.
J Hypertens 2017;35(1):76-88. journals.lww.com/jhypertension/

word-for-word citations within the running text stand out in italic type

2.3.2. EXPERIMENTAL PROTOCOL

After being placed, aortic rings are allowed to equilibrate for 60 minutes. During this phase the buffer is changed every 20 minutes and the initial tension is constantly set to zero using micrometer calipers. Finally, the vasotonus no longer changes spontaneously.

In order to check for the functionality of the aortic rings these are depolarized twice with 80 mM potassium chloride (final concentration in organ bath) and hence constricted. This test serves as equilibration for smooth muscle cells as the extent is considered to be the maximal possible constriction. After washing out several times, the initial tension is again adjusted. A further testing in terms of constriction is carried out by applying 10 µM phenylephrine. Then, in order to investigate endothelium-dependent relaxation, a preconstriction with 0.2 µM phenylephrine is performed and subsequently, increasing doses of acetylcholine (1 nM to 10 µM) are successively applied whenever a plateau was reached. Thus, a dose-response curve is obtained. Washing out and equilibration is performed as described above. Thereafter, to check reactivity to exogenous NO the NO-donor S-nitroso-N-acetyl-D,L-penicillamine (SNAP, own synthesis within the institute according to [63]), is applied in cumulative doses (1 nM to 10 µM) after preconstricting with 0.2 µM phenylephrine.

2.4. eNOS mRNA-Expression

Quantification of murine and bovine eNOS messenger RNA-expression is determined by real-time PCR utilizing TaqMan® technology. RNA of frozen thoracic aortic probes is extracted by RNeasy® Fibrous Tissue Mini Kit (Qiagen, Hilden, Germany) using the TissueRuptor® (Qiagen, Hilden, Germany) in accordance with the manufacturer's protocol. The concentration of RNA is determined by a NanoDrop 1000 Spectrophotometer (Thermo Fisher Scientific, Schwerte, Germany) and the supplier's software in its version 3.7.0. Following this, synthesis of cDNA is performed with 500 ng RNA using the QuantiTect® Reverse Transcription Kit (Qiagen, Hilden, Germany),

This work was published in

Suvorava T*, Pick S*, and Kojda G. (* equal contribution)
Selective impairment of blood pressure reduction by endothelial nitric oxide synthase dimer destabilization in mice.
J Hypertens 2017;35(1):76-88. journals.lww.com/jhypertension/

also pursuant to the manufacturer's protocol. This cDNA is then introduced in a concentration of 2 ng/µl as a template for real-time PCR applying TaqMan® Gene Expression Assay (Life Technologies GmbH, Darmstadt, Germany). The principle of this technology is described in fig. 2.8.

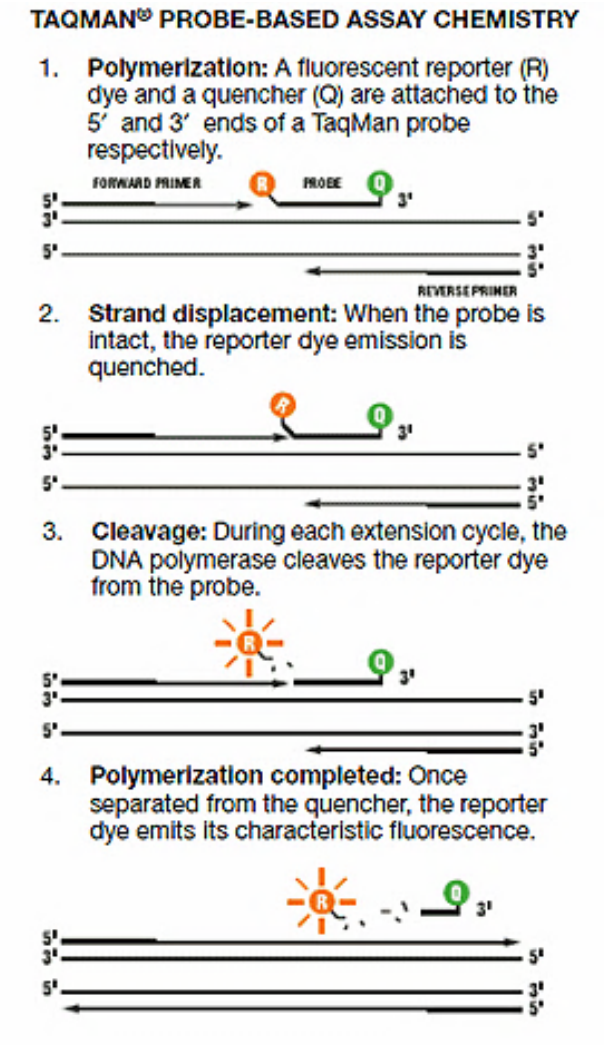

Fig. 2.8: *Principle of TaqMan® real-time PCR chemistry mechanism [64]. Each TaqMan® probe consists of an oligonucleotide probe with a fluorophore covalently attached to the 5'-end and a quencher at the 3'-end. Here 6-carboxyfluorescein (acronym: FAM) is used as the fluorophore. The quencher molecule inhibits the fluorescence emitted by the fluorophore via Fluorescence Resonance Energy Transfer as long as the fluorophore and the quencher are in proximity. If the target sequence is present the probe anneals downstream to single stranded DNA. Owing to the 5' to 3' exonuclease activity, the Taq polymerase extends the primer and the nascent strand is synthesized. Thus, the polymerase degrades the probe, releasing the fluorophore, and breaking the close proximity to the quencher. Thereby the quenching effect is relieved allowing fluorescence of the fluorophore to be detected as directly proportional to the amount of DNA template introduced.*

This work was published in

Suvorava T*, Pick S*, and Kojda G. (* equal contribution)
Selective impairment of blood pressure reduction by endothelial nitric oxide synthase dimer destabilization in mice.
J Hypertens 2017;35(1):76-88. journals.lww.com/jhypertension/

word-for-word citations within the running text stand out in italic type

Commercially available primers are chosen from Life Technologies GmbH, Darmstadt, Germany for murine and bovine eNOS mRNA, making sure that there is no cross-reactivity vice versa with either Bos taurus or Mus musculus. This is additionally ensured by applying the primers to appropriate negative controls. To allow internal standardization, RNA of murine large ribosomal protein (RPLP0, Life Technologies GmbH, Darmstadt, Germany), serving as an endogenous housekeeping control, is been coamplificated.

murine primer:		
Mm01134920_m1	amplicon length: 69	(probe spans exons 23-24)
bovine primer:		
Bt03217671_m1	amplicon length: 110	(probe spans exons 20-21)
housekeeping primer:		
Mm01974474_gH	amplicon length: 89	(probe binds within exon 3)

10 ng of cDNA are introduced to the total reaction volume of 25 µl containing 2x TaqMan® Gene Expression Master Mix (Life Technologies GmbH, Darmstadt, Germany) and 20x TaqMan® primer mix. The experiments are then performed using Abi Prism 7900HT Sequence Detector System (Applied Biosystems, Weiterstadt, Germany) under the following conditions:

stage 1:	50°C	2 min	
stage 2:	95°C	10 min	
stage 3:	95°C	15 sec	
	60°C	1 min	40 repeats within stage 3

In order to evaluate the relative murine eNOS mRNA-expression, the comparative C_T method is used. The C_T value is defined as the PCR cycle at which the fluorescent signal crosses an arbitrarily placed threshold. The ΔC_T is obtained by subtracting the internal

This work was published in

Suvorava T*, Pick S*, and Kojda G. (* equal contribution)
Selective impairment of blood pressure reduction by endothelial nitric oxide synthase dimer destabilization in mice.
J Hypertens 2017;35(1):76-88. journals.lww.com/jhypertension/

control value from the value of the gene of interest. By comparing a sample, e.g. transgenic mouse, with a control, e.g. wild-type animal, the $\Delta\Delta C_T$ is given as follows:

$$\Delta\Delta C_T = [(C_T\ gene\ of\ interest - C_T\ internal\ control)_{sample} - (C_T\ gene\ of\ interest - C_T\ internal\ control)_{control}]$$

As in every cycle the concentration of DNA is doubled, the relative expression is finally obtained by the following equation:

$$Fold\ change = 2^{-\Delta\Delta C_T}$$

Evaluation of the bovine eNOS expression cannot be standardized to a control as wild-type animals do not express bovine eNOS. Here individual data points are calculated by

$2^{-\Delta C_T}$ [65].

2.5. Western Blot

2.5.1. Preparation of organs

Protein fractions from aortic, myocardial, lung and skeletal muscle tissue are isolated in order to determine the protein expression by Western Blot analysis. The frozen organs are pulverized by using a metal mortar pre-cooled in liquid nitrogen. An adequate amount of cold lysis buffer is added immediately, and the tissue powder dispersed thoroughly therein. Further homogenization is achieved by utilizing an Ultra-Turrax (T8, Ika Labortechnik, Staufen, Germany) at its highest liquidizing level. In order to break up cell membranes, the probes are additionally placed in an ultrasonic bath at 4°C for 10 minutes. After centrifugation for 10 minutes at 100xg and 4°C, the supernatant is used for the further experiments.

2.5.2. Determination of protein concentrations

Protein concentrations are determined by the use of the Bradford method [66]. 100 µl of different dilutions of the protein solution (1:20 to 1:800) and 400 µl of Bradford reagent are measured at 595 nm in a spectrophotometer (DU 640 Spektrophotometer,

This work was published in

Suvorava T*, Pick S*, and Kojda G. (* equal contribution)
Selective impairment of blood pressure reduction by endothelial nitric oxide synthase dimer destabilization in mice.
J Hypertens 2017;35(1):76-88. journals.lww.com/jhypertension/

word-for-word citations within the running text stand out in italic type

Beckman, Krefeld, Germany) in standard cuvettes, applicable for the visible wavelength range. Prior to every single series of measurements, a calibration is carried out with various concentrations of bovine serum albumin (10 µg/ml to 140 µg/ml in 5 mM Tris, pH 7.6; see fig. 2.9). The calibration line is achieved by linear regression. Those dilutions of the protein fractions, which are inherent in the linear range of the calibration curve, are used for analysis.

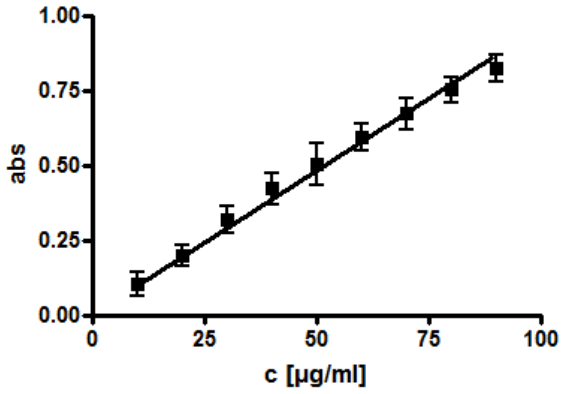

Fig. 2.9: *Exemplary calibration curve for increasing bovine serum albumin concentrations (10 µg/ml to 90 µg/ml) measured by Bradford method photometrically at 595 nm.*

2.5.3. GENERAL WESTERN BLOT PROTOCOL

The protein fractions are mixed 1:1 with sample buffer and denaturated by incubation at 95°C for 5 minutes. The same amount of total protein (20-100 µg) is loaded onto the gel of those probes that are supposed to be compared to each other. The separation of the proteins is achieved by a discontinuous and denaturating polyacrylamide gel electrophoresis [67,68]. 7.5%-10% acrylamide/bisacrylamide (37.5:1) containing running gels are used, depending on the size of the desired protein. Polymerization is achieved by adding 0.8 µg/ml ammonium persulfate and 0.6 µl/ml tetramethylethylenediamine. A stacking gel of 4.5% acrylamide/bisacrylamide (37.5:1) is poured above the running gel. Preparation of the gels, using Western Blot running gel buffer or Western Blot stacking gel buffer, and the following gel electrophoresis, are performed in equipment obtained from Bio-Rad (Munich, Germany). One slot on each gel is loaded with a pre-stained protein marker (PageRuler Plus Prestained Protein

This work was published in

Suvorava T*, Pick S*, and Kojda G. (* equal contribution)
Selective impairment of blood pressure reduction by endothelial nitric oxide synthase dimer destabilization in mice.
J Hypertens 2017;35(1):76-88. journals.lww.com/jhypertension/

Ladder; Thermo Fisher Scientific, Schwerte, Germany). Running of the gel is carried out in Western Blot tank buffer at 150 V for about 60 minutes.

The separated proteins are then transferred from the gel to a nitrocellulose membrane (Immobilon-NC Membrane, pore size 0.45 µm; Merck Millipore, Darmstadt, Germany) in Western Blot blotting buffer at 90 V for about 90 min using a Bio-Rad apparatus (Munich, Germany).

Membranes are then transferred into and blocked with Odyssey® Blocking Buffer (LI-COR Biosciences, Lincoln, NE, USA) in accordance with the manufacturer's protocol. Antibody incubations are performed herein as well. These are used in concentrations as shown in chapter 2.5.5. Detection and quantification of the signals are carried out at 680 nm and 800 nm on Odyssey® Infrared Imager 9120 (LI-COR Biosciences, Lincoln, NE, USA) with the supplier's software (Odyssey® Application Software Version 3.0.29). If stripping is necessary, the procedure followed the protocol provided with the Odyssey® equipment.

2.5.4. NATIVE GEL ELECTROPHORESIS

In order to determine eNOS dimer/monomer-ratio, 6% running gels are prepared and pre-cooled to 4°C. The probes are mixed 1:1 with the Western Blot sample buffer without β-mercaptoethanol. Thus, the probes are not denaturated but loaded immediately onto the gel. Running of the gel is performed at 30 mA for about 3 hours at 4°C in a cold room. The apparatus was additionally placed in an ice-bath.

2.5.5. ANTIBODIES

Here all antibodies employed in this study are shown including the size of the detected protein and the dilution used during incubation. Except for the secondary antibodies, the host organism is specified. Whether the antibody is of monoclonal or polyclonal design is also specified.

This work was published in

Suvorava T*, Pick S*, and Kojda G. (* equal contribution)
Selective impairment of blood pressure reduction by endothelial nitric oxide synthase dimer destabilization in mice.
J Hypertens 2017;35(1):76-88. journals.lww.com/jhypertension/

word-for-word citations within the running text stand out in italic type

PRIMARY ANTIBODIES

Purified Mouse Anti-eNOS/NOS Type III (BD Biosciences, Franklin Lakes, NJ, USA)	140 kDa Mouse IgG	1:1,000 monoclonal
Polyclonal Rabbit Anti-eNOS/NOS Type III (BD Biosciences, Franklin Lakes, NJ, USA)	140 kDa Rabbit IgG	1:1,000 polyclonal
phospho eNOS (Ser1177) (C9C3) Rabbit mAb (Cell Signaling Technology Inc., Danvers, MA, USA)	140 kDa Rabbit IgG	1:1,000 monoclonal
Anti-phopho-VASP (Ser239) Antibody, clone 16C2 (Merck Millipore, Darmstadt, Germany)	50 kDa Mouse IgG	1:1,000 monoclonal
Anti-VASP (Merck Millipore, Darmstadt, Germany)	45-49 kDa Rabbit IgG	1:2,000 polyclonal
Phospho-AMPKα (Thr172) Antibody (Cell Signaling Technology Inc., Danvers, MA, USA)	62 kDa Rabbit IgG	1:1,000 polyclonal
AMPKα (K6) Antibody (Cell Signaling Technology Inc., Danvers, MA, USA)	62 kDa Mouse IgG	1:1,000 monoclonal
Phospho Akt (Ser473) (587F11) Mouse mAb (Cell Signaling Technology Inc., Danvers, MA, USA)	60 kDa Mouse IgG	1:1,000 monoclonal
Akt Antibody (Cell Signaling Technology Inc., Danvers, MA, USA)	60 kDa Rabbit IgG	1:1,000 polyclonal
Anti-Nitro tyrosine antibody [HM.11] (abcam plc, Cambridge, UK)	25,45,55 kDa Mouse IgG	1:1,000 monoclonal
Mouse SOD3/EC-SOD Affinity Purified Polyclonal Ab (R&D Systems, Minneapolis, MN, USA)	~30 kDa Goat IgG	1:1,000 polyclonal
Anti-Actin antibody produced in rabbit (Sigma-Aldrich®, St. Louis, MO, USA)	42 kDa Rabbit IgG	1:5,000 polyclonal

This work was published in

Suvorava T*, Pick S*, and Kojda G. (* equal contribution)
Selective impairment of blood pressure reduction by endothelial nitric oxide synthase dimer destabilization in mice.
J Hypertens 2017;35(1):76-88. journals.lww.com/jhypertension/

SECONDARY ANTIBODIES

IRDye 680LT Goat anti-Mouse IgG (H + L) (LI-COR Biosciences, Lincoln, NE, USA)	1:10,000
IRDye 800CW Goat anti-Rabbit IgG (H + L) (LI-COR Biosciences, Lincoln, NE, USA)	1:10,000
IRDye 680RD Donkey anti-Goat IgG (H + L) (LI-COR Biosciences, Lincoln, NE, USA)	1:10,000

2.6. IMMUNOPRECIPITATION AND FLUORESCENCE DETECTION (DYNABEADS®)

Immunoprecipitation of eNOS is carried out by using Dynabeads® M-280 Sheep anti-Rabbit IgG (Life Technologies GmbH, Darmstadt, Germany) following the manufacturer's protocol, using a DynaMag™-2 magnet (Life Technologies GmbH, Darmstadt, Germany). In detail, 1 µg of polyclonal rabbit anti-eNOS antibody (BD Biosciences, Franklin Lakes, NJ, USA) is loaded on 10^7 beads. Per analysis 10^6 beads and 500 µg of total protein from whole tissue lysates are used. Neither cross-linking nor elution was performed. The analysis was then accomplished by a 1:1,000 incubation with phospho eNOS (Ser1177) rabbit monoclonal antibody (Cell Signaling Technology Inc., Danvers, MA, USA) in order to detect phosphorylated eNOS, with anti-Glutathione monoclonal antibody (Virogen, Watertown, MA, USA) to determine gluthathionylated eNOS or with anti-nitrotyrosine antibody (abcam plc, Cambridge, UK) to seek tyrosine-nitrated eNOS. Mouse anti-eNOS antibody (BD Biosciences, Franklin Lakes, NJ, USA) is used additionally to allow standardization to total eNOS protein. Finally, fluorescent detection on 96 well plates is achieved by labeling with either IRDye 680LT Goat anti-Mouse IgG or IRDye 800CW Goat anti-Rabbit IgG (both LI-COR Biosciences, Lincoln, NE, USA) at a concentration of 1:3,000, used during incubation.

To ensure the specificity of the method several negative control experiments are performed during each set. Thus, incubations with dyes, which should not give a signal, and which are used during the following procedure, are carried out. These controls also

This work was published in

Suvorava T*, Pick S*, and Kojda G. (* equal contribution)
Selective impairment of blood pressure reduction by endothelial nitric oxide synthase dimer destabilization in mice.
J Hypertens 2017;35(1):76-88. journals.lww.com/jhypertension/

ensure binding of the particular target in its step as certain dyes might give a signal if no binding is achieved. For example, after binding of eNOS protein from tissue lysate, no signal is achieved after application of anti-rabbit dye, whereas this particular dye gives a signal on the beads themselves or the bound anti-eNOS pAb respectively. This control experiment thus ensures saturated binding. Details are shown in fig. 2.10.

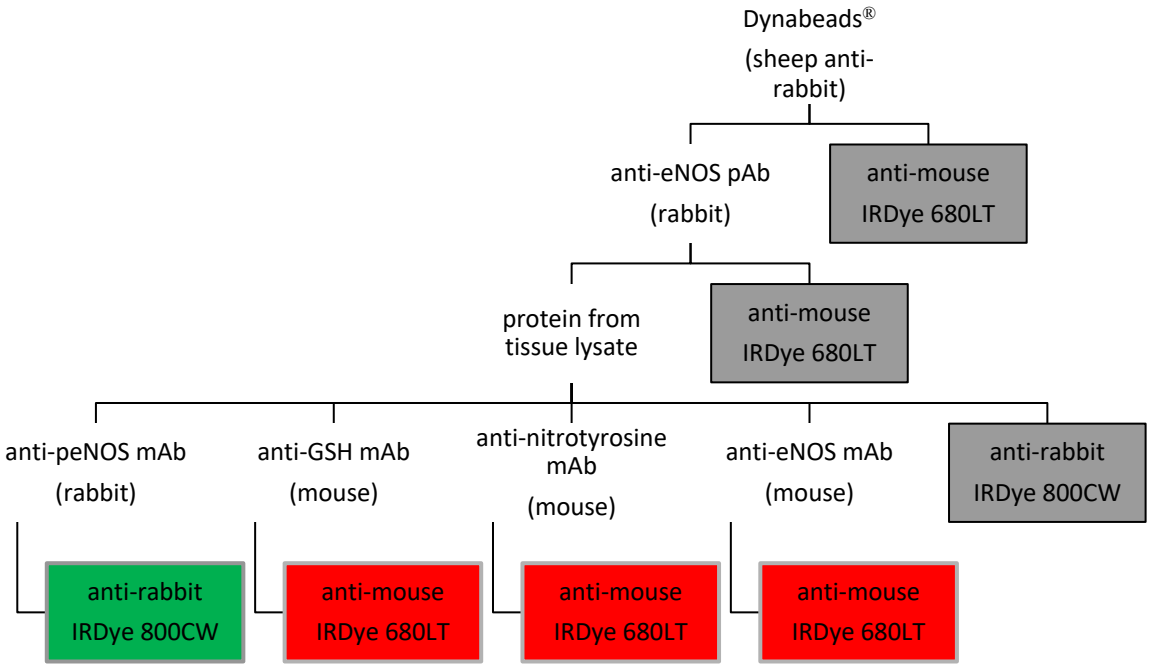

Fig. 2.10: *Experimental scheme of Dynabeads® immunoprecipitation and the subsequent fluorescent detection of phosphorylated, glutathionylated or tyrosine-nitrated eNOS. Negative controls give no signal and are marked in gray, whereas the fluorescing probes are marked in red or green, depending on the dye.*

Additionally, the whole Dynabeads® construct is mixed with Western Blot sample buffer containing β-mercaptoethanol and incubated at 95°C for 5 min. The supernatant is applied on a Western Blot as described above. A band at 140 kDa indicates that eNOS protein is detected, as presented in fig. 2.11A. To ensure detection of tyrosine-nitrated eNOS, a costaining of 3-nitrotyrosine and eNOS is performed after elution and running a Western Blot. Results are shown in fig. 2.11B.

This work was published in

Suvorava T*, Pick S*, and Kojda G. (* equal contribution)
Selective impairment of blood pressure reduction by endothelial nitric oxide synthase dimer destabilization in mice.
J Hypertens 2017;35(1):76-88. journals.lww.com/jhypertension/

word-for-word citations within the running text stand out in italic type

A **B**

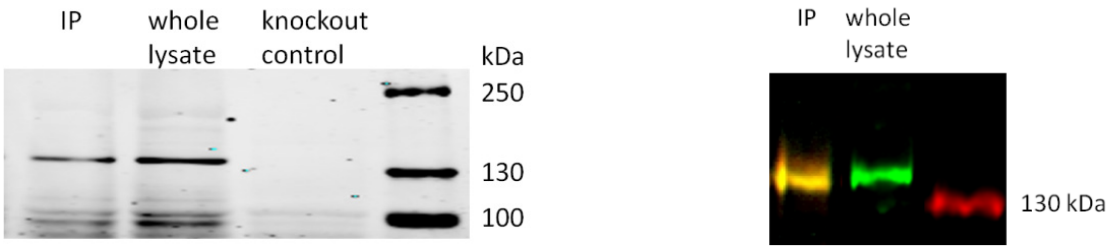

Fig. 2.11: *Western Blot experiments of both immunoprecipitated eNOS (IP; 500 µg total protein on 10^6 beads) and whole tissue lysate from the same lung tissue (100 µg total protein) of a C57BL/6 mouse. A quantization is not feasible because different amounts of protein are loaded.* ***A*** *eNOS is detected at 140 kDa by mouse anti-eNOS antibody (BD Biosciences, Franklin Lakes, NJ, USA). As a negative control, lung lysate (100 µg total protein) of an eNOS-knockout mouse [50] was used.* ***B*** *Co-staining with eNOS polyclonal antibody, finally detected in green, and anti-nitrotyrosine antibody, finally detected in red. In an overlay, red and green give a total signal in yellow, indicating a detection of tyrosine-nitrated eNOS after immunoprecipitation.*

2.7. Detection of Superoxide Anion Radical

Generation of $O_2^{-\bullet}$ radicals by mouse thoracic aorta, myocardium and skeletal muscle is measured by use of lucigenin-enhanced chemiluminescence assay [69,70]. The tissue probes are equilibrated in Krebs-Henseleit buffer (pH 7.4, 37°C) gassed with carbogen for at least 30 minutes, or until use. The measurements of $O_2^{-\bullet}$ radicals are performed at 37°C in PBSGA enriched with lucigenin (5 µM). Vials containing this buffer are preheated to 37°C by placing them in the luminometer (Packard Luminometer Analyzer, Picolite A6112, Packard, Downers Grove, IL, USA). A background measurement of 20 minutes is then performed before placing the tissue segments into the vials. Then the measurement itself is carried out for another 20 minutes. $O_2^{-\bullet}$ production in the vessel segment is analyzed by correction for background radiation and calculated per mg weight of dry tissue, which is obtained by drying the tissue over night at 100°C.

This work was published in

Suvorava T*, Pick S*, and Kojda G. (* equal contribution)
Selective impairment of blood pressure reduction by endothelial nitric oxide synthase dimer destabilization in mice.
J Hypertens 2017;35(1):76-88. journals.lww.com/jhypertension/

word-for-word citations within the running text stand out in italic type

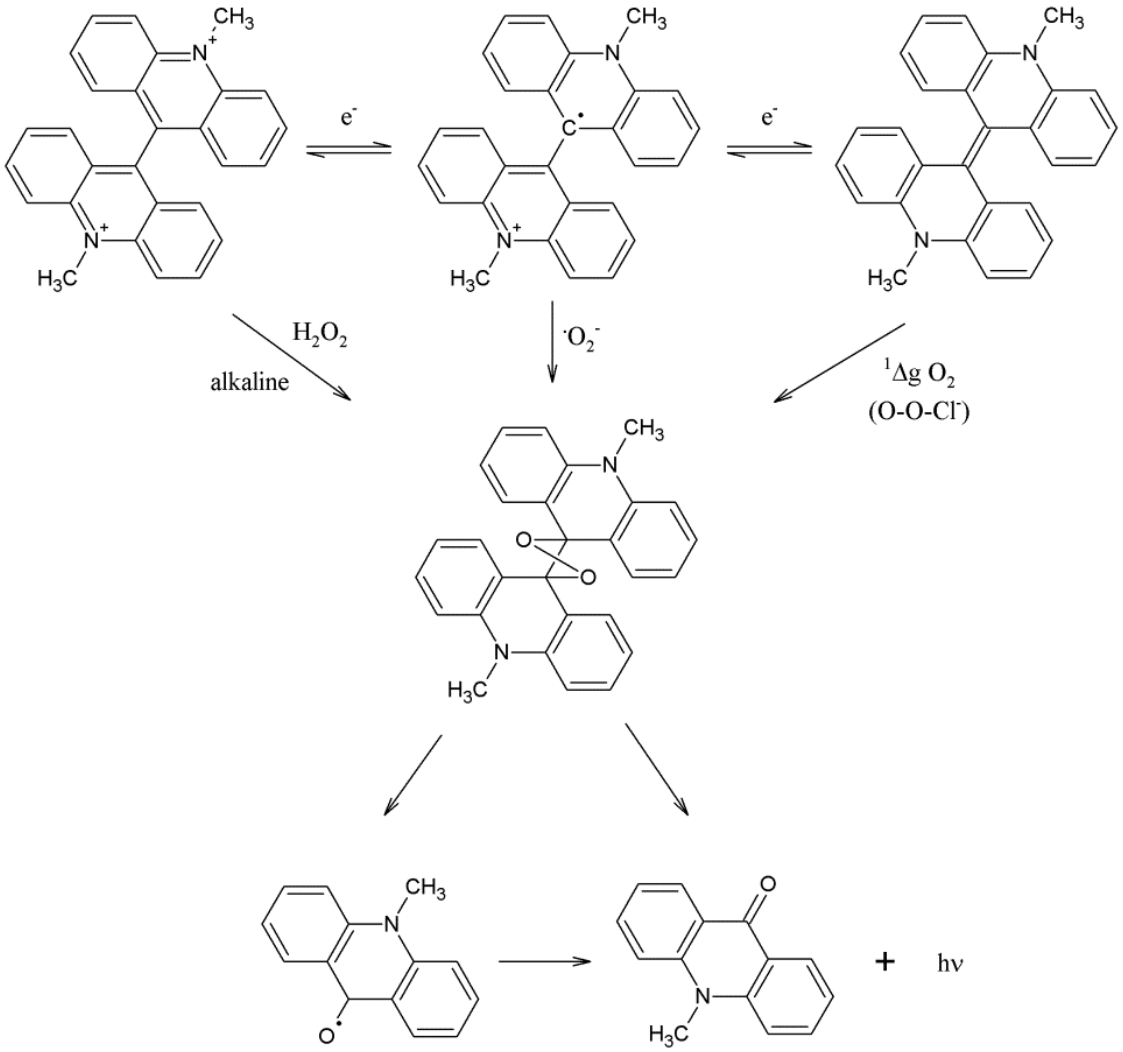

Fig. 2.12: *Lucigenin reaction. In alkaline solution, lucigenin reacts with hydrogen peroxide, a divalently reduced molecular oxygen, but only weakly in neutral or acid pH range. If lucigenin is reduced univalently, a reaction with $O_2^{-\bullet}$ in a radical-radical or in an anion-cation annihilation manner can take place. After divalent reduction, lucigenin can react with singlet oxygen. All three possibilities end up in formation of the dioxetane interstate, which finally disintegrates in one excited and one ground state of N-methylacridone [70].*

To ensure that $O_2^{-\bullet}$ is eNOS-derived, the NOS-blocker L-NAME is applied to the organ bath during equilibration. A final concentration of 0.1 mM was used [71]. In order to

check for the effect of the antioxidant Tempol®, a similar incubation for at least 20 minutes is carried out with an organ bath concentration of 1 mM [72].

2.8. STATISTICS

All results are presented as arithmetic mean ± standard error, in which n indicates the numbers of experiments performed. Statistical and graphical evaluations are performed with the software Graph Pad Prism, version 4.03 (GraphPad Software, San Diego, USA). In order to check different experimental conditions, unpaired t-tests are performed. Only if parameters are determined in one individual before and after intervention, a paired t-test is used. If more than two groups had to be compared, analysis of variance (one-way ANOVA) is carried out, including a following Newman-Keuls post-test. A statistically confirmed difference is achieved by a level of significance defined as $p < 0.05$ and marked by * if $p < 0.05$, ** if $p < 0.01$ and *** if $p < 0.005$ (and # respectively), or n.s. if $p > 0.05$. Proportional relations are characterized by determination of the correlation coefficient r^2.

Dose-response curves obtained by organ bath experiments are given as the remaining vessel tension in percent of the preconstruction value. This initial value is set to 100%. The curves are compared by a two-sided analysis of variance (two-way ANOVA).

This work was published in

Suvorava T*, Pick S*, and Kojda G. (* equal contribution)
Selective impairment of blood pressure reduction by endothelial nitric oxide synthase dimer destabilization in mice.
J Hypertens 2017;35(1):76-88. journals.lww.com/jhypertension/

3. RESULTS

3.1. OVEREXPRESSION OF ENOS

3.1.1. GENOTYPING

Genotyping is carried out with primers that only detect the transgenic construct but give no amplification product in wild-type probes. Visualized on an agarose gel the band is estimated at a size of 351 base pairs. Fig. 3.1 shows an exemplary PCR result carried out with DNA obtained from mouse tail biopsies. Transgenic positive mice show a discrete band at the right size whereas transgenic negative littermates do not give a signal. According to the PCR result mice are classified to be eNOS-tg or transgenic negative littermates (eNOS-tgn) and C101A-eNOS-tg or C101A-eNOS-tgn respectively.

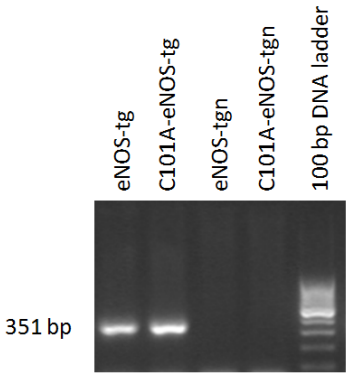

Fig. 3.1: *Results of a genotyping PCR visualized on an agarose gel. Transgenic mice show a band at 351 bp (eNOS-tg and C101A-eNOS-tg). Those animals showing no band are characterized to be transgenic negative littermates (eNOS-tgn and C101A-eNOS-tgn).*

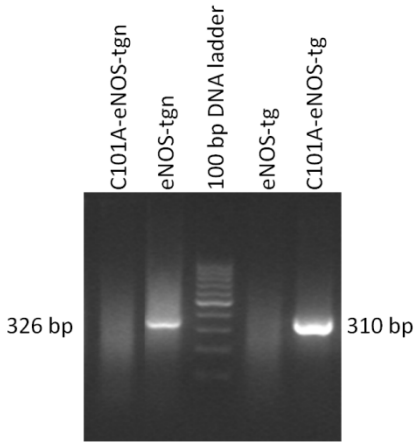

Fig. 3.2: *Results of a specific transgene genotyping PCR visualized on an agarose gel. eNOS-tg mice show a band at 326 bp for wild-type bovine eNOS and C101A-eNOS-tg mice show a band at 310 bp for C101A-mutated eNOS whereas the transgenic animals don't show a band vice-versa.*

This work was published in

Suvorava T*, Pick S*, and Kojda G. (* equal contribution)
Selective impairment of blood pressure reduction by endothelial nitric oxide synthase dimer destabilization in mice.
J Hypertens 2017;35(1):76-88. journals.lww.com/jhypertension/

word-for-word citations within the running text stand out in italic type

In order to ensure that the right mouse strains are used for experiments, a transgene-specific PCR is carried out at regular intervals. Here the native bovine eNOS gives a band at 326 bp whereas C101A-mutated eNOS shows a band at 310 bp (see fig. 3.2). Vice-versa no cross-reactivity could be detected. This ensures the specificity of the primers.

3.1.2. eNOS PROTEIN EXPRESSION

Western Blot analysis reveals the level of overexpression in aortic (50 µg total protein loaded), myocardial, lung and skeletal muscle tissue (100 µg total protein loaded) of both transgenic mouse strains. In all different kinds of tissue a significant increase as compared to C57BL/6 is detectable. Overall, there is always a significantly larger expression of eNOS in eNOS-tg than in C101A-eNOS-tg (see figs. 3.3-3.6).

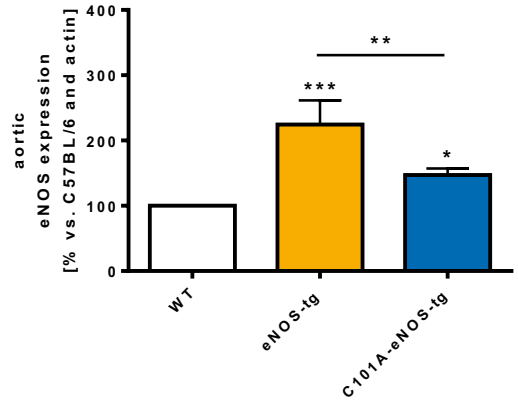

Fig. 3.3: *Evaluation of Western Blot results on aortic eNOS expression in eNOS-tg (224.6 ± 36.88%, n=6, p<0.001) and C101A-eNOS-tg (147.3 ± 9.796%, n=12, p<0.05; p<0.01 vs. eNOS-tg).*

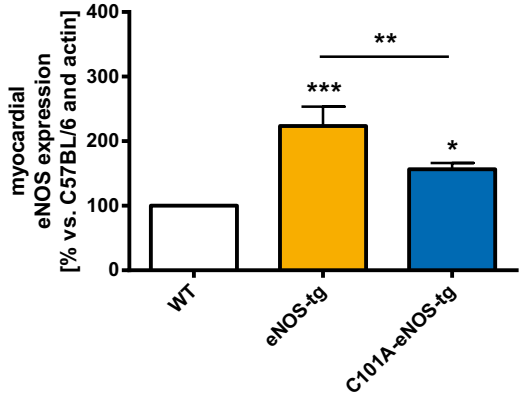

Fig. 3.4: *Evaluation of Western Blot results on myocardial eNOS expression in eNOS-tg (223.6 ± 29.74%, n=6, p<0.001) and C101A-eNOS-tg (156.5 ± 9.722%, n=10, p<0.05; p<0.01 vs. eNOS-tg).*

This work was published in

Suvorava T*, Pick S*, and Kojda G. (* equal contribution)
Selective impairment of blood pressure reduction by endothelial nitric oxide synthase dimer destabilization in mice.
J Hypertens 2017;35(1):76-88. journals.lww.com/jhypertension/

word-for-word citations within the running text stand out in italic type

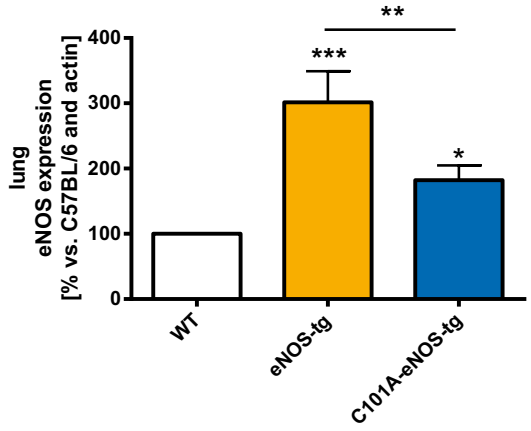

Fig. 3.5: *Evaluation of Western Blot results on lung eNOS expression in eNOS-tg (301.4 ± 47.96%, n=7, p<0.001) and C101A-eNOS-tg (172.5 ± 21.85%, n=7, p<0.05; p<0.01 vs. eNOS-tg).*

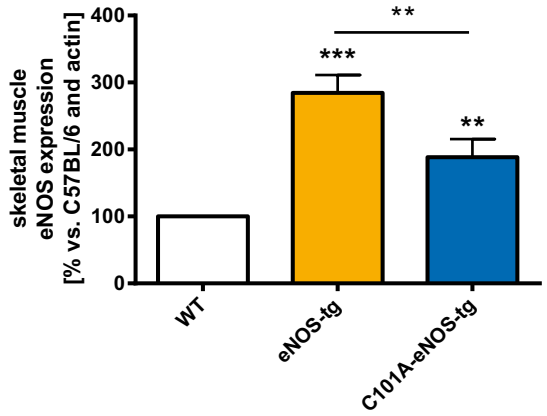

Fig. 3.6: *Evaluation of Western Blot results on skeletal muscle eNOS expression in eNOS-tg (284.3 ± 26.75%, n=6, p<0.001) and C101A-eNOS-tg (188.4 ± 26.96%, n=6, p<0.01, p=0.0128; p<0.01 vs. eNOS-tg).*

3.1.3. eNOS DIMER FORMATION

Loading 100 µg total protein of aortic samples of C101A-eNOS-tg on a native gel reveals a larger monomer signal than in transgenic negative littermates whereas the dimer signal remains nearly unchanged (see fig. 3.7). This indicates that the introduced mutated eNOS (see 2.2.1) in C101A-eNOS-tg mice has been successfully destabilized.

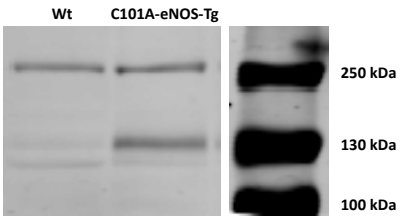

Fig. 3.7: *Representative native Western Blot showing increased aortic eNOS-monomer formation at 142 kDa in aortic tissue of C101A-eNOS-tg as compared to a transgenic negative littermate.*

This work was published in

Suvorava T*, Pick S*, and Kojda G. (* equal contribution)
Selective impairment of blood pressure reduction by endothelial nitric oxide synthase dimer destabilization in mice.
J Hypertens 2017;35(1):76-88. journals.lww.com/jhypertension/

word-for-word citations within the running text stand out in italic type

3.1.4. eNOS mRNA expression

Both introduced eNOS variants in the transgenic animal strains are of bovine origin. In order to determine the effect on murine eNOS expression a real-time PCR is carried out with aortic tissue by applying specific primers for either murine or bovine eNOS. Indeed, the additionally introduced bovine eNOS has an effect on the expression of native eNOS and significantly reduces the murine eNOS expression as seen in fig. 3.8.

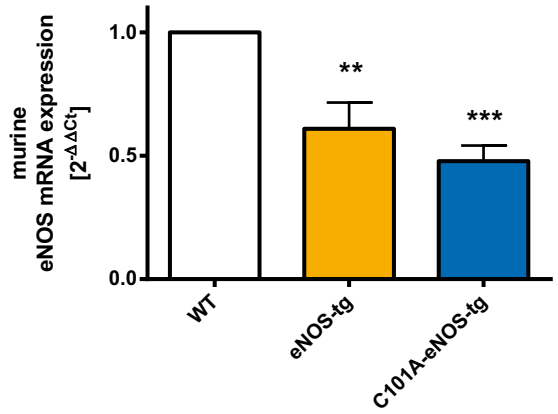

Fig. 3.8: *Evaluation of real-time PCR results on aortic murine eNOS expression in eNOS-tg (0.6090 ± 0.1002, n=6, p<0.01 vs. C57BL/6) and C101A-eNOS-tg (0.4777 ± 0.06365, n=6, p<0.001 vs. C57BL/6; n.s. vs. eNOS-tg).*

As expected, bovine eNOS in is not detectable in C57BL/6, giving further evidence for the specificity of the bovine primers. In accordance to those results observed by Western Blot analysis (see 3.1.2) mRNA expression of bovine eNOS is much larger in eNOS-tg than in C101A-eNOS-tg (fig. 3.9).

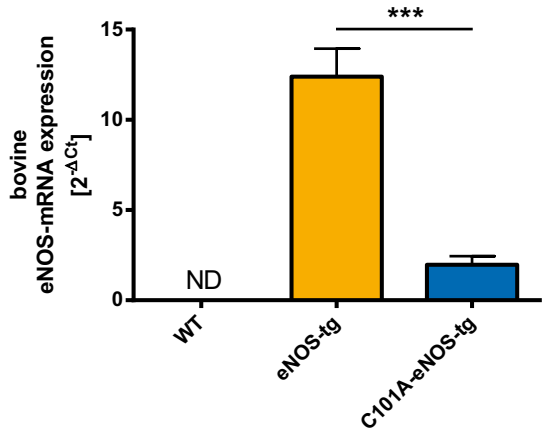

Fig. 3.9: *Evaluation of real-time PCR results on aortic bovine eNOS expression in eNOS-tg (12.40 ± 1.549, n=6) and C101A-eNOS-tg (1.975 ± 0.4677, n=6, p<0.001 vs. eNOS-tg). No expression is detectable in C57BL/6 (ND).*

This work was published in

Suvorava T*, Pick S*, and Kojda G. (* equal contribution)
Selective impairment of blood pressure reduction by endothelial nitric oxide synthase dimer destabilization in mice.
J Hypertens 2017;35(1):76-88. journals.lww.com/jhypertension/

word-for-word citations within the running text stand out in italic type

3.2. OXIDATIVE STRESS

3.2.1. SUPEROXIDE ANION RADICAL

Detection of $O_2^{-\bullet}$ by lucigenin-enhanced chemiluminescence assay is carried out with aortic, myocardial and skeletal muscle tissue (see figs. 3.10-3.12). Whereas in eNOS-tg there is no difference as compared to C57BL/6, the introduction of the destabilized eNOS variant significantly increases the level of $O_2^{-\bullet}$ in C101A-eNOS-tg. Application of the NOS-inhibitor L-NAME during calibration completely inhibits this increase indicating mutated eNOS being a source of ROS.

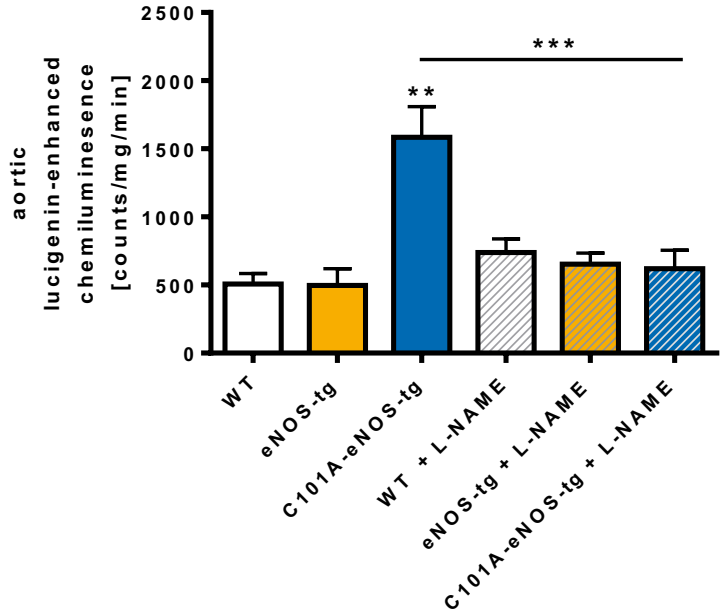

Fig. 3.10: *Evaluation of lucigenin assay results on aortic $O_2^{-\bullet}$ production in C57BL/6 (508.2 ± 76.33 counts/mg/min, n=5), eNOS-tg (496.9 ± 112.9 counts/mg/min, n=5, p>0.05 vs. C57BL/6) and C101A-eNOS-tg (1584 ± 225.2 counts/mg/min, n=5, p<0.001 vs. C57BL/6 and eNOS-tg). Incubation with L-NAME blunts the difference indicating $O_2^{-\bullet}$ being produced by NOS: C57BL/6 (739.0 ± 99.77 counts/mg/min, n=5), eNOS-tg (652.4 ± 82.41 counts/mg/min, n=5) and C101A-eNOS-tg (619.2 ± 135.0 counts/mg/min, n=5, p<0.001 vs. C101A-eNOS-tg).*

This work was published in

Suvorava T*, Pick S*, and Kojda G. (* equal contribution)
Selective impairment of blood pressure reduction by endothelial nitric oxide synthase dimer destabilization in mice.
J Hypertens 2017;35(1):76-88. journals.lww.com/jhypertension/

word-for-word citations within the running text stand out in italic type

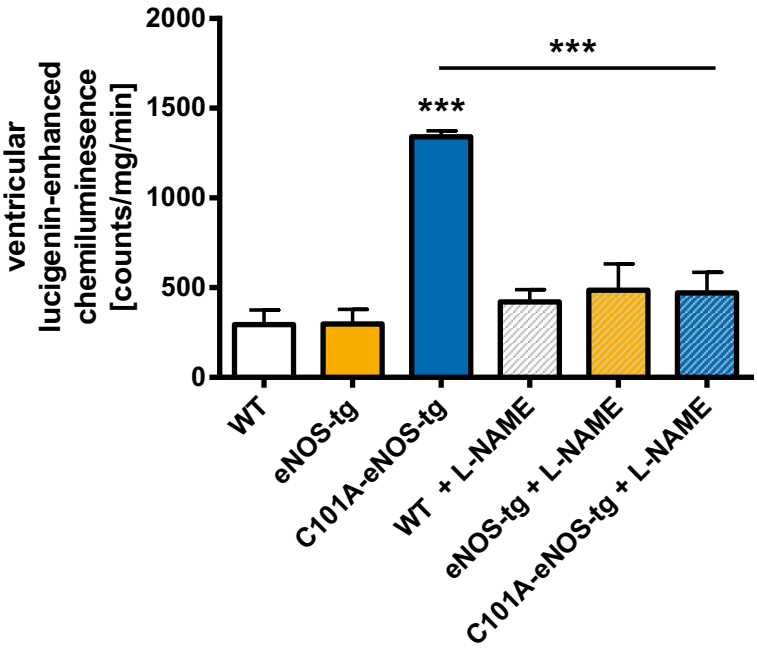

Fig. 3.11: *Evaluation of lucigenin assay results on ventricular $O_2^{-\bullet}$ production in C57BL/6 (294.8 ± 81.05 counts/mg/min, n=5), eNOS-tg (297.3 ± 82.05 counts/mg/min, n=5, p>0.05 vs. C57BL/6) and C101A-eNOS-tg (1341 ± 34.05 counts/mg/min, n=5, p<0.001 vs. C57BL/6 and eNOS-tg). Incubation with L-NAME blunts the difference indicating $O_2^{-\bullet}$ being produced by NOS: C57BL/6 (421.5 ± 67.27 counts/mg/min, n=5), eNOS-tg (470.7 ± 115.3 counts/mg/min, n=5) and C101A-eNOS-tg (486.1 ± 145.8 counts/mg/min, n=5, p<0.001 vs. C101A-eNOS-tg).*

This work was published in

Suvorava T*, Pick S*, and Kojda G. (* equal contribution)
Selective impairment of blood pressure reduction by endothelial nitric oxide synthase dimer destabilization in mice.
J Hypertens 2017;35(1):76-88. journals.lww.com/jhypertension/

word-for-word citations within the running text stand out in italic type

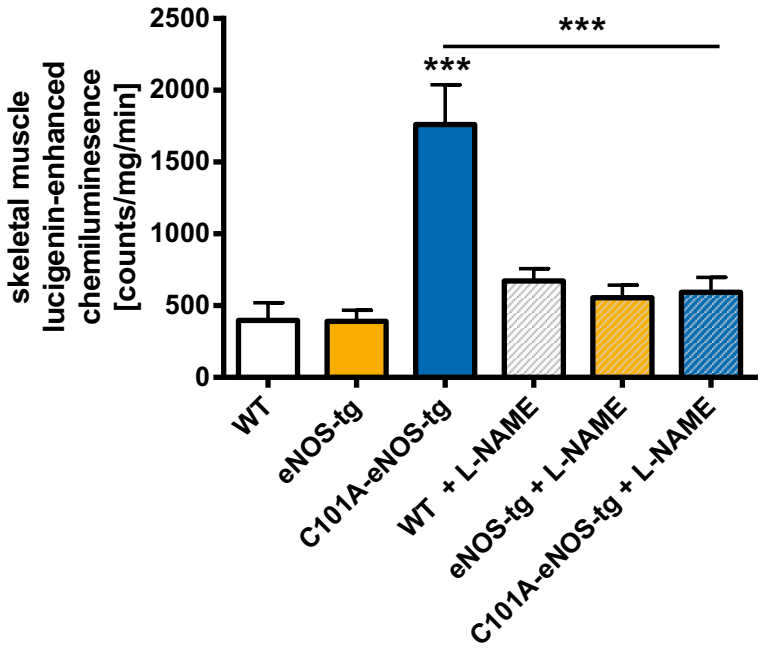

Fig. 3.12: *Evaluation of lucigenin assay results on skeletal muscle $O_2^{-\bullet}$ production in C57BL/6 (396.3 ± 124.3 counts/mg/min, n=5), eNOS-tg (390.2 ± 77.46 counts/mg/min, n=5, p>0.05 vs. C57BL/6) and C101A-eNOS-tg (1761 ± 277.5 counts/mg/min, n=5, p<0.001 vs. C57BL/6 and eNOS-tg). Incubation with L-NAME blunts the difference indicating $O_2^{-\bullet}$ being produced by NOS: C57BL/6 (671.0 ± 85.95 counts/mg/min, n=5), eNOS-tg (556.2 ± 86.03 counts/mg/min, n=5) and C101A-eNOS-tg (593.3 ± 104.6 counts/mg/min, n=5, p<0.001 vs. C101A-eNOS-tg).*

3.2.2. GLUTATHIONYLATED eNOS

Immunoprecipitation of aortic, myocardial, lung and skeletal muscle eNOS and subsequent detection with an antibody against S-glutathionylated protein reveals increased S-glutathionylation of eNOS in C101A-eNOS-tg as compared to transgenic negative littermates, but no difference in eNOS-tg (see figs. 3.13-3.16). This is regarded as a hint for successful destabilization, achieved by the replacement of Cys 101 by Ala, as S-glutathionylation is considered to be a marker for eNOS 'uncoupling' [73].

This work was published in

Suvorava T*, Pick S*, and Kojda G. (* equal contribution)
Selective impairment of blood pressure reduction by endothelial nitric oxide synthase dimer destabilization in mice.
J Hypertens 2017;35(1):76-88. journals.lww.com/jhypertension/

word-for-word citations within the running text stand out in italic type

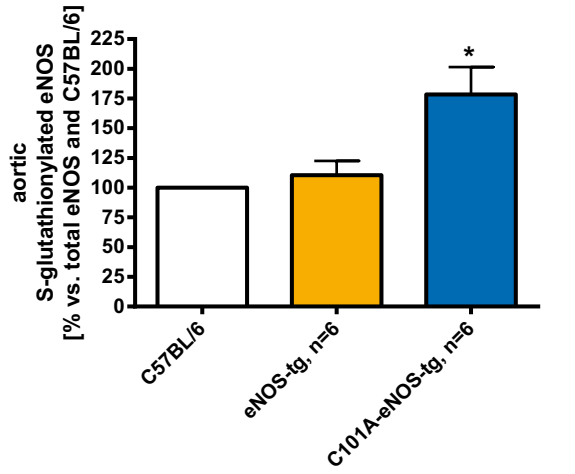

Fig. 3.13: *Evaluation of fluorescence results on immunoprecipitated aortic S-glutathionylated eNOS in eNOS-tg (110.5 ± 11.98%, n=6, n.s.) and C101A-eNOS-tg (178.4 ± 23.12%, n=6, p=0.0194).*

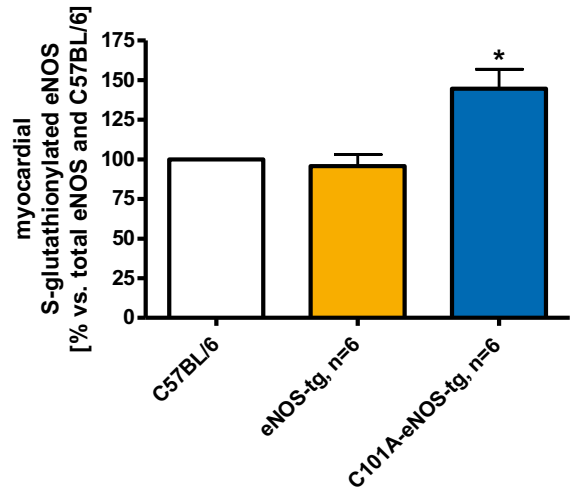

Fig. 3.14: *Evaluation of fluorescence results on immunoprecipitated myocardial S-glutathionylated eNOS in eNOS-tg (95.71 ± 7.272%, n=6, n.s.) and C101A-eNOS-tg (144.6 ± 12.29%, n=6, p=0.0151).*

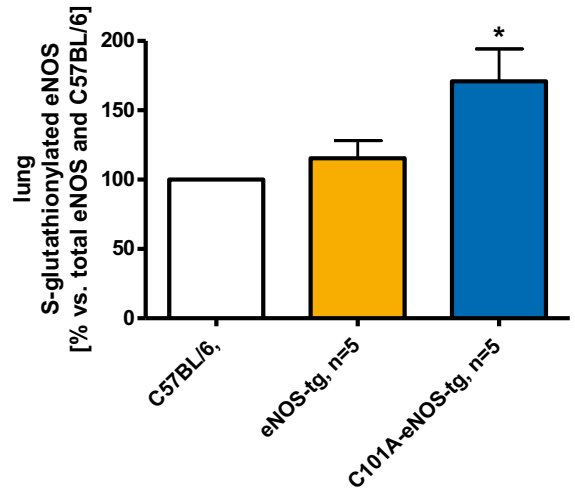

Fig. 3.15: *Evaluation of fluorescence results on immunoprecipitated lung S-glutathionylated eNOS in eNOS-tg (115.4 ± 12.60%, n=5, n.s.) and C101A-eNOS-tg (171.0 ± 23.26%, n=5, p=0.0194).*

This work was published in

Suvorava T*, Pick S*, and Kojda G. (* equal contribution)
Selective impairment of blood pressure reduction by endothelial nitric oxide synthase dimer destabilization in mice.
J Hypertens 2017;35(1):76-88. journals.lww.com/jhypertension/

word-for-word citations within the running text stand out in italic type

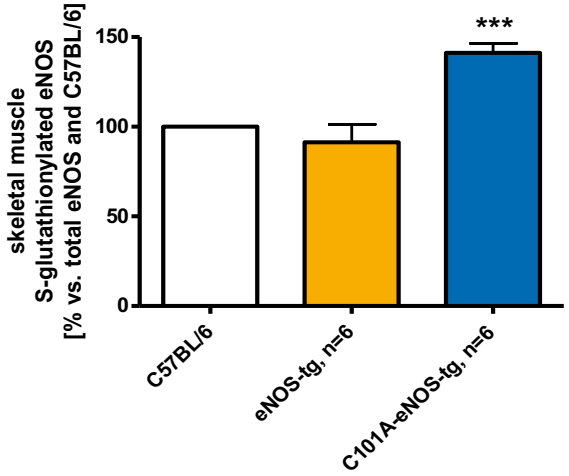

Fig. 3.16: *Evaluation of fluorescence results on immunoprecipitated skeletal muscle S-glutathionylated eNOS in eNOS-tg (91.32 ± 9.969%, n=6, n.s.) and C101A-eNOS-tg (141.2 ± 5.207%, n=6, p=0.0005).*

3.2.3. PROTEIN TYROSINE-NITRATION

Upon formation of peroxynitrite out of $O_2^{-\bullet}$ and nitric oxide, proteins can undergo nitration by a nucleophilic aromatic substitution at a tyrosine residue giving 3-nitrotyrosine. This is considered to be a marker for nitrosative stress [74]. As expected, 3-nitrotyrosine levels are increased in aortic (50 µg total protein loaded), myocardial, lung and skeletal muscle tissue (100 µg total protein loaded) of C101A-eNOS-tg as compared to their transgenic negative littermates, and not in eNOS-tg (see figs. 3.17-3.20).

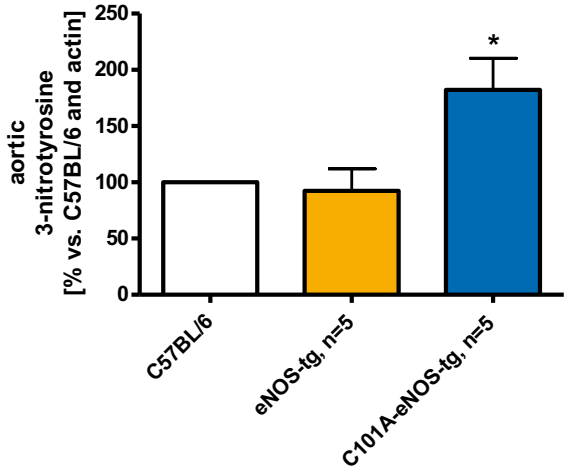

Fig. 3.17: *Evaluation of Western Blot results on aortic 3-nitrotyrosine in eNOS-tg (92.44 ± 19.56%, n=5, n.s.) and C101A-eNOS-tg (182.2 ± 28.20%, n=5, p=0.0435).*

This work was published in

Suvorava T*, Pick S*, and Kojda G. (* equal contribution)
Selective impairment of blood pressure reduction by endothelial nitric oxide synthase dimer destabilization in mice.
J Hypertens 2017;35(1):76-88. journals.lww.com/jhypertension/

word-for-word citations within the running text stand out in italic type

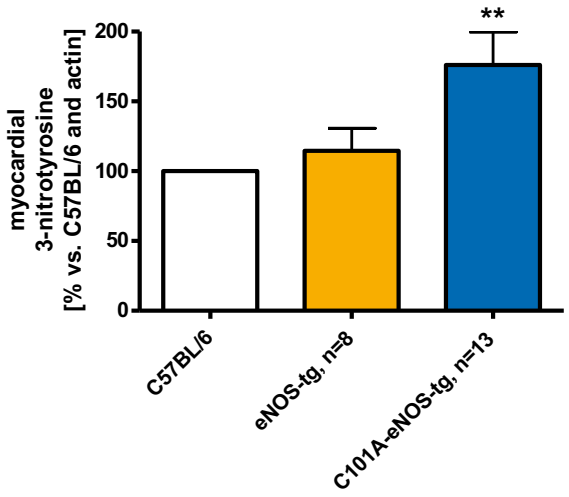

Fig. 3.18: *Evaluation of Western Blot results on myocardial 3-nitrotyrosine in eNOS-tg (114.6 ± 16.24%, n=8, n.s.) and C101A-eNOS-tg (176.1 ± 23.74%, n=5, p=0.0076).*

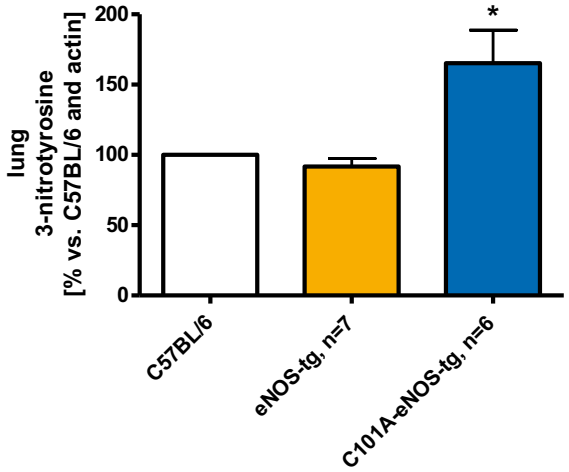

Fig. 3.19: *Evaluation of Western Blot results on lung 3-nitrotyrosine in eNOS-tg (91.78 ± 5.574%, n=7, n.s.) and C101A-eNOS-tg (165.2 ± 23.5%, n=6, p=0.0391).*

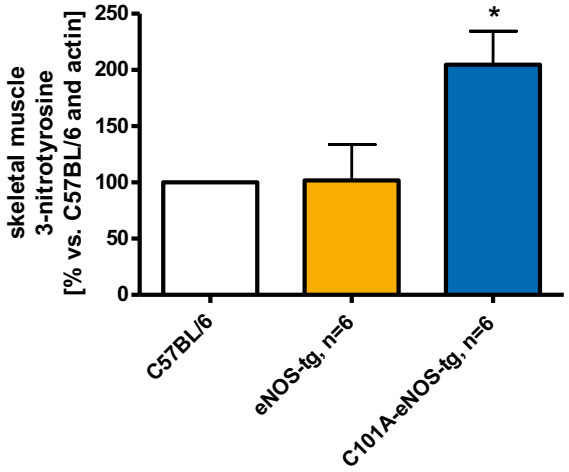

Fig. 3.20: *Evaluation of Western Blot results on skeletal muscle 3-nitrotyrosine in eNOS-tg (101.9 ± 31.77%, n=6, n.s.) and C101A-eNOS-tg (204.6 ± 29.76%, n=6, p=0.0170).*

This work was published in

Suvorava T*, Pick S*, and Kojda G. (* equal contribution)
Selective impairment of blood pressure reduction by endothelial nitric oxide synthase dimer destabilization in mice.
J Hypertens 2017;35(1):76-88. journals.lww.com/jhypertension/

word-for-word citations within the running text stand out in italic type

3.2.4. PHOSPHORYLATION OF eNOS AT SER1176/9

Phosphorylation of eNOS at Ser1176/9 is connected to the activity of eNOS, i.e. the production of nitric oxide or, in case of 'uncoupling', $O_2^{-\bullet}$ respectively. In C101A-eNOS-tg an augmentation in phosphorylation at Ser1176/9 is detectable after immunoprecipitation of eNOS, whereas in eNOS-tg there is no effect as compared to C57BL/6 (see figs. 3.21-3.24). Experiments are performed with aortic, myocardial, lung and skeletal muscle tissue.

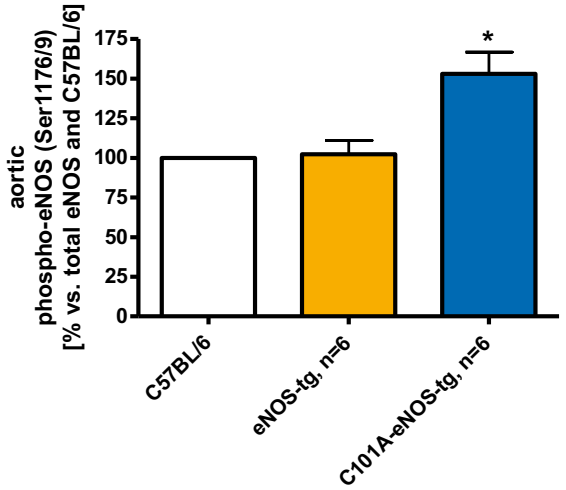

Fig. 3.21: *Evaluation of fluorescence results on immunoprecipitated aortic phosphorylated eNOS at Ser1176/9 in eNOS-tg (102.3 ± 8.822%, n=6, n.s.) and C101A-eNOS-tg (153.1 ± 13.75%, n=6, p=0.0119).*

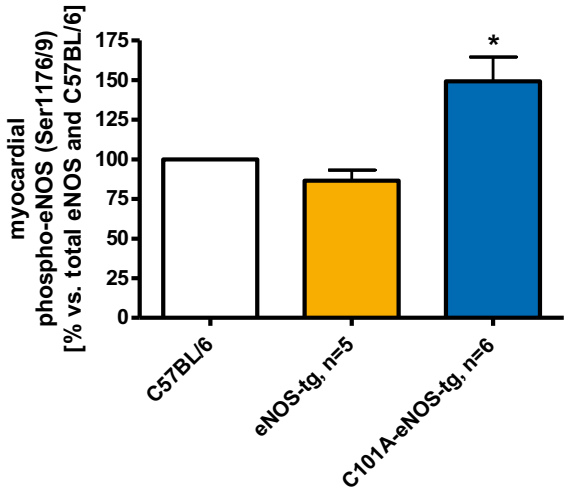

Fig. 3.22: *Evaluation of fluorescence results on immunoprecipitated myocardial phosphorylated eNOS at Ser1176/9 in eNOS-tg (86.60 ± 6.634%, n=5, n.s.) and C101A-eNOS-tg (149.3 ± 15.36%, n=6, p=0.0238).*

This work was published in

Suvorava T*, Pick S*, and Kojda G. (* equal contribution)
Selective impairment of blood pressure reduction by endothelial nitric oxide synthase dimer destabilization in mice.
J Hypertens 2017;35(1):76-88. journals.lww.com/jhypertension/

word-for-word citations within the running text stand out in italic type

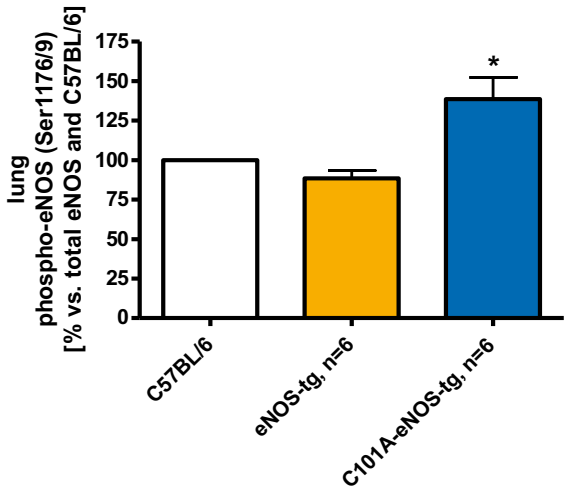

Fig. 3.23: *Evaluation of fluorescence results on immunoprecipitated lung phosphorylated eNOS at Ser1176/9 in eNOS-tg (88.45 ± 4.881%, n=6, n.s.) and C101A-eNOS-tg (138.6 ± 13.63%, n=6, p=0.0365).*

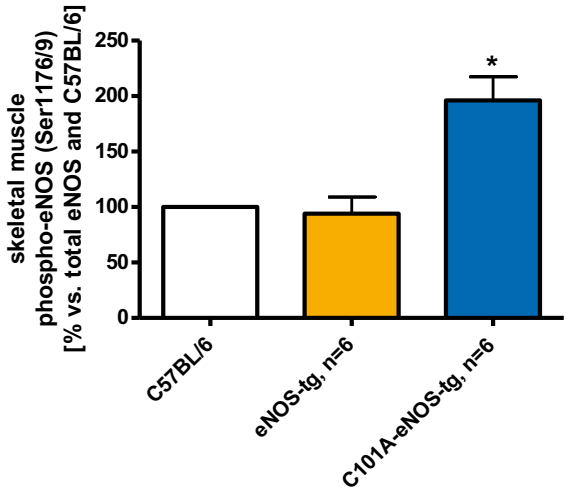

Fig. 3.24: *Evaluation of fluorescence results on immunoprecipitated skeletal muscle phosphorylated eNOS at Ser1176/9 in eNOS-tg (94.03 ± 15.05%, n=6, n.s.) and C101A-eNOS-tg (196.2 ± 21.23%, n=6, p=0.0062).*

3.2.4.1. PHOSPHORYLATION OF AMPK AT THR172

Phosphorylation of eNOS at Ser1176/9 can be either driven by AMPKα [75] or Akt [76,77] which are both themselves phosphorylated upon activation. AMPKα is phosphorylated at Thr472 in stages of oxidative stress, mainly by peroxynitrite [78]. Indeed, in C101A-eNOS-tg an increased phosphorylation can be detected whereas total AMPKα expression is not changed (see figs. 3.25-3.28). Experiments are performed with 50 µg of aortic and 100 µg of skeletal muscle tissue total protein.

This work was published in

Suvorava T*, Pick S*, and Kojda G. (* equal contribution)
Selective impairment of blood pressure reduction by endothelial nitric oxide synthase dimer destabilization in mice.
J Hypertens 2017;35(1):76-88. journals.lww.com/jhypertension/

word-for-word citations within the running text stand out in italic type

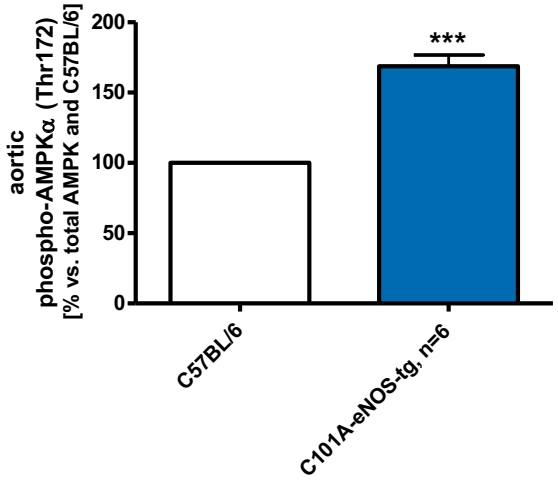

Fig. 3.25: *Evaluation of Western Blot results on aortic AMPKα phosphorylation at Thr172 in C101A-eNOS-tg (168.7 ± 7.982%, n=6, p=0.0003).*

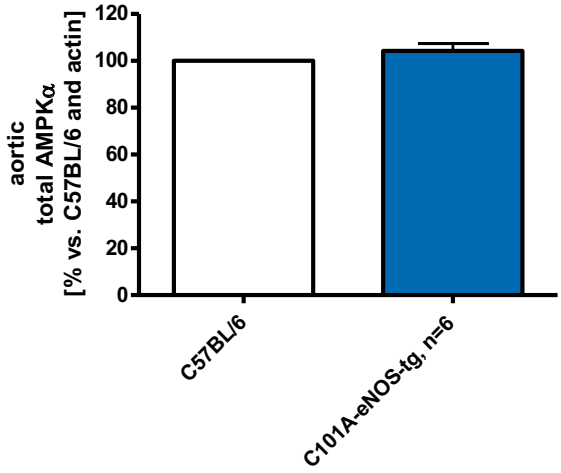

Fig. 3.26: *Evaluation of Western Blot results on aortic AMPKα expression in C101A-eNOS-tg (104.2 ± 3.154%, n=6) showed no difference.*

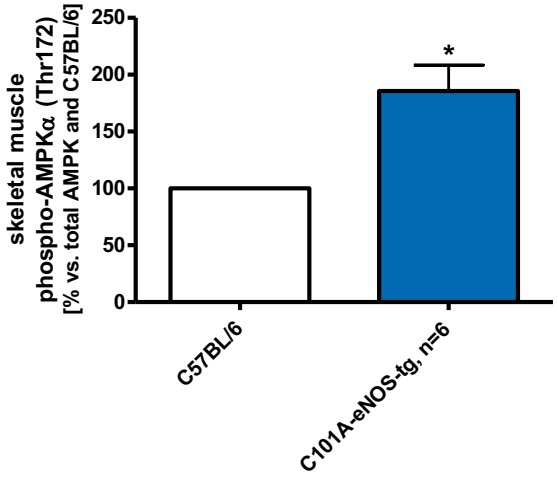

Fig. 3.27: *Evaluation of Western Blot results on skeletal muscle AMPKα phosphorylation at Thr172 in C101A-eNOS-tg (185.6 ± 22.79%, n=6, p=0.0132).*

This work was published in

Suvorava T*, Pick S*, and Kojda G. (* equal contribution)
Selective impairment of blood pressure reduction by endothelial nitric oxide synthase dimer destabilization in mice.
J Hypertens 2017;35(1):76-88. journals.lww.com/jhypertension/

word-for-word citations within the running text stand out in italic type

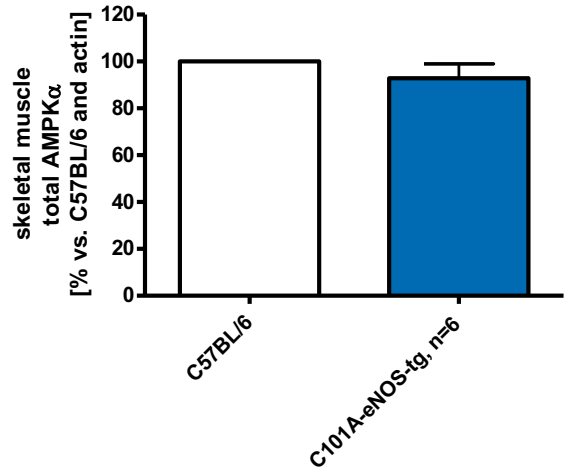

Fig. 3.28: *Evaluation of Western Blot results on skeletal muscle AMPKα expression in C101A-eNOS-tg (92.87 ± 6.077%, n=6) showed no difference.*

3.2.4.2. PHOSPHORYLATION OF AKT AT SER473

No changes, neither in phosphorylation of Akt at Ser473 nor in total expression are detectable in aortic (50 µg total protein loaded) or skeletal muscle tissue (100 µg total protein loaded) of C101A-eNOS-tg as compared to transgenic negative littermates (see figs. 3.29-3.32). This indicates that increased phosphorylation of eNOS in these transgenic animals is not driven by activation of Akt but of AMPKα (see 3.2.4.1).

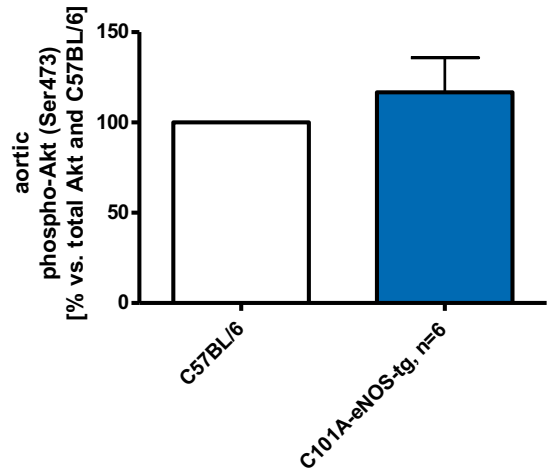

Fig. 3.29: *Evaluation of Western Blot results on aortic Akt phosphorylation at Ser473 in C101A-eNOS-tg (116.7 ± 19.10%, n=6, n.s.).*

This work was published in

Suvorava T*, Pick S*, and Kojda G. (* equal contribution)
Selective impairment of blood pressure reduction by endothelial nitric oxide synthase dimer destabilization in mice.
J Hypertens 2017;35(1):76-88. journals.lww.com/jhypertension/

word-for-word citations within the running text stand out in italic type

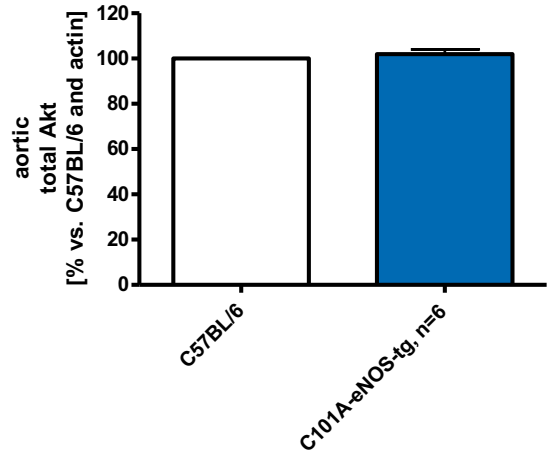

Fig. 3.30: *Evaluation of Western Blot results on aortic Akt expression in C101A-eNOS-tg (101.9 ± 2.080%, n=6) showed no difference.*

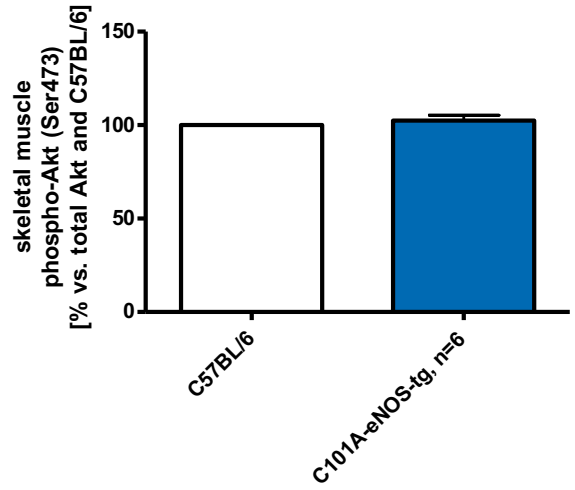

Fig. 3.31: *Evaluation of Western Blot results on skeletal muscle Akt phosphorylation at Ser473 in C101A-eNOS-tg (102.4 ± 2.923%, n=6, n.s.).*

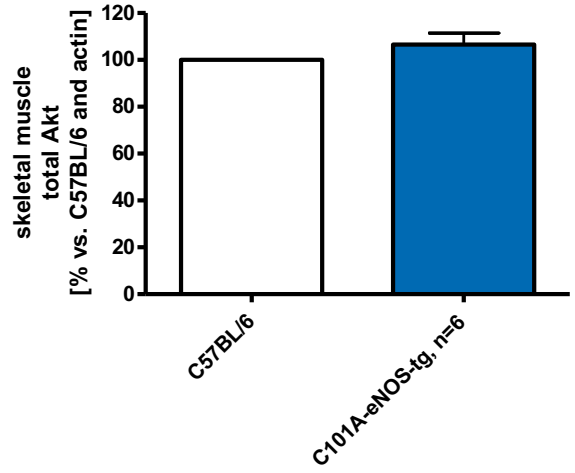

Fig. 3.32: *Evaluation of Western Blot results on skeletal muscle Akt expression in C101A-eNOS-tg (106.6 ± 4.877%, n=6) showed no difference.*

This work was published in

Suvorava T*, Pick S*, and Kojda G. (* equal contribution)
Selective impairment of blood pressure reduction by endothelial nitric oxide synthase dimer destabilization in mice.
J Hypertens 2017;35(1):76-88. journals.lww.com/jhypertension/

word-for-word citations within the running text stand out in italic type

3.3. FUNCTIONAL STUDIES

3.3.1. ENDOTHELIUM-DEPENDENT RELAXATION

Functional studies on isolated mouse aorta are performed using organ bath equipment. Here, endothelium-dependent relaxation after preconstriction with 0.2 µM phenylephrine is determined by cumulative doses of acetylcholine (1 nM-10 µM). Augmented eNOS expression has no effect on acetylcholine induced relaxation, neither by native bovine eNOS in eNOS-tg (see fig. 3.33), nor by the destabilized eNOS variant in C101A-eNOS-tg (see fig. 3.34).

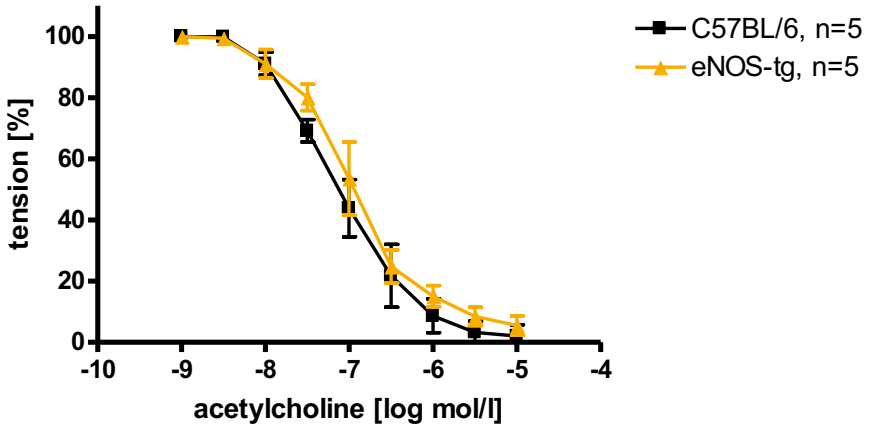

Fig. 3.33: *Endothelium-dependent relaxation determined by cumulative doses of acetylcholine after preconstriction with 0.2 µM phenylephrine reveales no difference in eNOS-tg as compared to C57BL/6.*

This work was published in

Suvorava T*, Pick S*, and Kojda G. (* equal contribution)
Selective impairment of blood pressure reduction by endothelial nitric oxide synthase dimer destabilization in mice.
J Hypertens 2017;35(1):76-88. journals.lww.com/jhypertension/

word-for-word citations within the running text stand out in italic type

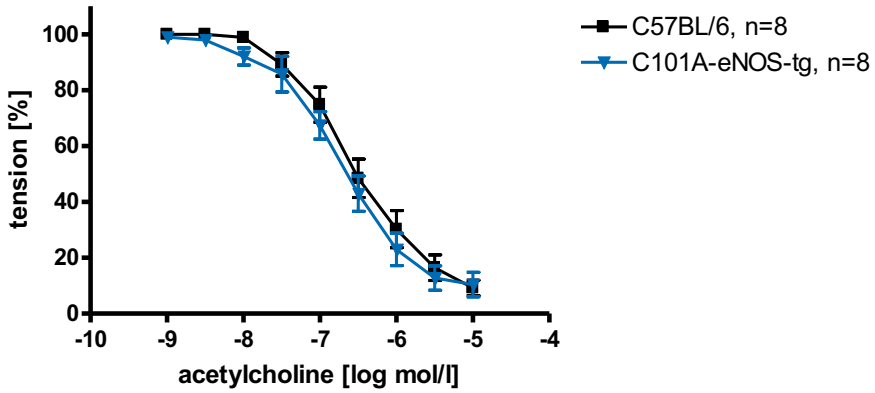

Fig. 3.34: *Endothelium-dependent relaxation determined by cumulative doses of acetylcholine after preconstriction with 0.2 µM phenylephrine reveales no difference in C101A-eNOS-tg as compared to C57BL/6.*

3.3.2. ENDOTHELIUM-INDEPENDENT RELAXATION

Responses to exogenous NO are achieved by cumulative doses of the NO donor SNAP (1 nM-10 mM) after preconstiction with 0.2 µM phenylephrine. Similar to the results obtained by endogenous NO release by acetylcholine (see 3.3.1), here no effect is obtainable either in both transgenic strains (see figs. 3.35-3.36).

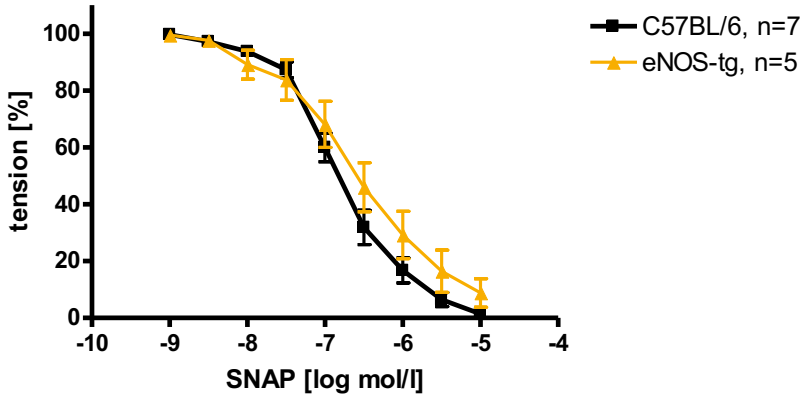

Fig. 3.35: *Relaxation to cumulative doses of the NO-donor SNAP after preconstriction with 0.2 µM phenylephrine reveals no difference in eNOS-tg as compared to C57BL/6.*

This work was published in

Suvorava T*, Pick S*, and Kojda G. (* equal contribution)
Selective impairment of blood pressure reduction by endothelial nitric oxide synthase dimer destabilization in mice.
J Hypertens 2017;35(1):76-88. journals.lww.com/jhypertension/

word-for-word citations within the running text stand out in italic type

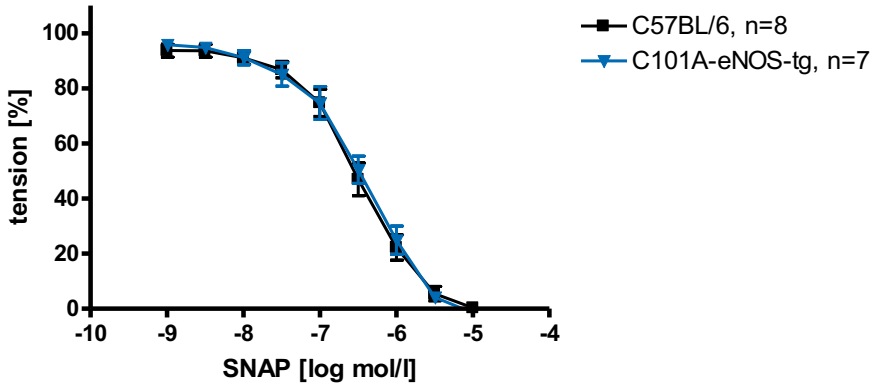

Fig. 3.36: *Relaxation to cumulative doses of the NO-donor SNAP after preconstriction with 0.2 µM phenylephrine reveals no difference in C101A-eNOS-tg as compared to C57BL/6.*

3.3.3. BLOOD PRESSURE AND HEART RATE

Systolic blood pressure and heart rate are measured by tail-cuff method in awake mice over a period of six days. As expected and due to increased endogenous NO bioavailability, a reduction in blood pressure is determined in eNOS-tg mice (see fig. 3.37). Heart rate is measured simultaneously and not changed in these animals (see fig. 3.38).

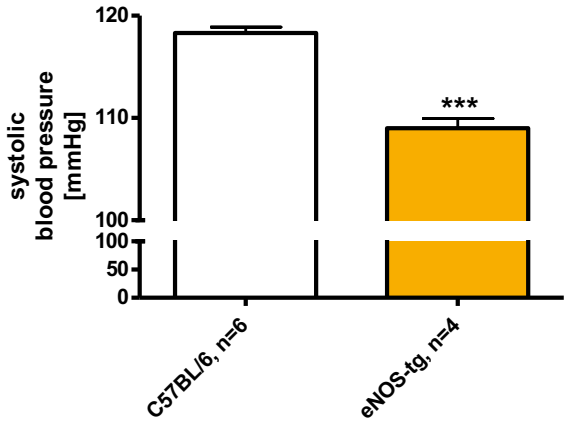

Fig. 3.37: *Blood pressure results in eNOS-tg (109.0 ± 0.9500 mmHg, n=4, p<0.0001) and their transgenic negative littermates (C57BL/6: 118.3 ± 0.5797 mmHg, n=6).*

This work was published in

Suvorava T*, Pick S*, and Kojda G. (* equal contribution)
Selective impairment of blood pressure reduction by endothelial nitric oxide synthase dimer destabilization in mice.
J Hypertens 2017;35(1):76-88. journals.lww.com/jhypertension/

word-for-word citations within the running text stand out in italic type

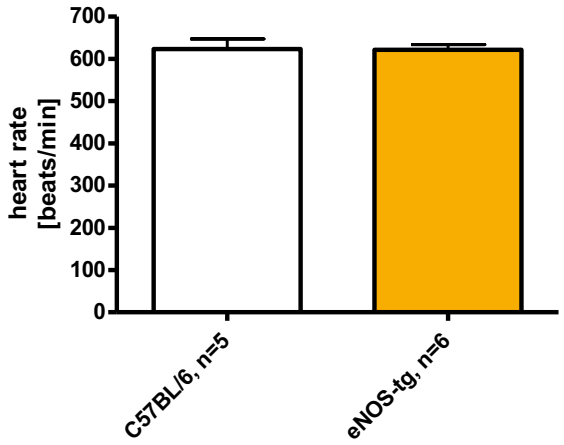

Fig. 3.38: *Heart rate results in eNOS-tg (621.3 ± 12.21 beats per minute, n=6) and their transgenic negative littermates (C57BL/6: 623.2 ±23.87 beats per minute, n=5) showing no difference.*

Surprisingly, and notwithstanding increased eNOS expression, in C101A-eNOS-tg no changes are determinable, neither for blood pressure (see fig. 3.39), nor for heart rate (see fig. 3.40). This may indicate that the destabilized eNOS variant is not producing enough endogenous NO to lower blood pressure.

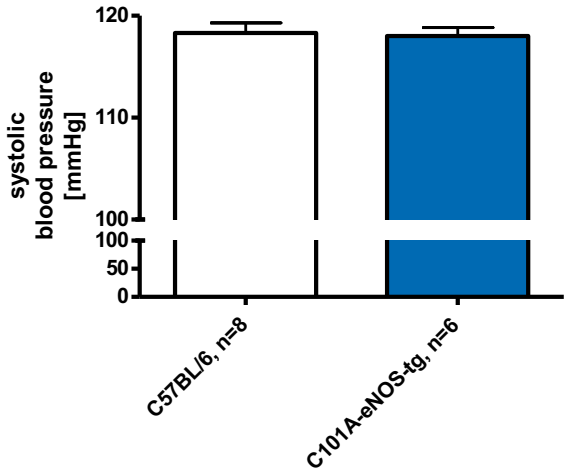

Fig. 3.39: *Blood pressure results in C101A-eNOS-tg (118.0 ± 0.8447 mmHg, n=6) and their transgenic negative littermates (C57BL/6: 118.3 ± 0.9899 mmHg, n=8) showing no difference.*

This work was published in

Suvorava T*, Pick S*, and Kojda G. (* equal contribution)
Selective impairment of blood pressure reduction by endothelial nitric oxide synthase dimer destabilization in mice.
J Hypertens 2017;35(1):76-88. journals.lww.com/jhypertension/

word-for-word citations within the running text stand out in italic type

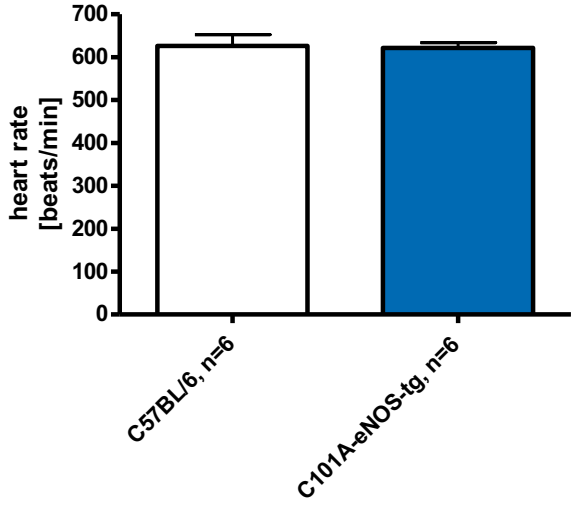

Fig. 3.40: *Heart rate results in C101A-eNOS-tg (621.6 ± 11.99 beats per minute, n=6) and their transgenic negative littermates (C57BL/6: 626.5 ± 26.10 beats per minute, n=6) showing no difference.*

3.3.4. PHOSPHORYLATION OF VASP AT SER239

In order to seek for NO/cGMP-pathway activation [79] and thus for NO bioavailability in all transgenic animal strains used, phosphorylation of VASP at Ser239 is measured by Western Blot analysis. In figs. 3.41-3.44 the phosphorylation relative to total VASP expression is shown for aortic (50 µg total protein loaded), myocardial, lung and skeletal muscle tissue (100 µg total protein loaded) in eNOS-tg and C101A-eNOS-tg.

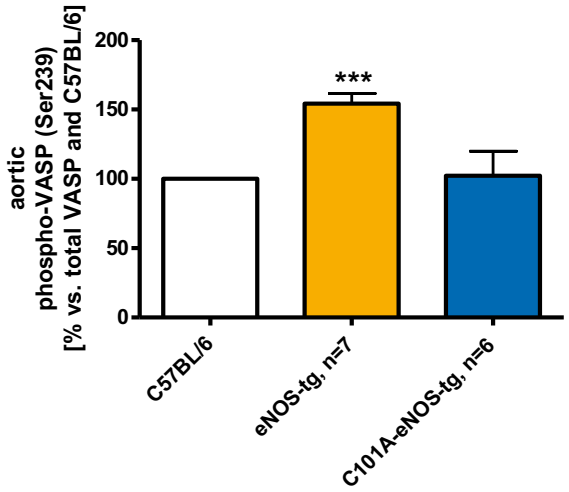

Fig. 3.41: *Evaluation of Western Blot results on aortic VASP phosphorylation at Ser239 in eNOS-tg (153.3 ± 7.276%, n=7, p=0.0003) and C101A-eNOS-tg (102.2 ± 17.69%, n=6, n.s.).*

This work was published in

Suvorava T*, Pick S*, and Kojda G. (* equal contribution)
Selective impairment of blood pressure reduction by endothelial nitric oxide synthase dimer destabilization in mice.
J Hypertens 2017;35(1):76-88. journals.lww.com/jhypertension/

word-for-word citations within the running text stand out in italic type

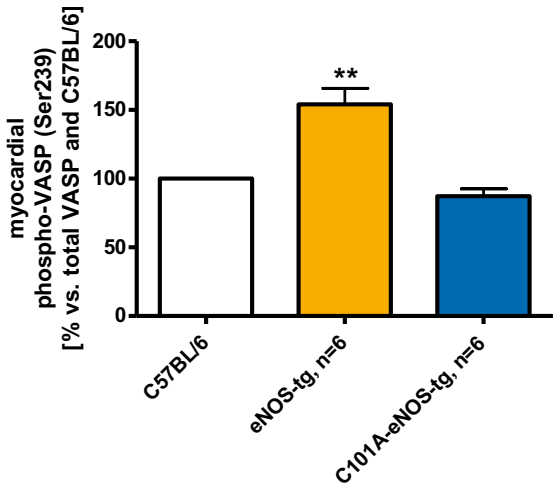

Fig. 3.42: *Evaluation of Western Blot results on myocardial VASP phosphorylation at Ser239 in eNOS-tg (154.2 ± 11.6%, n=7, p=0.0055) and C101A-eNOS-tg (87.19 ± 5.337%, n=6, n.s.).*

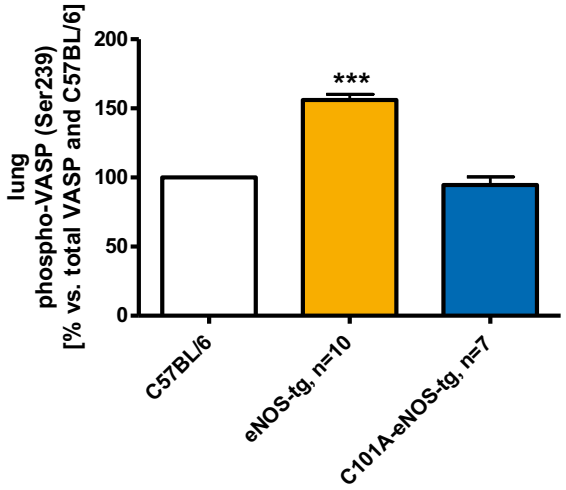

Fig. 3.43: *Evaluation of Western Blot results on lung VASP phosphorylation at Ser239 in eNOS-tg (156.1 ± 4.069%, n=10, p<0.0001) and C101A-eNOS-tg (94.56 ± 5.786%, n=7, n.s.).*

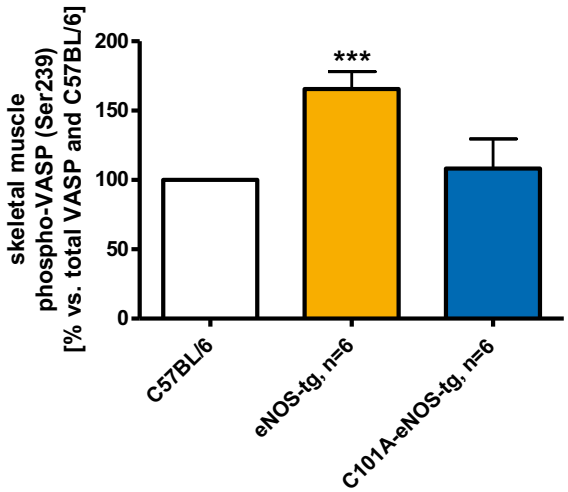

Fig. 3.44: *Evaluation of Western Blot results on skeletal muscle VASP phosphorylation at Ser239 in eNOS-tg (165.6 ± 12.41%, n=6, p=0.0032) and C101A-eNOS-tg (108.3 ± 21.34%, n=6, n.s.).*

This work was published in

Suvorava T*, Pick S*, and Kojda G. (* equal contribution)
Selective impairment of blood pressure reduction by endothelial nitric oxide synthase dimer destabilization in mice.
J Hypertens 2017;35(1):76-88. journals.lww.com/jhypertension/

word-for-word citations within the running text stand out in italic type

3.3.5. ecSOD EXPRESSION

As NO is an important mediator in its regulation [80], ecSOD expression is determined in both transgenic animal strains by Western Blot analysis. Experiments are done with 50 µg total protein loaded of aortic, and 100 µg of myocardial, lung and skeletal muscle tissue.

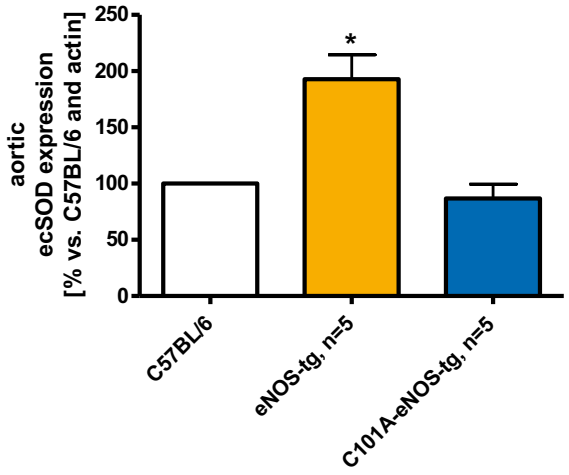

Fig. 3.45: *Evaluation of Western Blot results on aortic ecSOD expression in eNOS-tg (192.8 ± 21.68%, n=5, p=0.0128) and C101A-eNOS-tg (86.76 ± 12.79%, n=5, n.s.).*

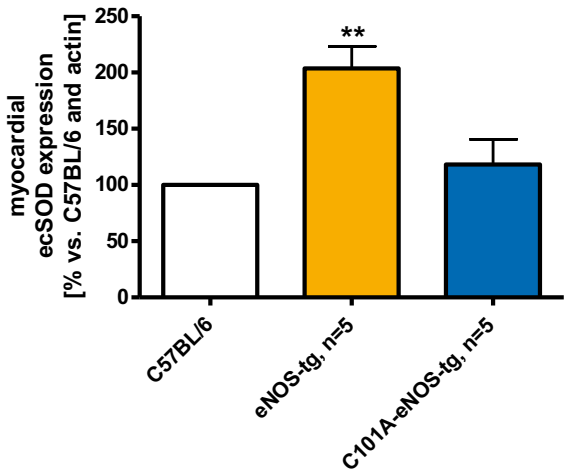

Fig. 3.46: *Evaluation of Western Blot results on myocardial ecSOD expression in eNOS-tg (203.6 ± 19.63%, n=5, p=0.0033) and C101A-eNOS-tg (86.76 ± 12.79%, n=5, n.s.).*

This work was published in

Suvorava T*, Pick S*, and Kojda G. (* equal contribution)
Selective impairment of blood pressure reduction by endothelial nitric oxide synthase dimer destabilization in mice.
J Hypertens 2017;35(1):76-88. journals.lww.com/jhypertension/

word-for-word citations within the running text stand out in italic type

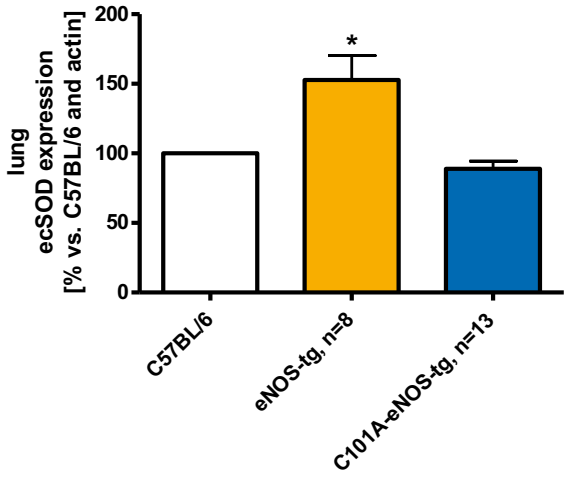

Fig. 3.47: *Evaluation of Western Blot results on lung ecSOD expression in eNOS-tg (152.8 ± 17.55%, n=8, p=0.0198) and C101A-eNOS-tg (88.87 ± 5.577%, n=13, n.s.).*

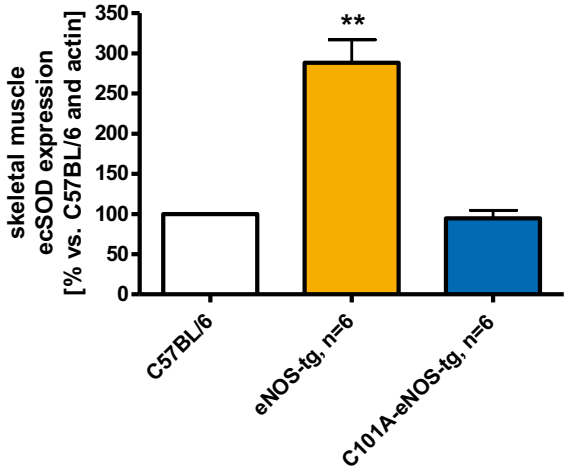

Fig. 3.48: *Evaluation of Western Blot results on skeletal muscle ecSOD expression in eNOS-tg (288.4 ± 28.47%, n=6, p=0.0012) and C101A-eNOS-tg (94.77 ± 9.692%, n=6, n.s.).*

According to the evidences for increased NO bioavailability in eNOS-tg, obtained by blood pressure data (see 3.3.3) and VASP Ser239 phosphorylation results (see 3.3.4), ecSOD expression is increased in this strain as compared to transgenic negative littermates (see figs. 3.45-3.48). No changes can be found in C101A-eNOS-tg, giving another hint for no increased bioavailability despite increased eNOS expression levels.

3.4. Effects of Tempol®

In C101A-eNOS-tg increased levels of oxidative stress are determined (see 3.2.1). In order to distinguish the effects of $O_2^{-\bullet}$, the SOD-mimetic Tempol® is applied orally in

This work was published in

Suvorava T*, Pick S*, and Kojda G. (* equal contribution)
Selective impairment of blood pressure reduction by endothelial nitric oxide synthase dimer destabilization in mice.
J Hypertens 2017;35(1):76-88. journals.lww.com/jhypertension/

word-for-word citations within the running text stand out in italic type

C101A-eNOS-tg mice as well as in their transgenic negative littermates for a period of three weeks.

3.4.1. eNOS PROTEIN EXPRESSION

Expression of total eNOS is not influenced by Tempol® treatment, neither in C101A-eNOS-tg (see figs. 3.49,3.50), nor in C57BL/6 (see figs. 3.51,3.52).

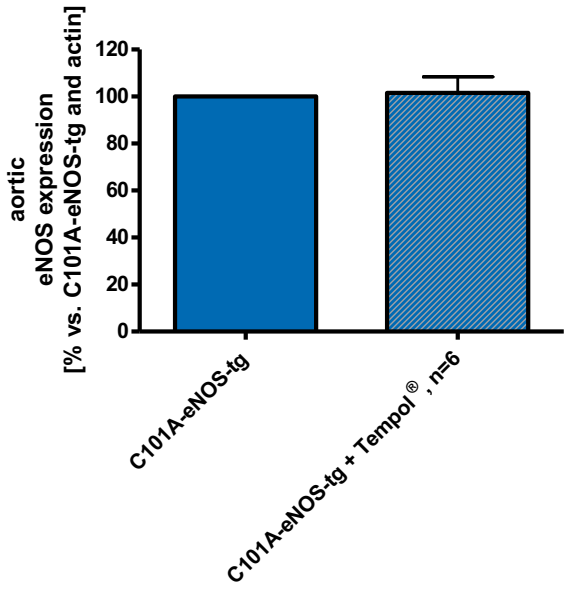

Fig. 3.49: *Evaluation of Western Blot results on aortic eNOS expression in C101A-eNOS-tg after Tempol® treatment (101.6 ± 6.798%, n=6, n.s.).*

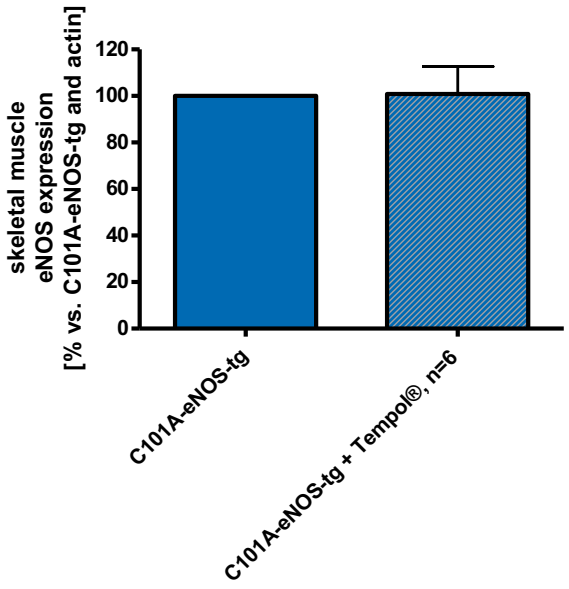

Fig. 3.50: *Evaluation of Western Blot results on skeletal muscle eNOS expression in C101A-eNOS-tg after Tempol® treatment (100.8 ± 11.80%, n=6, n.s.).*

This work was published in

Suvorava T*, Pick S*, and Kojda G. (* equal contribution)
Selective impairment of blood pressure reduction by endothelial nitric oxide synthase dimer destabilization in mice.
J Hypertens 2017;35(1):76-88. journals.lww.com/jhypertension/

word-for-word citations within the running text stand out in italic type

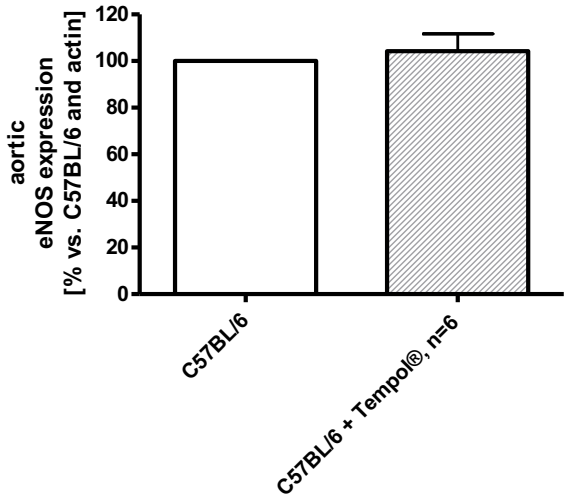

Fig. 3.51: *Evaluation of Western Blot results on aortic eNOS expression in C57BL/6 after Tempol® treatment (104.3 ± 7.378%, n=6, n.s.).*

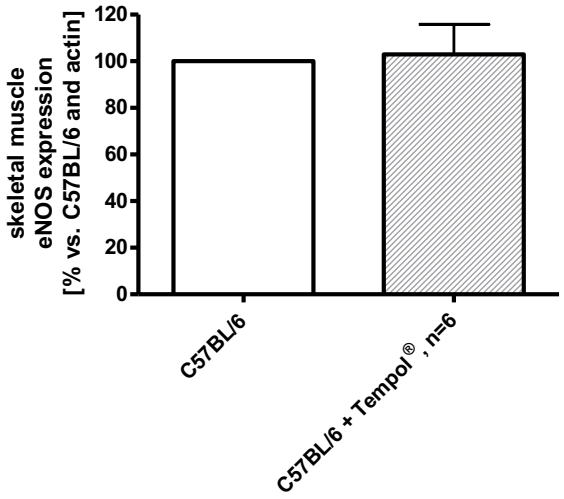

Fig. 3.52: *Evaluation of Western Blot results on skeletal muscle eNOS expression in C57BL/6 after Tempol® treatment (102.9 ± 12.95%, n=6, n.s.).*

Experiments are carried out in aortic (50 µg total protein loaded) and skeletal muscle (100 µg total protein loaded) samples.

3.4.2. DETECTION OF SUPEROXIDE ANION RADICAL

After one week of oral Tempol® treatment already, $O_2^{-\bullet}$ ss not detectable by lucigenin method any longer. In order to ensure the measurement itself, Tempol® is added to tissue of non-treated mice during calibration (1 mM). Here no quantification is possible either.

This work was published in

Suvorava T*, Pick S*, and Kojda G. (* equal contribution)
Selective impairment of blood pressure reduction by endothelial nitric oxide synthase dimer destabilization in mice.
J Hypertens 2017;35(1):76-88. journals.lww.com/jhypertension/

word-for-word citations within the running text stand out in italic type

3.4.3. GLUTATHIONYLATED eNOS

The effect of Tempol® treatment on S-glutathionylated eNOS is determined in aortic, myocardial, lung and skeletal muscle tissue after immunoprecipitation of eNOS. The previous results shown in 3.2.2 are reproducible in non-treated control mice: There is a significant augmentation in S-glutathionylated eNOS detectable in C101A-eNOS-tg. This effect is abrogated by the treatment with Tempol® (see figs. 3.53-3.56).

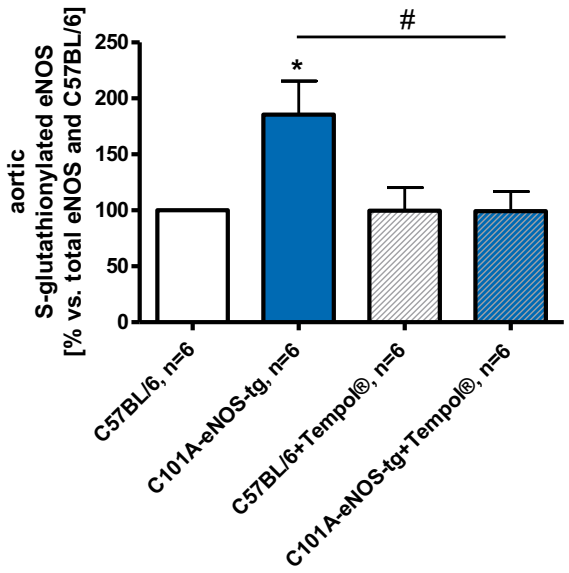

Fig. 3.53: *Evaluation of fluorescence results on immunoprecipitated aortic S-glutathionylated eNOS in C101A-eNOS-tg (185.4 ± 30.06%, n=6, p=0.0362) and their transgenic negative littermates (C57BL/6) before and after Tempol® treatment (C101A-eNOS-tg: 99.18 ± 17.63%, n=6, p<0.05 vs. C101A-eNOS-tg by 1-way ANOVA and Newman-Keuls post test; C57BL/6: 99.18 ± 17.63%, n=6).*

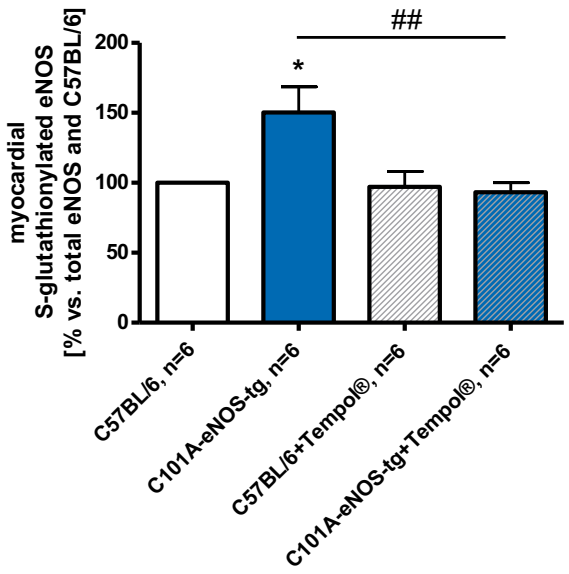

Fig. 3.54: *Evaluation of fluorescence results on immunoprecipitated myocardial S-glutathionylated eNOS in C101A-eNOS-tg (150.3 ± 18.37%, n=6, p=0.0410) and their transgenic negative littermates (C57BL/6) before and after Tempol® treatment (C101A-eNOS-tg: 93.22 ± 6.891%, n=6, p<0.01 vs. C101A-eNOS-tg by 1-way ANOVA and Newman-Keuls post test; C57BL/6: 97.02 ± 11.00%, n=6).*

This work was published in

Suvorava T*, Pick S*, and Kojda G. (* equal contribution)
Selective impairment of blood pressure reduction by endothelial nitric oxide synthase dimer destabilization in mice.
J Hypertens 2017;35(1):76-88. journals.lww.com/jhypertension/

word-for-word citations within the running text stand out in italic type

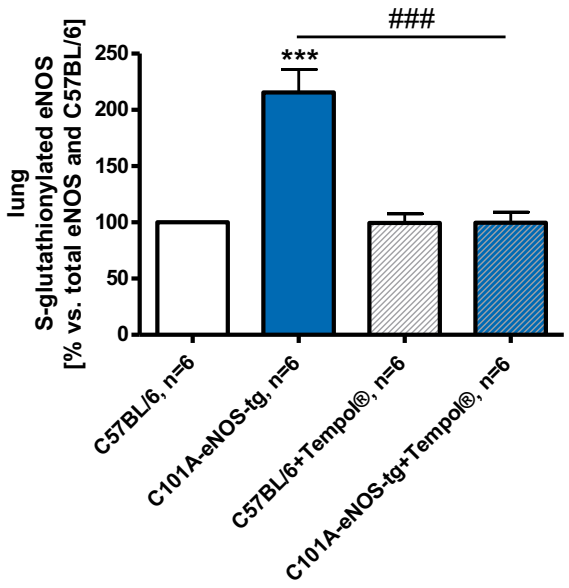

Fig. 3.55: *Evaluation of fluorescence results on immunoprecipitated lung S-glutathionylated eNOS in C101A-eNOS-tg (215.5 ± 20.41%, n=6, p=0.0024) and their transgenic negative littermates (C57BL/6) before and after Tempol® treatment (C101A-eNOS-tg: 99.77 ± 9.281%, n=6, p<0.001 vs. C101A-eNOS-tg by 1-way ANOVA and Newman-Keuls post test; C57BL/6: 99.53 ± 8.140%, n=6).*

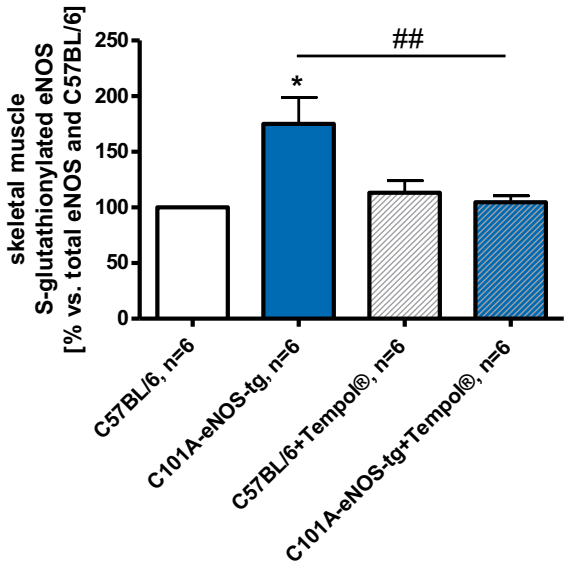

Fig. 3.56: *Evaluation of fluorescence results on immunoprecipitated skeletal muscle S-glutathionylated eNOS in C101A-eNOS-tg (175.1 ± 23.66%, n=6, p=0.0247) and their transgenic negative littermates (C57BL/6) before and after Tempol® treatment (C101A-eNOS-tg: 104.7 ± 5.726%, n=6, p<0.01 vs. C101A-eNOS-tg by 1-way ANOVA and Newman-Keuls post test; C57BL/6: 113.2 ± 10.94%, n=6).*

3.4.4. eNOS TYROSINE-NITRATION

The effect of Tempol® treatment on eNOS tyrosine-nitration is determined in aortic, myocardial, lung and skeletal muscle tissue after immunoprecipitation of eNOS. The previous data obtained by Western Blot analysis on total protein nitration shown in 3.2.3 give similar results in non-treated control mice: There is a significant

augmentation in tyrosine-nitrated eNOS detectable in C101A-eNOS-tg. This effect is abolished by the treatment with Tempol® (see figs. 3.57-3.60).

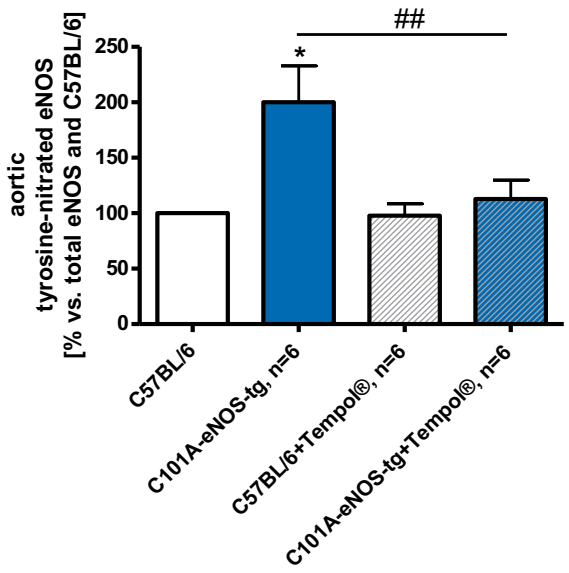

Fig. 3.57: *Evaluation of fluorescence results on immunoprecipitated aortic tyrosine-nitrated eNOS in C101A-eNOS-tg (200.1 ± 32.76%, n=6, p=0.0282) and their transgenic negative littermates (C57BL/6) before and after Tempol® treatment (C101A-eNOS-tg: 112.9 ± 16.93%, n=6, p<0.01 vs. C101A-eNOS-tg by 1-way ANOVA and Newman-Keuls post test; C57BL/6: 97.78 ± 10.60%, n=6).*

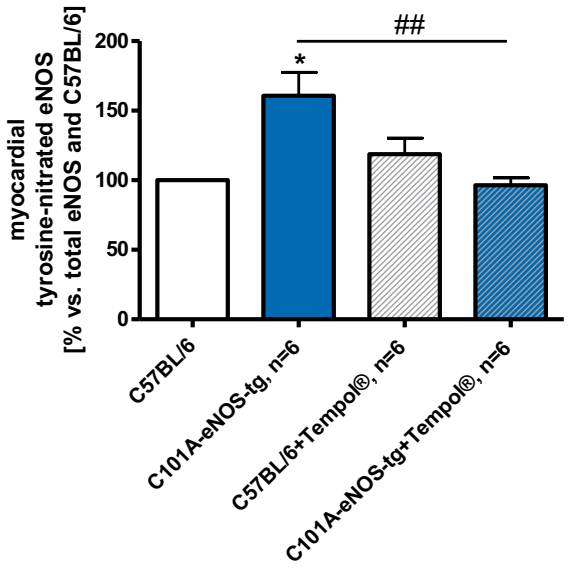

Fig. 3.58: *Evaluation of fluorescence results on immunoprecipitated myocardial tyrosine-nitrated eNOS in C101A-eNOS-tg (160.8 ± 13.83%, n=6, p=0.0153) and their transgenic negative littermates (C57BL/6) before and after Tempol® treatment (C101A-eNOS-tg: 96.44 ± 5.384%, n=6, p<0.01 vs. C101A-eNOS-tg by 1-way ANOVA and Newman-Keuls post test; C57BL/6: 118.7 ± 11.54%, n=6).*

This work was published in

Suvorava T*, Pick S*, and Kojda G. (* equal contribution)
Selective impairment of blood pressure reduction by endothelial nitric oxide synthase dimer destabilization in mice.
J Hypertens 2017;35(1):76-88. journals.lww.com/jhypertension/

word-for-word citations within the running text stand out in italic type

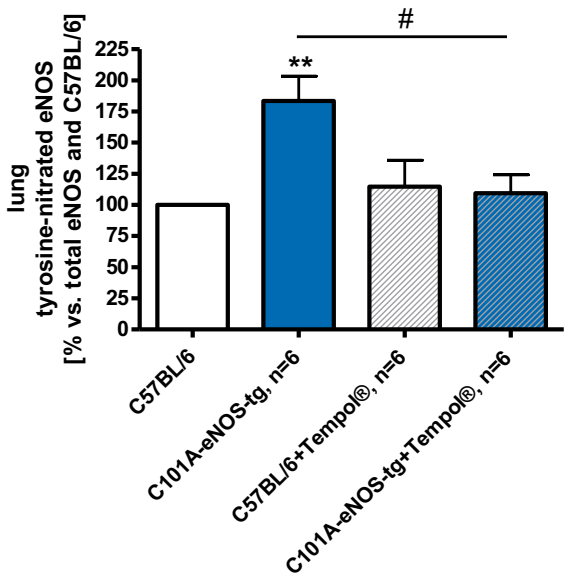

Fig. 3.59: *Evaluation of fluorescence results on immunoprecipitated lung tyrosine-nitrated eNOS in C101A-eNOS-tg (183.3 ± 19.83%, n=6, p=0.0084) and their transgenic negative littermates (C57BL/6) before and after Tempol® treatment (C101A-eNOS-tg: 109.3 ± 14.94%, n=6, p<0.05 vs. C101A-eNOS-tg by 1-way ANOVA and Newman-Keuls post test; C57BL/6: 114.6 ± 21.15%, n=6).*

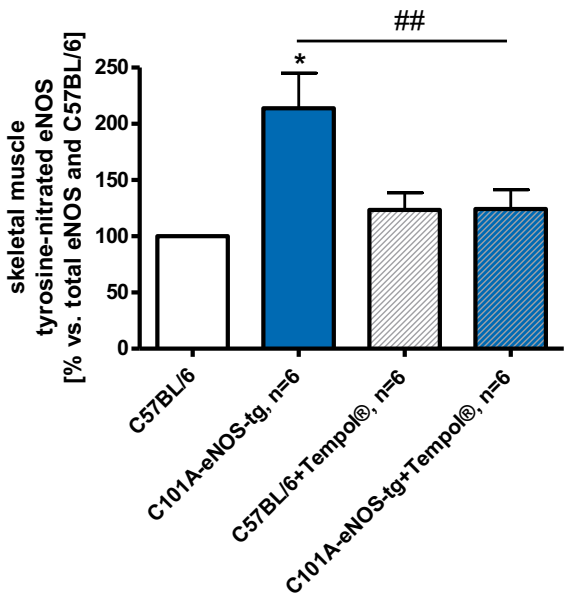

Fig. 3.60: *Evaluation of fluorescence results on immunoprecipitated skeletal muscle tyrosine-nitrated eNOS in C101A-eNOS-tg (213.8 ± 31.22%, n=6, p=0.0148) and their transgenic negative littermates (C57BL/6) before and after Tempol® treatment (C101A-eNOS-tg: 124.3 ± 16.99%, n=6, p<0.01 vs. C101A-eNOS-tg by 1-way ANOVA and Newman-Keuls post test; C57BL/6: 123.5 ± 15.16%, n=6).*

3.4.5. PHOSPHORYLATION OF eNOS AT SER1176/9

The effect of Tempol® treatment on phosphorylated eNOS at Ser1176/9 is determined in aortic, myocardial, lung and skeletal muscle tissue after immunoprecipitation of eNOS. The previous results shown in 3.2.4 are reproducible in non-treated control

This work was published in

Suvorava T*, Pick S*, and Kojda G. (* equal contribution)
Selective impairment of blood pressure reduction by endothelial nitric oxide synthase dimer destabilization in mice.
J Hypertens 2017;35(1):76-88. journals.lww.com/jhypertension/

word-for-word citations within the running text stand out in italic type

mice: There is a significant augmentation in phosphorylated eNOS detectable in C101A-eNOS-tg. This effect is abrogated by the treatment with Tempol® (see figs. 3.61-3.64).

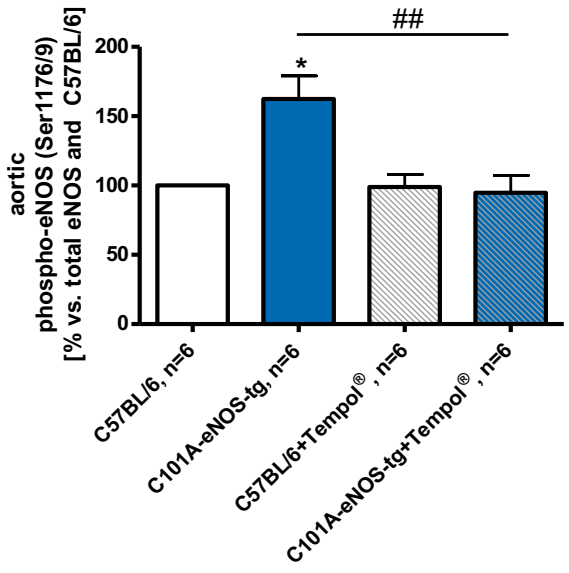

Fig. 3.61: *Evaluation of fluorescence results on immunoprecipitated aortic phosphorylated eNOS at Ser1176/9 in C101A-eNOS-tg (162.3 ± 16.78%, n=6, p=0.0138) and their transgenic negative littermates (C57BL/6) before and after Tempol® treatment (C101A-eNOS-tg: 94.80 ± 12.40%, n=6, p<0.01 vs. C101A-eNOS-tg by 1-way ANOVA and Newman-Keuls post test; C57BL/6: 98.94 ± 8.992%, n=6).*

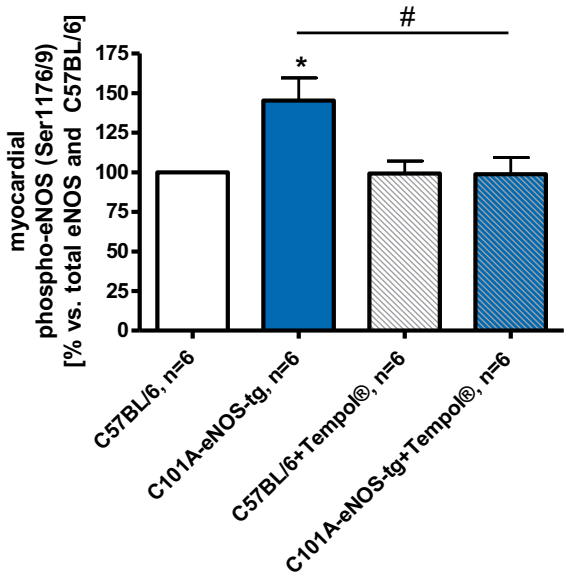

Fig. 3.62: *Evaluation of fluorescence results on immunoprecipitated myocardial phosphorylated eNOS at Ser1176/9 in C101A-eNOS-tg (145.4 ± 14.27%, n=6, p=0.0245) and their transgenic negative littermates (C57BL/6) before and after Tempol® treatment (C101A-eNOS-tg: 98.73 ± 10.57%, n=6, p<0.05 vs. C101A-eNOS-tg by 1-way ANOVA and Newman-Keuls post test; C57BL/6: 99.28 ± 7.801%, n=6).*

This work was published in

Suvorava T*, Pick S*, and Kojda G. (* equal contribution)
Selective impairment of blood pressure reduction by endothelial nitric oxide synthase dimer destabilization in mice.
J Hypertens 2017;35(1):76-88. journals.lww.com/jhypertension/

word-for-word citations within the running text stand out in italic type

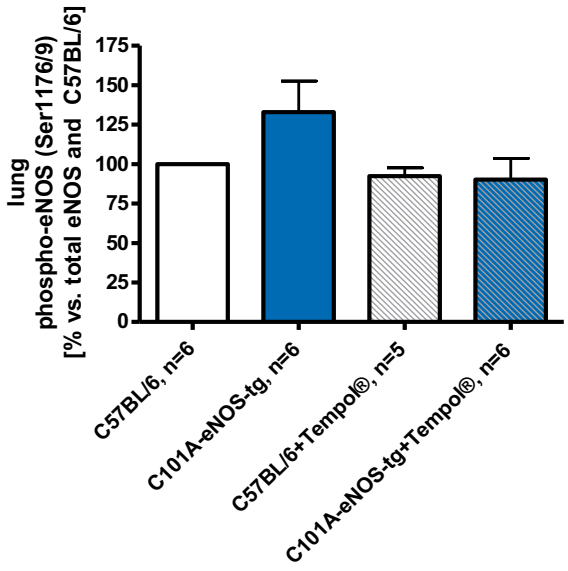

Fig. 3.63: *Evaluation of fluorescence results on immunoprecipitated lung phosphorylated eNOS at Ser1176/9 in C101A-eNOS-tg (133.0 ± 19.70%, n=6, n.s.) and their transgenic negative littermates (C57BL/6) before and after Tempol® treatment (C101A-eNOS-tg: 90.17 ± 13.39%, n=6, n.s. vs. C101A-eNOS-tg by 1-way ANOVA and Newman-Keuls post test; C57BL/6: 92.32 ± 5.250%, n=6).*

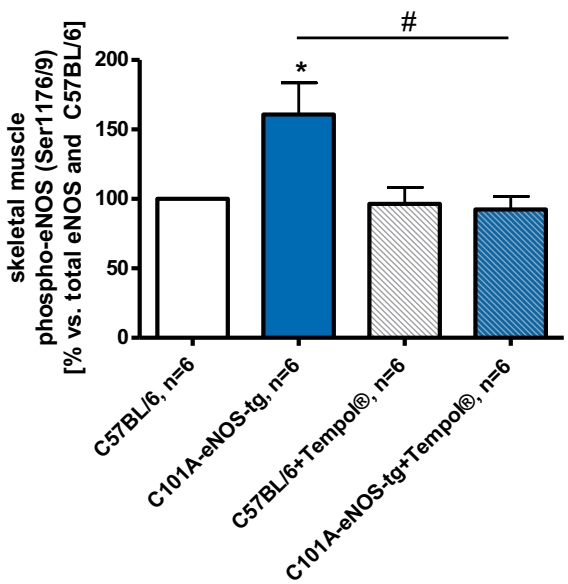

Fig. 3.64: *Evaluation of fluorescence results on immunoprecipitated skeletal muscle phosphorylated eNOS at Ser1176/9 in C101A-eNOS-tg (160.8 ± 22.77%, n=6, p=0.0444) and their transgenic negative littermates (C57BL/6) before and after Tempol® treatment (C101A-eNOS-tg: 92.43 ± 9.398%, n=6, p<0.05 vs. C101A-eNOS-tg by 1-way ANOVA and Newman-Keuls post test; C57BL/6: 96.49 ± 11.77%, n=6).*

3.4.5.1. PHOSPHORYLATION OF AMPK AT THR172

Phosphorylation of AMPKα at Thr172 is previously (see 3.2.4.1) identified as being responsible for phosphorylation of eNOS at Ser1176/9 in C101A-eNOS-tg. These results are reproduced by this particular set of Western Blot experiments achieved by loading

This work was published in

Suvorava T*, Pick S*, and Kojda G. (* equal contribution)
Selective impairment of blood pressure reduction by endothelial nitric oxide synthase dimer destabilization in mice.
J Hypertens 2017;35(1):76-88. journals.lww.com/jhypertension/

word-for-word citations within the running text stand out in italic type

50 µg of aortic and 100 µg of skeletal muscle tissue. As this augmented phosphorylation of AMPKα is abrogated after Tempol® treatment (see figs. 3.65-3.68) there is growing evidence that this finding is dependent on oxidative stress.

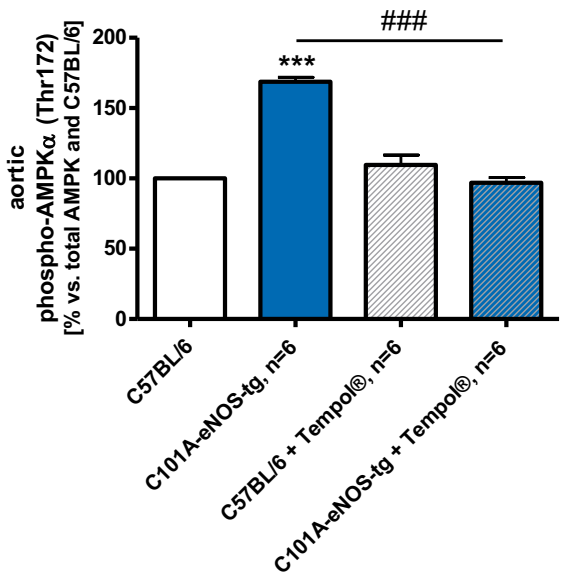

Fig. 3.65: *Evaluation of Western Blot results on aortic AMPKα phosphorylation at Thr172 in C101A-eNOS-tg (168.7 ± 7.982%, n=6, p=0.0003) and their transgenic negative littermates (C57BL/6) before and after Tempol® treatment (C101A-eNOS-tg: 96.86 ± 9.052%, n=6, p<0.001 vs. C101A-eNOS-tg by 1-way ANOVA and Newman-Keuls post test; C57BL/6: 109.6 ± 17.15%, n=6).*

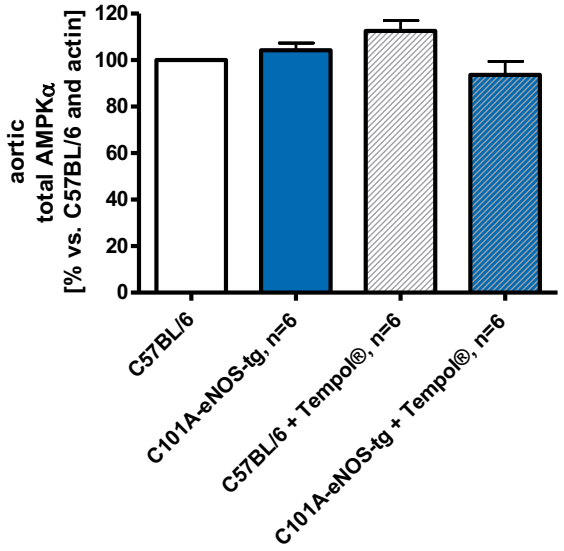

Fig. 3.66: *Evaluation of Western Blot results on aortic AMPKα expression in C101A-eNOS-tg (104.2 ± 3.154%, n=6, n.s.) and their transgenic negative littermates (C57BL/6) before and after Tempol® treatment (C101A-eNOS-tg: 93.68 ± 5.756%, n=6, n.s.; C57BL/6: 107.5 ± 4.614%, n=6, n.s.).*

This work was published in

Suvorava T*, Pick S*, and Kojda G. (* equal contribution)
Selective impairment of blood pressure reduction by endothelial nitric oxide synthase dimer destabilization in mice.
J Hypertens 2017;35(1):76-88. journals.lww.com/jhypertension/

word-for-word citations within the running text stand out in italic type

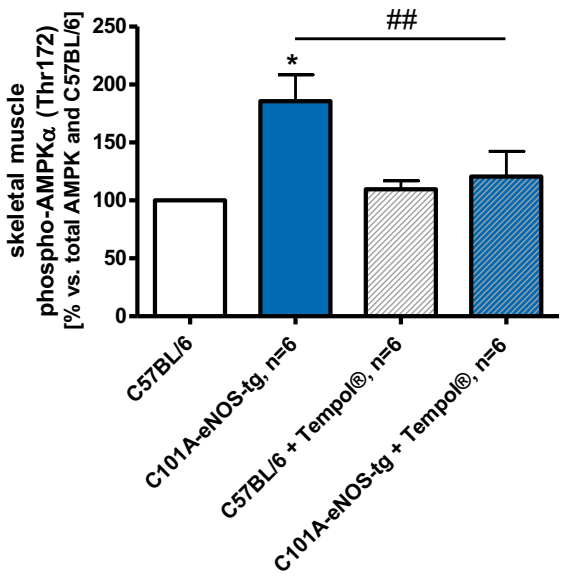

Fig. 3.67: *Evaluation of Western Blot results on skeletal muscle AMPKα phosphorylation at Thr172 in C101A-eNOS-tg (185.6 ± 22.79%, n=6, p=0.0132) and their transgenic negative littermates (C57BL/6) before and after Tempol® treatment (C101A-eNOS-tg: 120.7 ± 21.64%, n=6, p<0.01 vs. C101A-eNOS-tg by 1-way ANOVA and Newman-Keuls post test; C57BL/6: 109.7 ± 7.329%, n=6).*

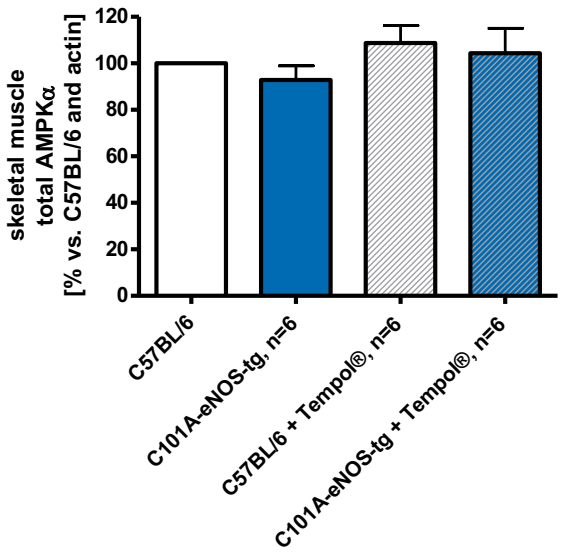

Fig. 3.68: *Evaluation of Western Blot results on skeletal muscle AMPKα expression in C101A-eNOS-tg (92.87 ± 6.077%, n=6, n.s.) and their transgenic negative littermates (C57BL/6) before and after Tempol® treatment (C101A-eNOS-tg: 104.3 ± 10.69%, n=6, n.s.; C57BL/6: 108.8 ± 7.449%, n=6, n.s.).*

3.4.5.2. PHOSPHORYLATION OF AKT AT SER473

As already shown in 3.2.4.2 there is no influence on phosphorylation of eNOS at Ser1176/9 of Akt and its activation by phosphorylation at Ser473. This is confirmed by the data of this set of experiments. Western Blot results are shown for aortic (50 µg total protein loaded) and skeletal muscle (100 µg total protein loaded) probes of

This work was published in

Suvorava T*, Pick S*, and Kojda G. (* equal contribution)
Selective impairment of blood pressure reduction by endothelial nitric oxide synthase dimer destabilization in mice.
J Hypertens 2017;35(1):76-88. journals.lww.com/jhypertension/

word-for-word citations within the running text stand out in italic type

C101A-eNOS-tg and their transgenic negative littermates before and after Tempol® treatment, which itself also has no effect on the expression of total Akt or the extend of its phosphorylation (see figs. 3.69-3.72).

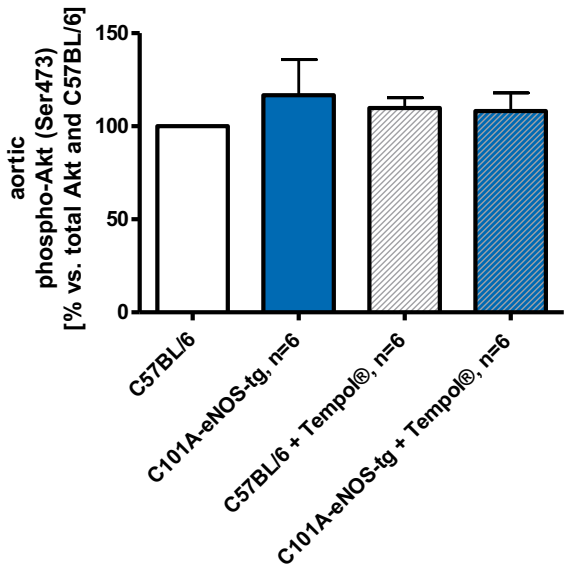

Fig. 3.69: *Evaluation of Western Blot results on aortic Akt phosphorylation at Ser473 in C101A-eNOS-tg (116.7 ± 19.10%, n=6, n.s.) and their transgenic negative littermates (C57BL/6) before and after Tempol® treatment (C101A-eNOS-tg: 108.2 ± 9.662%, n=6, n.s.; C57BL/6: 109.8 ± 5.552%, n=6, n.s.).*

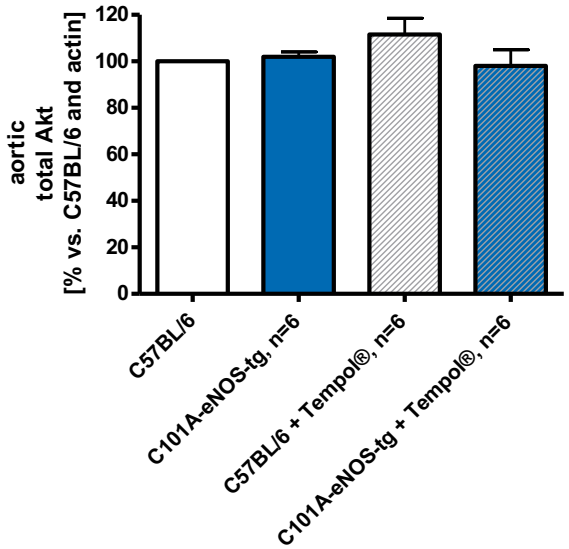

Fig. 3.70: *Evaluation of Western Blot results on aortic Akt expression in C101A-eNOS-tg (101.9 ± 2.080%, n=6, n.s.) and their transgenic negative littermates (C57BL/6) before and after Tempol® treatment (C101A-eNOS-tg: 98.08 ± 6.891%, n=6, n.s.; C57BL/6: 116.6 ± 6.965%, n=6, n.s.).*

This work was published in

Suvorava T*, Pick S*, and Kojda G. (* equal contribution)
Selective impairment of blood pressure reduction by endothelial nitric oxide synthase dimer destabilization in mice.
J Hypertens 2017;35(1):76-88. journals.lww.com/jhypertension/

word-for-word citations within the running text stand out in italic type

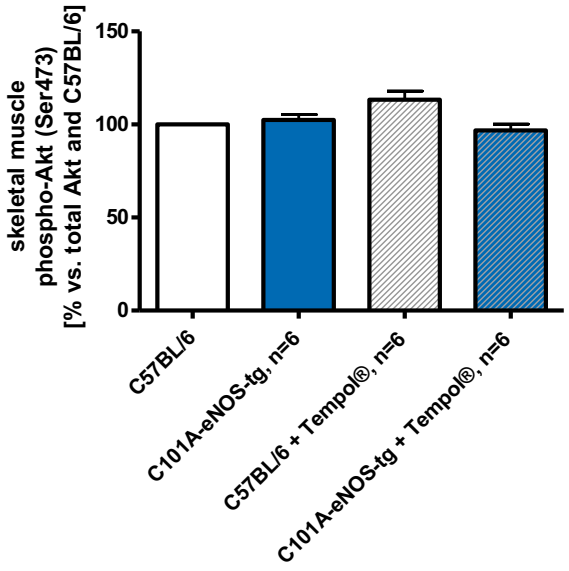

Fig. 3.71: *Evaluation of Western Blot results on skeletal muscle Akt phosphorylation at Ser473 in C101A-eNOS-tg (102.4 ± 2.923%, n=6, n.s.) and their transgenic negative littermates (C57BL/6) before and after Tempol® treatment (C101A-eNOS-tg: 96.75 ± 3.475%, n=6, n.s.; C57BL/6: 107.2 ± 4.488%, n=6, n.s.).*

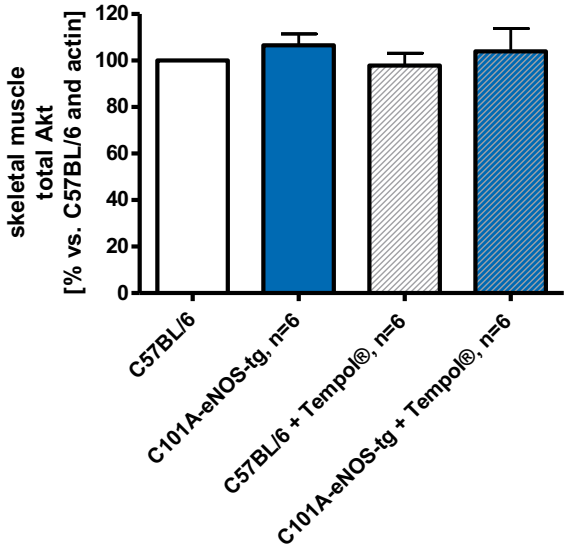

Fig. 3.72: *Evaluation of Western Blot results on skeletal muscle Akt expression in C101A-eNOS-tg (106.6 ± 4.877%, n=6, n.s.) and their transgenic negative littermates (C57BL/6) before and after Tempol® treatment (C101A-eNOS-tg: 104.0 ± 9.751%, n=6, n.s.; C57BL/6: 97.89 ± 5.213%, n=6, n.s.).*

3.4.6. BLOOD PRESSURE AND HEART RATE

By treatment with the antioxidant and SOD-mimetic Tempol® blood pressure is significantly reduced in C101A-eNOS-tg, but not in their transgenic negative littermates (see figs. 3.73-3.75). This can be due to reduced $O_2^{-\bullet}$ levels and therefore reduced peroxynitrite formation which can finally result in increased bioavailable NO. After a

This work was published in

Suvorava T*, Pick S*, and Kojda G. (* equal contribution)
Selective impairment of blood pressure reduction by endothelial nitric oxide synthase dimer destabilization in mice.
J Hypertens 2017;35(1):76-88. journals.lww.com/jhypertension/

word-for-word citations within the running text stand out in italic type

wash-out phase of two weeks, blood pressure is back to normal values again (see fig. 3.75). Heart rates are not changed by the antioxidative treatment (see figs. 3.76-3.77)

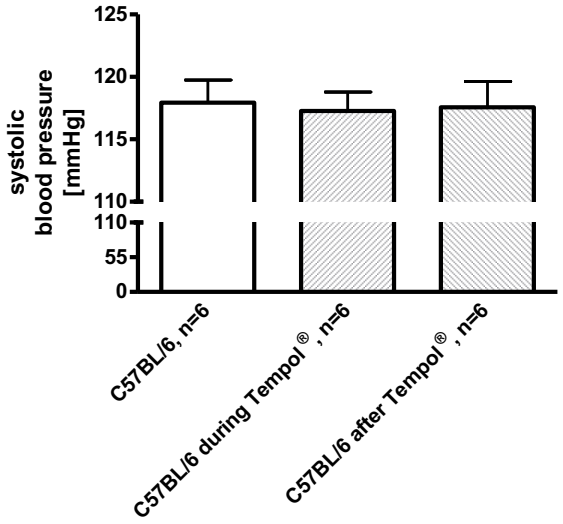

Fig. 3.73: *Blood pressure results in C57BL/6 (117.9 ± 1.823, n=6) and in the same animals during (117.3 ± 1.515 mmHg, n=6) and after (117.6 ± 2.079 mmHg, n=6) Tempol® treatment showing no difference.*

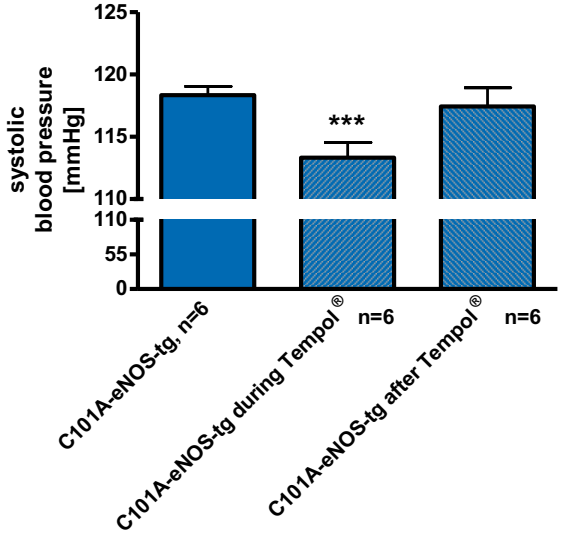

Fig. 3.74: *Blood pressure results in C101A-eNOS-tg (118.3 ± 0.7112, n=6) and in the same animals during (113.3 ± 1.234 mmHg, n=6, p=0.0019) and after (117.4 ± 1.495 mmHg, n=6) Tempol® treatment.*

This work was published in

Suvorava T*, Pick S*, and Kojda G. (* equal contribution)
Selective impairment of blood pressure reduction by endothelial nitric oxide synthase dimer destabilization in mice.
J Hypertens 2017;35(1):76-88. journals.lww.com/jhypertension/

word-for-word citations within the running text stand out in italic type

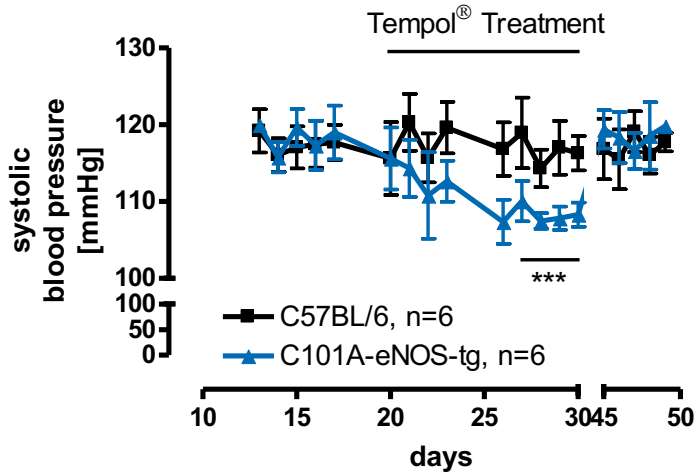

Fig. 3.75: *Time dependent blood pressure results in C57BL/6 (n=6) and C101A-eNOS-tg (n=6) without and during Tempol® treatment showing a significant decrease in C101A-eNOS-tg as compared to their transgenic negative littermates (see also Fig. XX).*

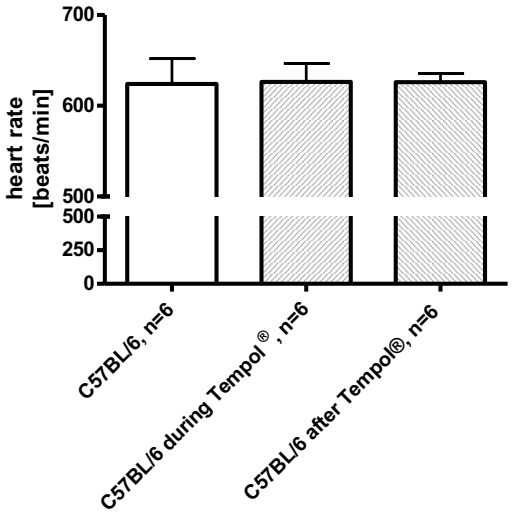

Fig. 3.76: *Heart rate results in C57BL/6 before (624.1 ± 28.02 beats per minute, n=6), during (626.2 ±20.34 beats per minute, n=6) and after (626.1 ±9.291 beats per minute, n=6) Tempol® treatment showing no difference.*

This work was published in

Suvorava T*, Pick S*, and Kojda G. (* equal contribution)
Selective impairment of blood pressure reduction by endothelial nitric oxide synthase dimer destabilization in mice.
J Hypertens 2017;35(1):76-88. journals.lww.com/jhypertension/

word-for-word citations within the running text stand out in italic type

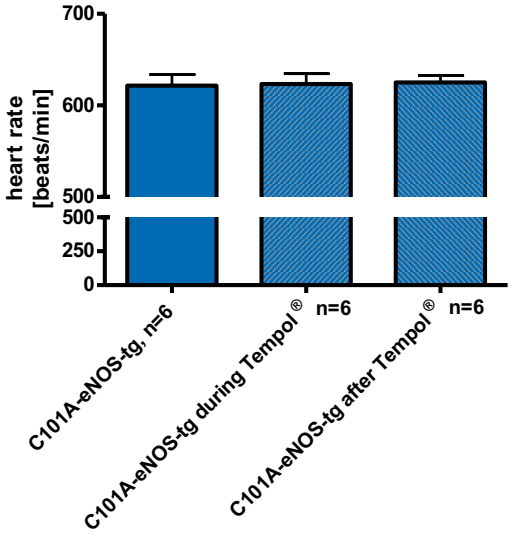

Fig. 3.77: *Heart rate results in C101A-eNOS-tg before (621.6 ± 11.99 beats per minute, n=6), during (623.4 ±11.32 beats per minute, n=6) and after (624.9 ± 7.653 beats per minute, n=6) Tempol® treatment showing no difference.*

A correlation of systolic blood pressure in different transgenic strains (eNOS-KO, C57BL/6, another transgenic strain with a higher overexpression of eNOS [37] and eNOS-tg) and their eNOS expression as detected by Western Blot analysis is performed to predict the expected blood pressure reduction in C101A-eNOS-tg (see fig. 3.86). The resulting equation is highly significant (R^2=0.9992) and given by

$$systolic\ blood\ pressure = 35.92e^{-0.007267X} + 102.0\ [mmHg]$$

wherein X is the percentage of aortic eNOS expression related to wild-type animals. Given the eNOS expression value in C101A-eNOS-tg of 147.3%, the equation yields a systolic blood pressure of 114.3 mmHg.

If the same approximation is carried out with values of eNOS expression in the skeletal muscle, the resulting equation is still significant (R^2=0.992):

$$systolic\ blood\ pressure = 35.56e^{-0.007202X} + 102.3\ [mmHg].$$

Given the eNOS expression value measured in skeletal muscle with 188.4%, the calculated expected systolic blood pressure is 111.5 mmHg.

This work was published in

Suvorava T*, Pick S*, and Kojda G. (* equal contribution)
Selective impairment of blood pressure reduction by endothelial nitric oxide synthase dimer destabilization in mice.
J Hypertens 2017;35(1):76-88. journals.lww.com/jhypertension/

word-for-word citations within the running text stand out in italic type

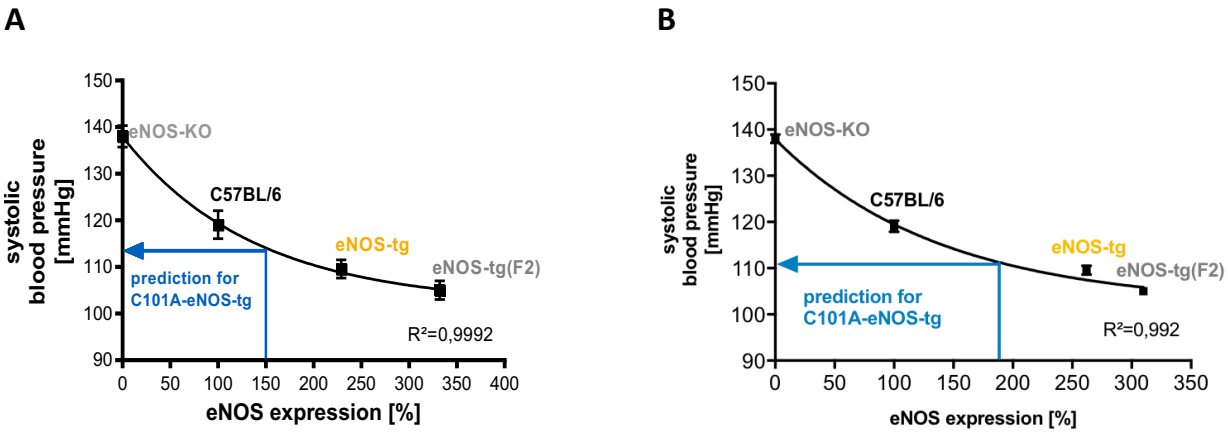

***Fig. 3.78**: Correlation of systolic blood pressure in different transgenic strains (eNOS-KO, C57BL/6, eNOS-tg, eNOS-tg(F2) [37]) and their **A** aortic and **B** skeletal muscle eNOS expression as detected by Western Blot analysis.*

3.4.7. PHOSPHORYLATION OF VASP AT SER239

Matching the results on blood pressure (see 3.4.6), VASP is stronger phosphorylated at Ser239, possibly due to increased endogenous NO bioavailable (see figs. 3.79-3.82). Data are obtained from Western Blots achieved by loading 50 µg of aortic or 100 µg of skeletal muscle tissue.

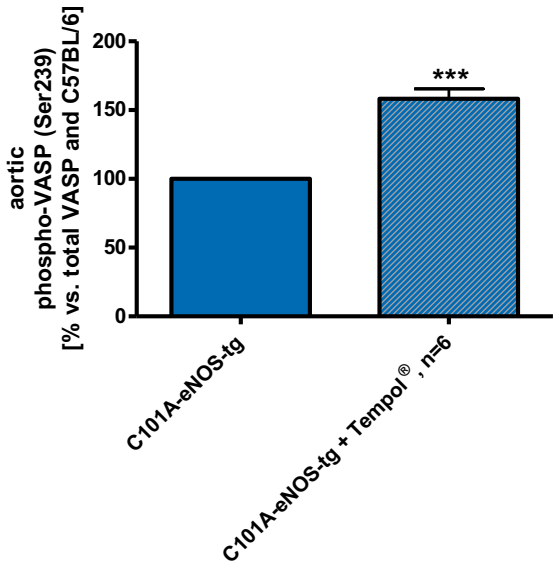

***Fig. 3.79:** Evaluation of Western Blot results on aortic VASP phosphorylation at Ser239 in C101A-eNOS-tg after Tempol® treatment (158.2 ± 7.245%, n=6, p=0.0005).*

This work was published in

Suvorava T*, Pick S*, and Kojda G. (* equal contribution)
Selective impairment of blood pressure reduction by endothelial nitric oxide synthase dimer destabilization in mice.
J Hypertens 2017;35(1):76-88. journals.lww.com/jhypertension/

word-for-word citations within the running text stand out in italic type

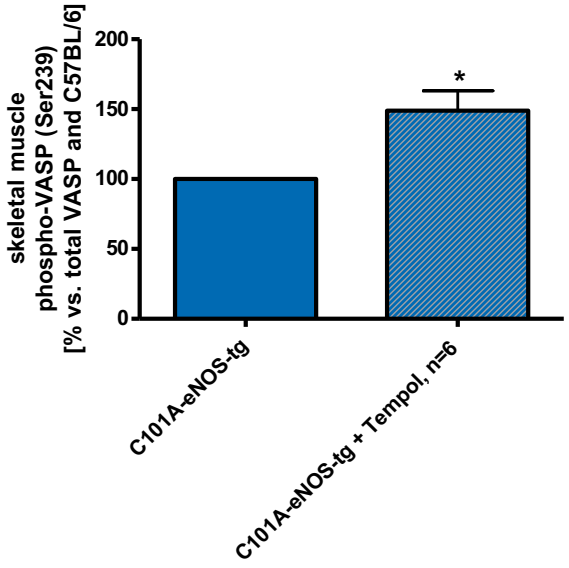

Fig. 3.80: *Evaluation of Western Blot results on skeletal muscle VASP phosphorylation at Ser239 in C101A-eNOS-tg after Tempol® treatment (149.0 ± 14.07%, n=6, p=0.0177).*

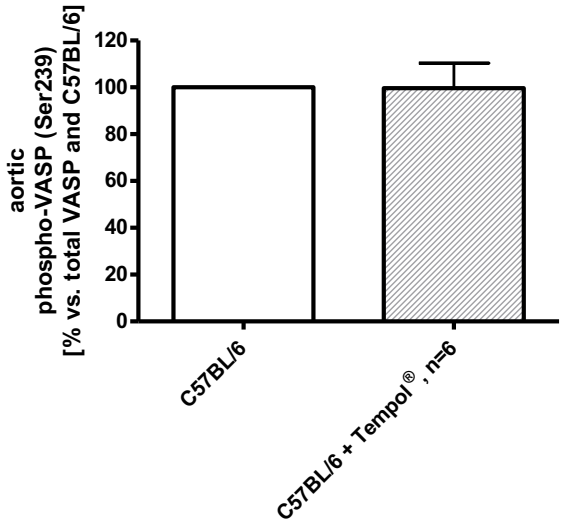

Fig. 3.81: *Evaluation of Western Blot results on aortic VASP phosphorylation at Ser239 in C57BL/6 after Tempol® treatment (99.70 ± 10.65%, n=6, n.s.).*

This work was published in

Suvorava T*, Pick S*, and Kojda G. (* equal contribution)
Selective impairment of blood pressure reduction by endothelial nitric oxide synthase dimer destabilization in mice.
J Hypertens 2017;35(1):76-88. journals.lww.com/jhypertension/

word-for-word citations within the running text stand out in italic type

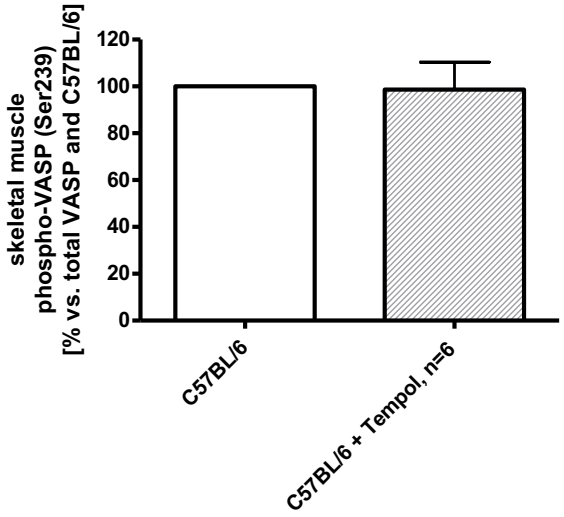

Fig. 3.82: *Evaluation of Western Blot results on skeletal muscle VASP phosphorylation at Ser239 in C57BL/6 after Tempol® treatment (98.70 ± 11.68%, n=6, n.s.).*

3.4.8. ecSOD EXPRESSION

Despite all hints for increased NO bioavailability after Tempol® treatment in C101A-eNOS-tg, as lowered blood pressure (see 3.4.6) and increased VASP phosphorylation at Ser239, there is no difference obtainable in ecSOD expression by Western Blot analysis, neither in aortic (50 µg total protein loaded), nor in skeletal muscle (100 µg total protein loaded) tissue (see figs. 3.83-3.86).

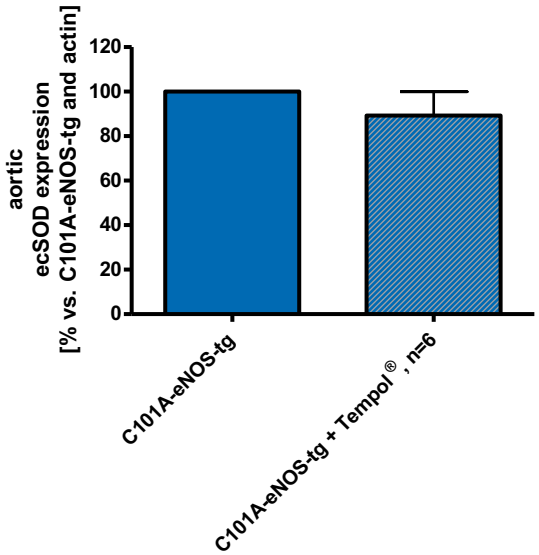

Fig. 3.83: *Evaluation of Western Blot results on aortic ecSOD expression in C101A-eNOS-tg after Tempol® treatment (89.23 ± 10.73%, n=6, n.s.).*

This work was published in

Suvorava T*, Pick S*, and Kojda G. (* equal contribution)
Selective impairment of blood pressure reduction by endothelial nitric oxide synthase dimer destabilization in mice.
J Hypertens 2017;35(1):76-88. journals.lww.com/jhypertension/

word-for-word citations within the running text stand out in italic type

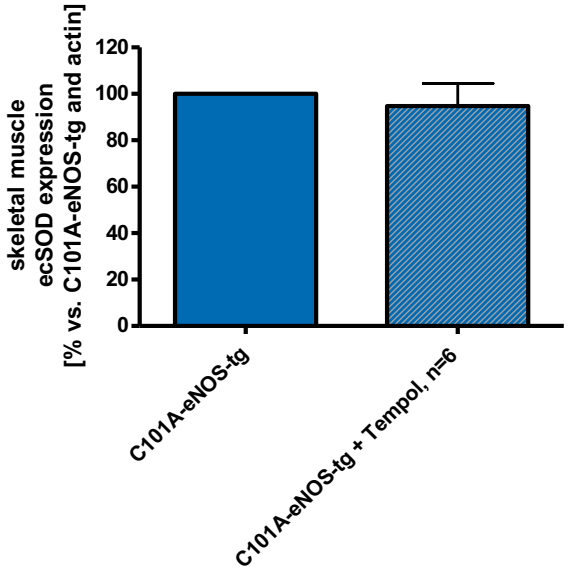

Fig. 3.84: *Evaluation of Western Blot results on skeletal muscle ecSOD expression in C101A-eNOS-tg after Tempol® treatment (94.77 ± 9.692%, n=6, n.s.).*

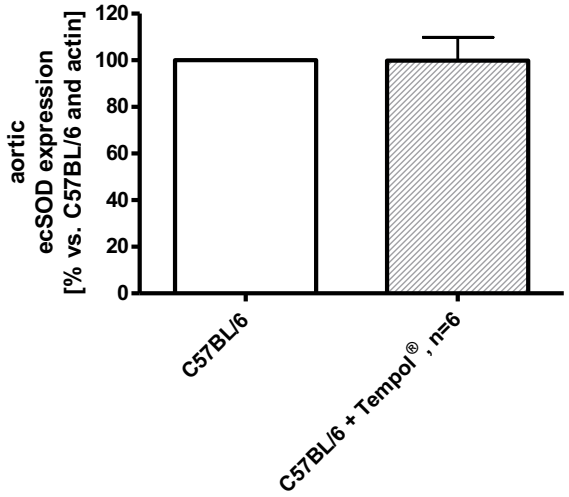

Fig. 3.85: *Evaluation of Western Blot results on aortic ecSOD expression in C57BL/6 after Tempol® treatment (99.81 ± 9.996%, n=6, n.s.).*

This work was published in

Suvorava T*, Pick S*, and Kojda G. (* equal contribution)
Selective impairment of blood pressure reduction by endothelial nitric oxide synthase dimer destabilization in mice.
J Hypertens 2017;35(1):76-88. journals.lww.com/jhypertension/

word-for-word citations within the running text stand out in italic type

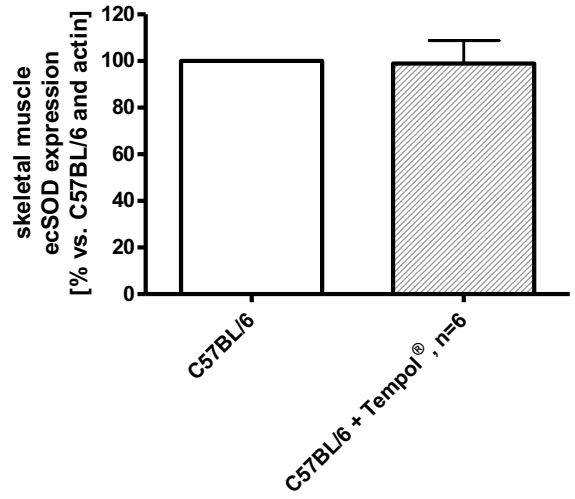

Fig. 3.86: *Evaluation of Western Blot results on skeletal muscle ecSOD expression in C57BL/6 after Tempol® treatment (98.92 ± 9.835%, n=6, n.s.).*

3.5. MECHANISTICAL STUDIES

In order to get further insights into the regulation of eNOS activity and the influence of oxidative stress, voluntary exercise training in C101A-eNOS-tg and their transgenic negative littermates is performed.

3.5.1. EXERCISE PARAMETERS

The efficacy of exercise training can be ascertained by daily running distance and by heart weight/body weight ratio. The running distance in C101A-eNOS-tg is 5,596 ± 82.21 m/day and does not differ to the running distance of C57BL/6 (5,421 ± 82.21 m/day). According heart weight/body weight ratio results are shown in fig. 3.86. Hereby, training efficacy is further ensured as the ratio is significantly higher in the exercised groups.

This work was published in

Suvorava T*, Pick S*, and Kojda G. (* equal contribution)
Selective impairment of blood pressure reduction by endothelial nitric oxide synthase dimer destabilization in mice.
J Hypertens 2017;35(1):76-88. journals.lww.com/jhypertension/

word-for-word citations within the running text stand out in italic type

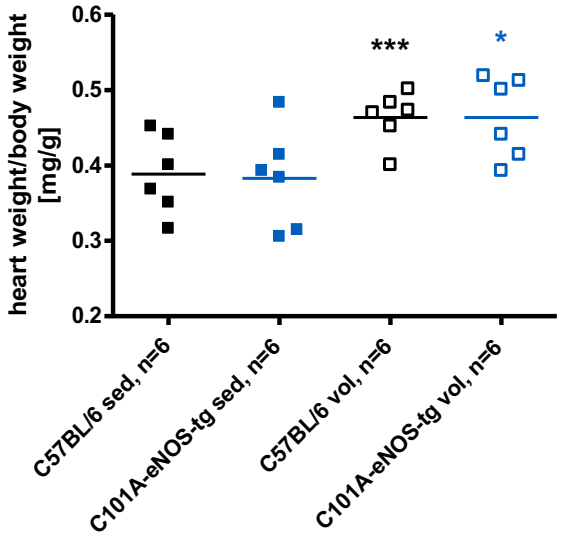

Fig. 3.87: *Heart weight/body weight results after three weeks of voluntary exercise training in C57BL/6 (0.4635 ± 0.01417 mg/g, n=6, p=0.0032 vs. C57BL/6 sed) and C101A-eNOS-tg (0.4635 ± 0.02218 mg/g, n=6, p=0.0148 vs. C101A-eNOS-tg sed) as compared to sedentary controls (C57BL/6: 0.3884 ± 0.02157 mg/g, n=6, C101A-eNOS-tg: 0.3827 ± 0.02697 mg/g, n=6).*

3.5.2. eNOS PROTEIN EXPRESSION

Expression of total eNOS is significantly increased after voluntary exercise (see figs. 3.88-3.91) as determined by Western Blot analysis in aortic and skeletal muscle tissue (50 µg and 100µg total protein loaded respectively).

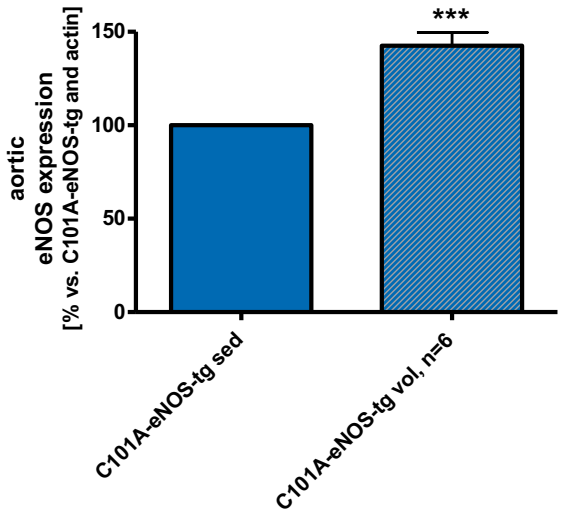

Fig. 3.88: *Evaluation of Western Blot results on aortic eNOS expression in C101A-eNOS-tg after voluntary exercise (142.6 ± 7.111%, n=6, p=0.0019.).*

This work was published in

Suvorava T*, Pick S*, and Kojda G. (* equal contribution)
Selective impairment of blood pressure reduction by endothelial nitric oxide synthase dimer destabilization in mice.
J Hypertens 2017;35(1):76-88. journals.lww.com/jhypertension/

word-for-word citations within the running text stand out in italic type

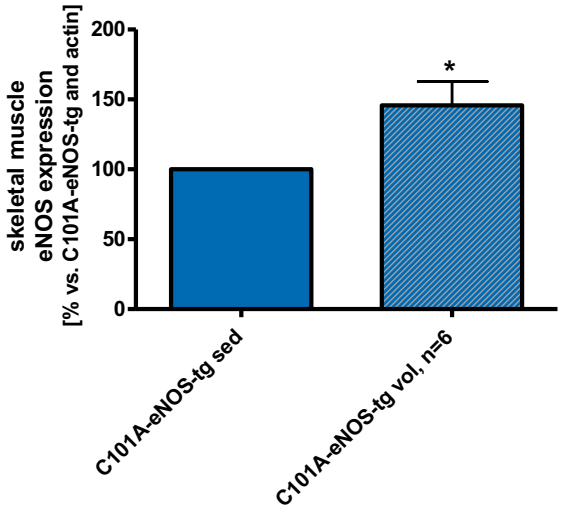

Fig. 3.89: *Evaluation of Western Blot results on skeletal muscle eNOS expression in C101A-eNOS-tg after voluntary exercise (145.8 ± 16.99%, n=6, p=0.0430).*

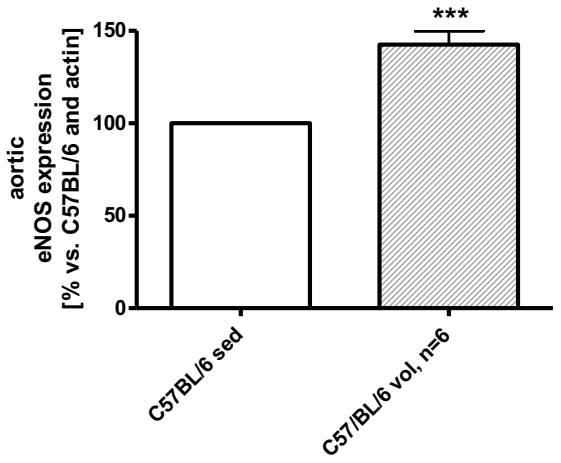

Fig. 3.90: *Evaluation of Western Blot results on aortic eNOS expression in C57BL/6 after voluntary exercise (142.6 ± 17.89%, n=6, p=0.0021).*

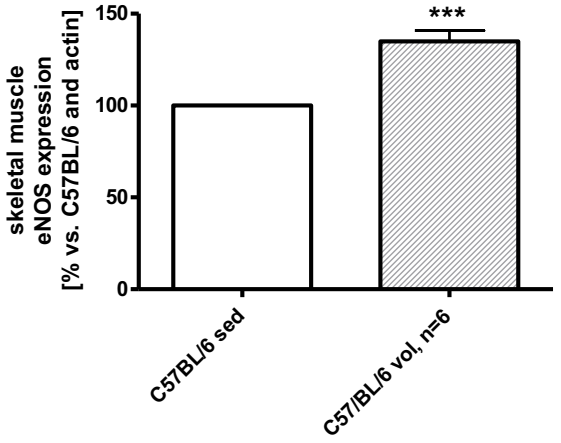

Fig. 3.91: *Evaluation of Western Blot results on skeletal muscle eNOS expression in C57BL/6 after voluntary exercise (134.9 ± 5.872%, n=6, p=0.0019).*

This work was published in

Suvorava T*, Pick S*, and Kojda G. (* equal contribution)
Selective impairment of blood pressure reduction by endothelial nitric oxide synthase dimer destabilization in mice.
J Hypertens 2017;35(1):76-88. journals.lww.com/jhypertension/

word-for-word citations within the running text stand out in italic type

3.5.3. GLUTHATHIONYLATED eNOS

Fluorescence staining after immunoprecipitation of eNOS reveals a significant reduction for S-glutathionylated eNOS in C101A-eNOS-tg and transgenic negative littermates after voluntary training in aortic, myocardial, skeletal muscle tissue, and in C101A-eNOS-tg lung samples (see figs. 3.92-3.95). This suggests a possible reduction of oxidative stress by exercise. Only in lung tissue of C57BL/6 no effect is measurable. The results obtained in sedentary mice are similar to those presented earlier in 3.2.2.

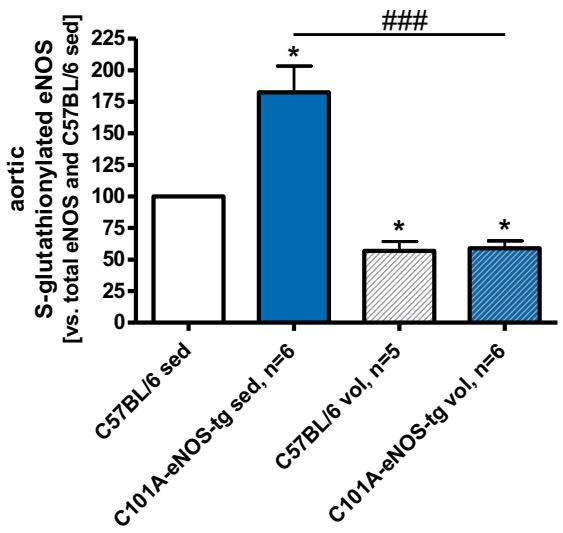

Fig. 3.92: *Evaluation of fluorescence results on immunoprecipitated aortic S-glutathionylated eNOS in sedentary C101A-eNOS-tg (182.4 ± 20.80%, n=6, p=0.0107) and their transgenic negative littermates (C57BL/6) as well as after voluntary exercise (C57BL/6: 56.92 ± 7.371%, n=6, p= 0.0043; C101A-eNOS-tg: 59.01 ± 5.818%, n=6, p=0.0009, p<0.001 vs. C101A-eNOS-tg sed by 1-way ANOVA and Newman-Keuls post test).*

This work was published in

Suvorava T*, Pick S*, and Kojda G. (* equal contribution)
Selective impairment of blood pressure reduction by endothelial nitric oxide synthase dimer destabilization in mice.
J Hypertens 2017;35(1):76-88. journals.lww.com/jhypertension/

word-for-word citations within the running text stand out in italic type

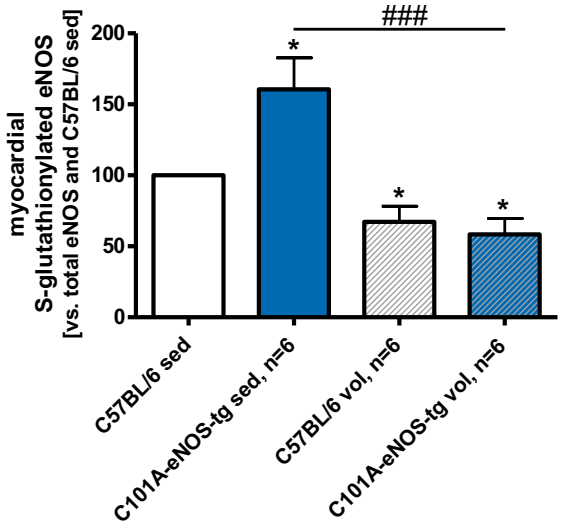

Fig. 3.93: *Evaluation of fluorescence results on immunoprecipitated myocardial S-glutathionylated eNOS in sedentary C101A-eNOS-tg (160.5 ± 22.20%, n=6, p=0.0415) and their transgenic negative littermates (C57BL/6) as well as after voluntary exercise (C57BL/6: 67.30 ± 10.91%, n=6, p=0.0302; C101A-eNOS-tg: 58.47 ± 11.10%, n=6, p=0.0134, p<0.001 vs. C101A-eNOS-tg sed by 1-way ANOVA and Newman-Keuls post test).*

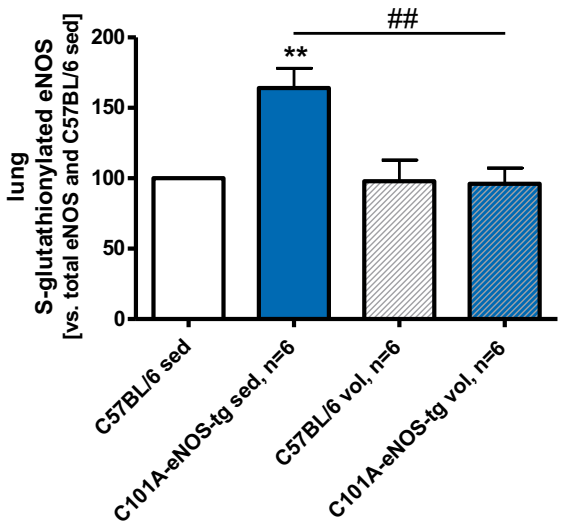

Fig. 3.94: *Evaluation of fluorescence results on immunoprecipitated lung S-glutathionylated eNOS in sedentary C101A-eNOS-tg (164.1 ± 14.02%, n=6, p=0.0060) and their transgenic negative littermates (C57BL/6) as well as after voluntary exercise (C57BL/6: 97.91 ± 14.93%, n=6, n.s.; C101A-eNOS-tg: 96.07 ± 11.23%, n=6, n.s., p<0.01 vs. C101A-eNOS-tg sed by 1-way ANOVA and Newman-Keuls post test).*

This work was published in

Suvorava T*, Pick S*, and Kojda G. (* equal contribution)
Selective impairment of blood pressure reduction by endothelial nitric oxide synthase dimer destabilization in mice.
J Hypertens 2017;35(1):76-88. journals.lww.com/jhypertension/

word-for-word citations within the running text stand out in italic type

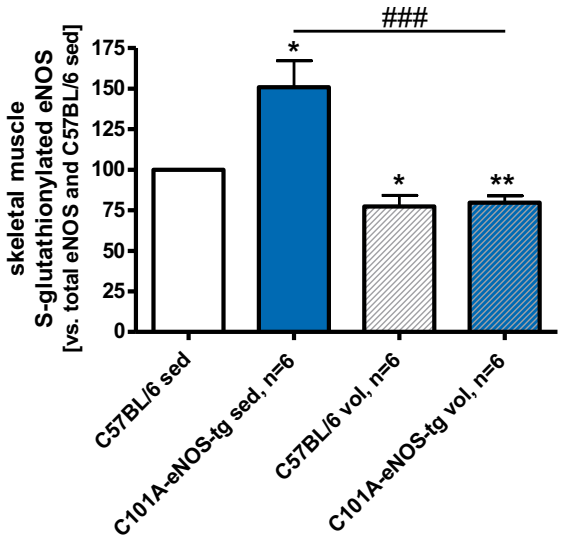

Fig. 3.95: *Evaluation of fluorescence results on immunoprecipitated skeletal muscle S-glutathionylated eNOS in sedentary C101A-eNOS-tg (150.9 ± 16.22%, n=6, p=0.0257) and their transgenic negative littermates (C57BL/6) as well as after voluntary exercise (C57BL/6: 77.41 ± 6.8%, n=6, p= 0.0211; C101A-eNOS-tg: 79.66 ± 4.206%, n=6, p=0.0047, p<0.001 vs. C101A-eNOS-tg sed by 1-way ANOVA and Newman-Keuls post test).*

3.5.4. eNOS TYROSINE-NITRATION

Evaluation of tyrosine-nitrated eNOS after immunoprecipitation of eNOS gives similar results in sedentary mice as described in the previous chapter 3.2.3. After voluntary exercise, tyrosine-nitration is significantly reduced in C101A-eNOS-tg and C57BL/6 in aortic, myocardial and skeletal muscle tissue. In contrast to the results in transgenic animals, where a significant reduction in tyrosine-nitrated eNOS is detectable after exercise, in C57BL/6 lung tissue no effect is apparent (see figs. 3.96-3.99).

This work was published in

Suvorava T*, Pick S*, and Kojda G. (* equal contribution)
Selective impairment of blood pressure reduction by endothelial nitric oxide synthase dimer destabilization in mice.
J Hypertens 2017;35(1):76-88. journals.lww.com/jhypertension/

word-for-word citations within the running text stand out in italic type

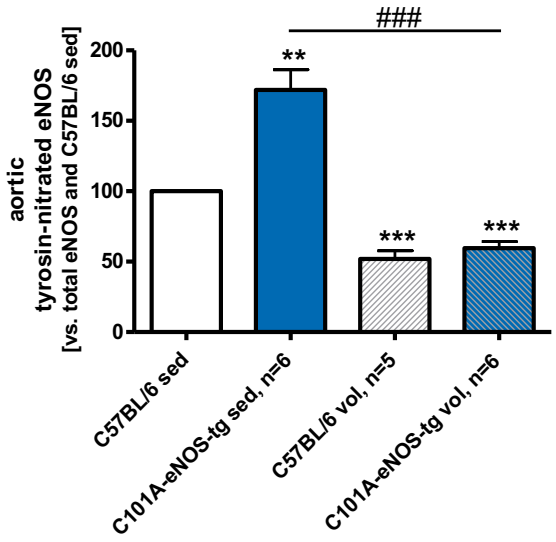

Fig. 3.96: *Evaluation of fluorescence results on immunoprecipitated aortic tyrosine-nitrated eNOS in sedentary C101A-eNOS-tg (172.0 ± 14.34%, n=6, p=0.0040) and their transgenic negative littermates (C57BL/6) as well as after voluntary exercise (C57BL/6: 51.93 ± 5.848%, n=6, p= 0.0004; C101A-eNOS-tg: 59.58 ± 4.723%, n=6, p=0.0004, p<0.001 vs. C101A-eNOS-tg sed by 1-way ANOVA and Newman-Keuls post test).*

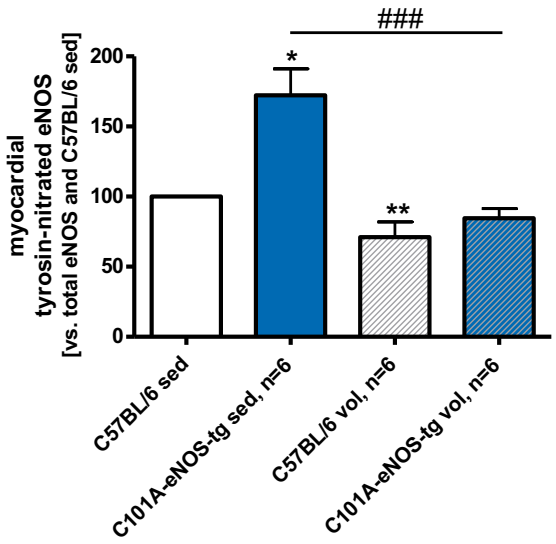

Fig. 3.97: *Evaluation of fluorescence results on immunoprecipitated myocardial tyrosine-nitrated eNOS in sedentary C101A-eNOS-tg (172.3 ± 18.88%, n=6, p=0.0123) and their transgenic negative littermates (C57BL/6) as well as after voluntary exercise (C57BL/6: 71.17 ± 10.70%, n=6, p=0.0430; C101A-eNOS-tg: 84.58 ± 6.898%, n=6, n.s., p<0.001 vs. C101A-eNOS-tg sed by 1-way ANOVA and Newman-Keuls post test).*

This work was published in

Suvorava T*, Pick S*, and Kojda G. (* equal contribution)
Selective impairment of blood pressure reduction by endothelial nitric oxide synthase dimer destabilization in mice.
J Hypertens 2017;35(1):76-88. journals.lww.com/jhypertension/

word-for-word citations within the running text stand out in italic type

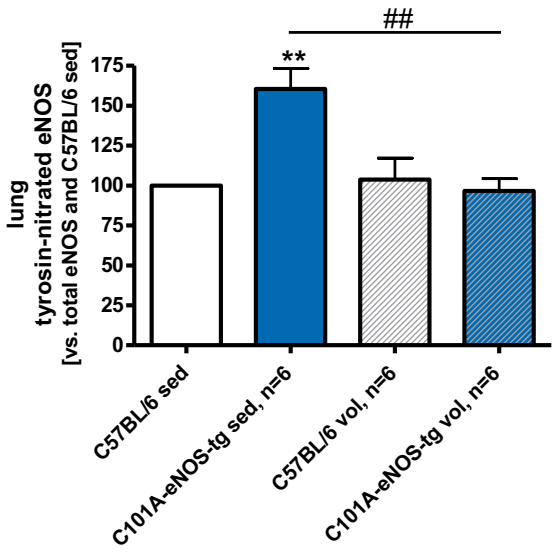

Fig. 3.98: *Evaluation of fluorescence results on immunoprecipitated lung tyrosine-nitrated eNOS in sedentary C101A-eNOS-tg (160.5 ± 12.81%, n=6, p=0.0053) and their transgenic negative littermates (C57BL/6) as well as after voluntary exercise (C57BL/6: 103.8 ± 13.88%, n=6, n.s.; C101A-eNOS-tg: 96.56 ± 7.815%, n=6, n.s., p<0.01 vs. C101A-eNOS-tg sed by 1-way ANOVA and Newman-Keuls post test).*

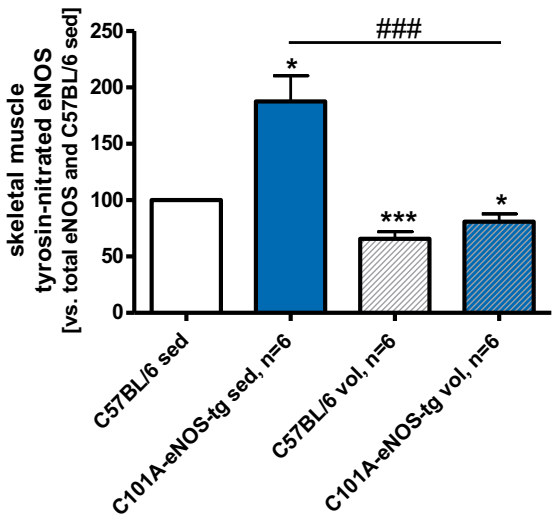

Fig. 3.99: *Evaluation of fluorescence results on immunoprecipitated skeletal muscle tyrosine-nitrated eNOS in sedentary C101A-eNOS-tg (187.5 ± 22.78%, n=6, p=0.0121) and their transgenic negative littermates (C57BL/6) as well as after voluntary exercise (C57BL/6: 65.64 ± 6.375%, n=6, p= 0.0030; C101A-eNOS-tg: 80.88 ± 7.001%, n=6, p=0.0412, p<0.001 vs. C101A-eNOS-tg sed by 1-way ANOVA and Newman-Keuls post test).*

3.5.5. PHOSPHORYLATION OF eNOS AT SER1176/9

Activation of eNOS is investigated by determination of phosphorylated eNOS at Ser1176/9. In C57BL/6 mice an increase is observable after voluntary training, whereas in C101A-eNOS-tg the basal augmented phosphorylation as compared to transgenic

This work was published in

Suvorava T*, Pick S*, and Kojda G. (* equal contribution)
Selective impairment of blood pressure reduction by endothelial nitric oxide synthase dimer destabilization in mice.
J Hypertens 2017;35(1):76-88. journals.lww.com/jhypertension/

word-for-word citations within the running text stand out in italic type

negative littermates could not be further enhanced (see figs. 3.100-3.103). Experiments are carried out using aortic, myocardial, lung and skeletal muscle samples after immunoprecipitation of eNOS and subsequent fluorescence detection.

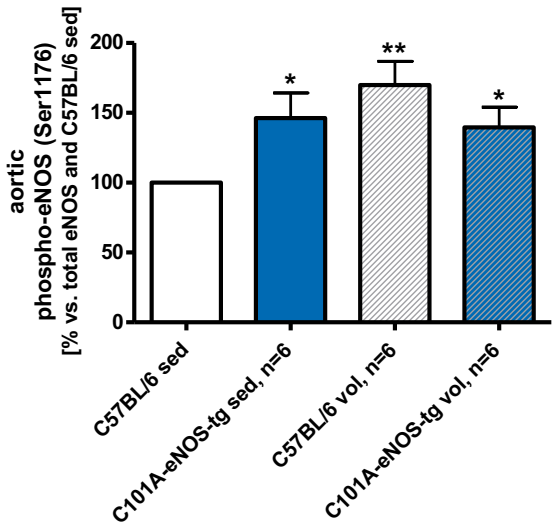

Fig. 3.100: *Evaluation of fluorescence results on immunoprecipitated aortic phosphorylated eNOS at Ser1176/9 in sedentary C101A-eNOS-tg (146.3 ± 17.99%, n=6, p=0.0499) and their transgenic negative littermates (C57BL/6) as well as after voluntary exercise (C101A-eNOS-tg: 139.9 ± 14.34%, n=6, p=0.0395; C57BL/6: 169.9 ± 16.91%, n=6, p=0.0090).*

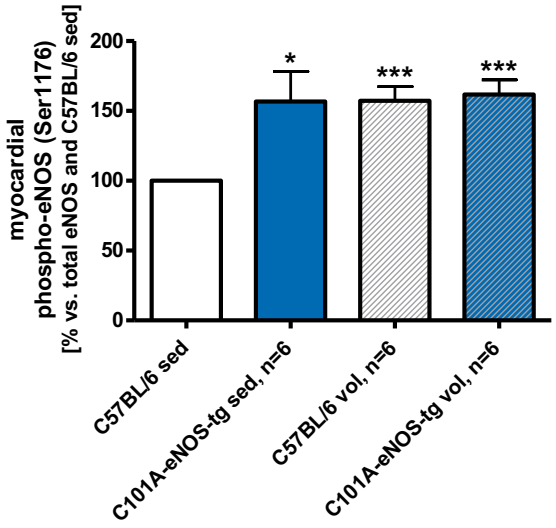

Fig. 3.101: *Evaluation of fluorescence results on immunoprecipitated myocardial phosphorylated eNOS at Ser1176/9 in sedentary C101A-eNOS-tg (156.7 ± 21.60%, n=6, p=0.0469) and their transgenic negative littermates (C57BL/6) as well as after voluntary exercise (C101A-eNOS-tg: 161.7 ± 10.48%, n=6, p=0.0020; C57BL/6: 157.2 ± 10.20%, n=6, p=0.0025).*

This work was published in

Suvorava T*, Pick S*, and Kojda G. (* equal contribution)
Selective impairment of blood pressure reduction by endothelial nitric oxide synthase dimer destabilization in mice.
J Hypertens 2017;35(1):76-88. journals.lww.com/jhypertension/

word-for-word citations within the running text stand out in italic type

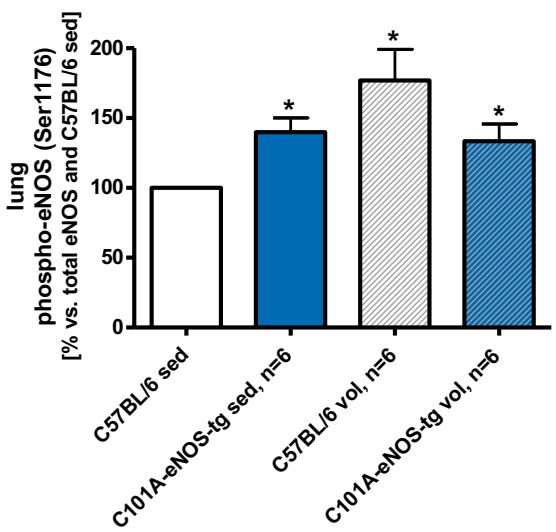

Fig. 3.102: *Evaluation of fluorescence results on immunoprecipitated lung phosphorylated eNOS at Ser1176/9 in sedentary C101A-eNOS-tg (139.9 ± 10.21%, n=6, p=0.0113) and their transgenic negative littermates (C57BL/6) as well as after voluntary exercise (C101A-eNOS-tg: 133.4 ± 12.31%, n=6, p=0.0419; C57BL/6: 176.9 ± 22.27%, n=6, p=0.0181).*

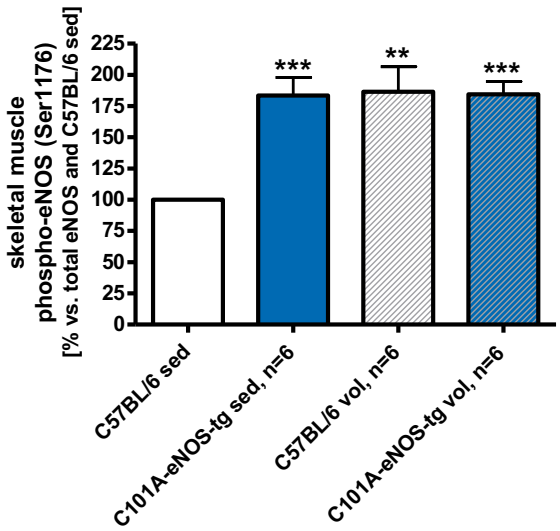

Fig. 3.103: *Evaluation of fluorescence results on immunoprecipitated skeletal muscle phosphorylated eNOS at Ser1176/9 in sedentary C101A-eNOS-tg (183.4 ± 14.59%, n=6, p=0.0023) and their transgenic negative littermates (C57BL/6) as well as after voluntary exercise (C101A-eNOS-tg: 184.4 ± 10.41%, n=6, p=0.0005; C57BL/6: 186.5 ± 20.13%, n=6, p=0.0077).*

3.5.5.1. PHOSPHORYLATION OF AMPK AT THR172

Activation of eNOS by phosphorylation at Ser1176/9 is likely to be driven by AMPKα activation. This is confirmed by results obtained on its own phosphorylation at Thr172. In aortic (50 µg total protein loaded) and skeletal muscle (100 µg total protein loaded) tissue of C57BL/6 an increase in phosphorylation of AMPKα is detectable by Western

This work was published in

Suvorava T*, Pick S*, and Kojda G. (* equal contribution)
Selective impairment of blood pressure reduction by endothelial nitric oxide synthase dimer destabilization in mice.
J Hypertens 2017;35(1):76-88. journals.lww.com/jhypertension/

word-for-word citations within the running text stand out in italic type

Blot analysis, whereas total expression remains unchanged. Similar to the results obtained on phosphorylation of eNOS at Ser1176/9 (3.5.5), in C101A-eNOS-tg, a further increase of the already augmented basal level of AMPKα phosphorylation seems to be not possible (see figs. 3.104-3.107). Total expression is as well not affected at all in the transgenic strain.

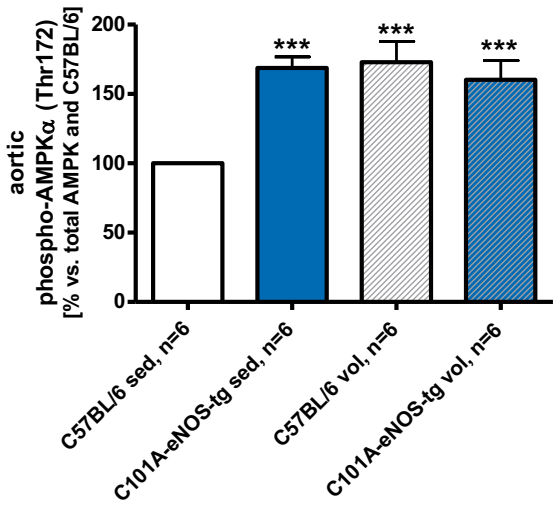

Fig. 3.104: *Evaluation of Western Blot results on aortic AMPKα phosphorylation at Thr172 in sedentary C101A-eNOS-tg (168.7 ± 7.982%, n=6, p=0.0003) and their transgenic negative littermates (C57BL/6) as well as after voluntary exercise (C101A-eNOS-tg: 160.3 ± 13.76%, n=6, p=0.0071; C57BL/6: 172.9 ± 14.97%, n=6, p=0.0046).*

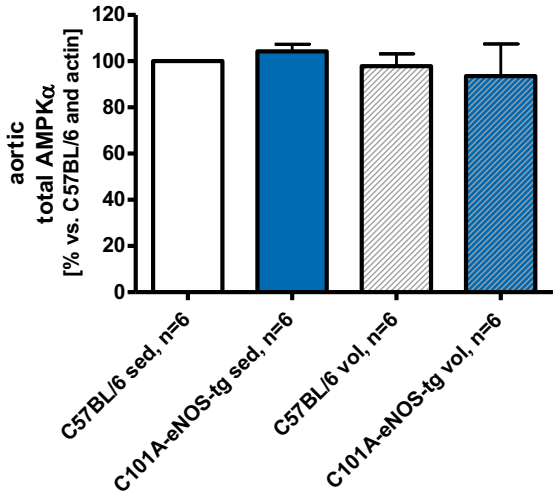

Fig. 3.105: *Evaluation of Western Blot results on aortic AMPKα expression in sedentary C101A-eNOS-tg (104.2 ± 3.154%, n=6) and their transgenic negative littermates (C57BL/6) as well as after voluntary exercise (C101A-eNOS-tg: 97.89 ± 5.213%, n=6, n.s.; C57BL/6: 93.52 ± 13.91%, n=6, n.s.).*

This work was published in

Suvorava T*, Pick S*, and Kojda G. (* equal contribution)
Selective impairment of blood pressure reduction by endothelial nitric oxide synthase dimer destabilization in mice.
J Hypertens 2017;35(1):76-88. journals.lww.com/jhypertension/

word-for-word citations within the running text stand out in italic type

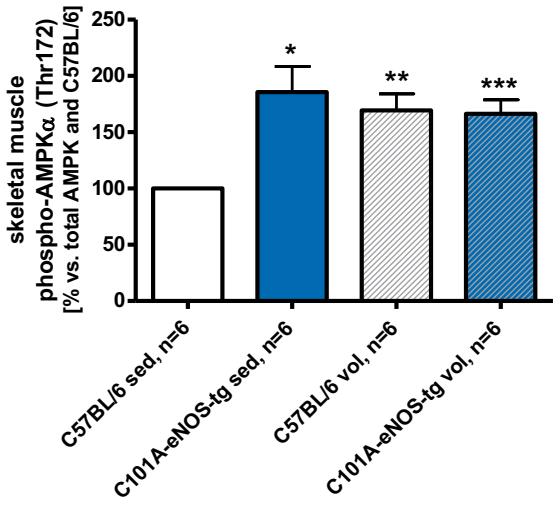

Fig. 3.106: *Evaluation of Western Blot results on skeletal muscle AMPKα phosphorylation at Thr172 in sedentary C101A-eNOS-tg (185.6 ± 22.79%, n=6, p=0.0132) and their transgenic negative littermates (C57BL/6) as well as after voluntary exercise (C101A-eNOS-tg: 166.3 ± 12.50%, n=6, p=0.0032; C57BL/6: 169.3 ± 14.74%, n=6, p=0.0053).*

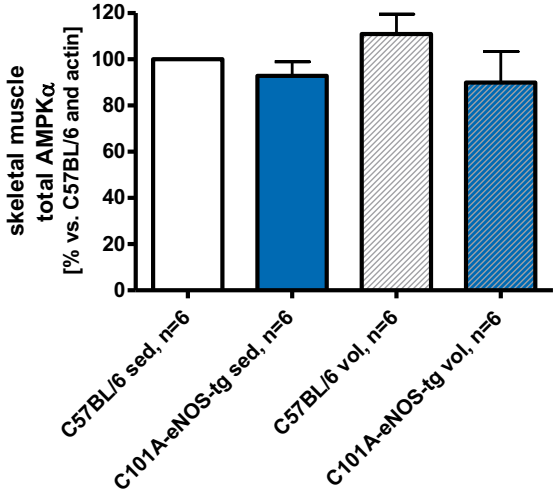

Fig. 3.107: *Evaluation of Western Blot results on skeletal muscle AMPKα expression in C101A-eNOS-tg (92.87 ± 6.077%, n=6, n.s.) and their transgenic negative littermates (C57BL/6) as well as after voluntary exercise (C101A-eNOS-tg: 89.91 ± 13.49%, n=6, n.s.; C57BL/6: 110.9 ± 8.656%, n=6, n.s.).*

3.5.5.2. PHOSPHORYLATION OF AKT AT SER473

As already observed previously (3.2.4.2 and 3.4.5.2), no changes in phosphorylation of Akt at Ser473 is detectable. After voluntary training this fact is as well the case, suggesting Akt not being involved in shear-dependent activation of eNOS. Results are obtained by performing Western Blots analysis using 50 µg of total aortic protein and 100 µg of total skeletal muscle protein of C101A-eNOS-tg and their transgenic negative littermates. Neither for phosphorylation nor for total expression of Akt changes are detectable (see figs. 3.108-3.111).

This work was published in

Suvorava T*, Pick S*, and Kojda G. (* equal contribution)
Selective impairment of blood pressure reduction by endothelial nitric oxide synthase dimer destabilization in mice.
J Hypertens 2017;35(1):76-88. journals.lww.com/jhypertension/

word-for-word citations within the running text stand out in italic type

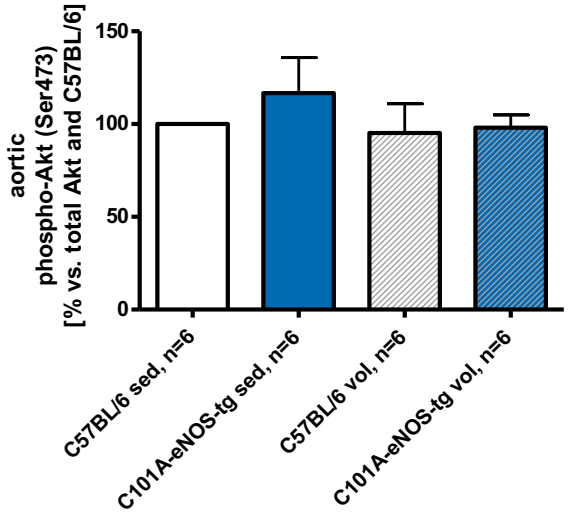

Fig. 3.108: *Evaluation of Western Blot results on aortic Akt phosphorylation at Ser473 in sedentary C101A-eNOS-tg (116.7 ± 19.10%, n=6, n.s.) and their transgenic negative littermates (C57BL/6) as well as after voluntary exercise (C101A-eNOS-tg: 98.08 ± 6.891%, n=6, n.s.; C57BL/6: 95.20 ± 15.74%, n=6, n.s.).*

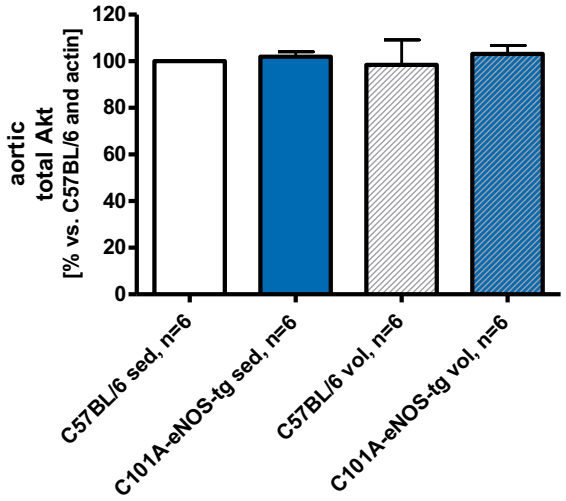

Fig. 3.109: *Evaluation of Western Blot results on aortic Akt expression in sedentary C101A-eNOS-tg (101.9 ± 2.080%, n=6, n.s.) and their transgenic negative littermates (C57BL/6) as well as after voluntary exercise (C101A-eNOS-tg: 103.2 ± 3.567%, n=6, n.s.; C57BL/6: 98.49 ± 10.67%, n=6, n.s.).*

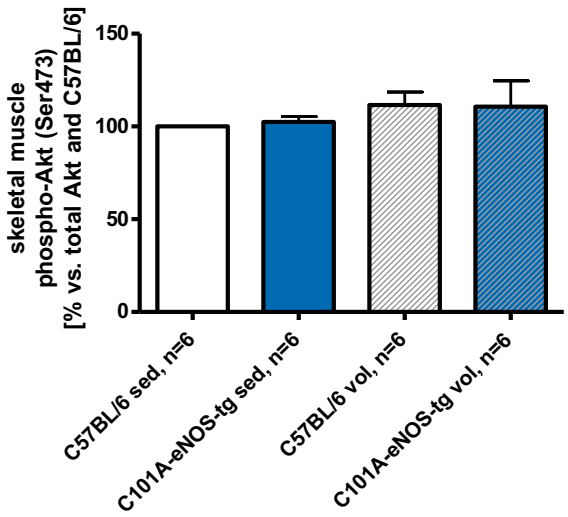

Fig. 3.110: *Evaluation of Western Blot results on skeletal muscle Akt phosphorylation at Ser473 in sedentary C101A-eNOS-tg (102.4 ± 2.923%, n=6, n.s.) and their transgenic negative littermates (C57BL/6) as well as after voluntary exercise (C101A-eNOS-tg: 110.6 ± 13.97%, n=6, n.s.; C57BL/6: 111.6 ± 6.965%, n=6, n.s.).*

This work was published in

Suvorava T*, Pick S*, and Kojda G. (* equal contribution)
Selective impairment of blood pressure reduction by endothelial nitric oxide synthase dimer destabilization in mice.
J Hypertens 2017;35(1):76-88. journals.lww.com/jhypertension/

word-for-word citations within the running text stand out in italic type

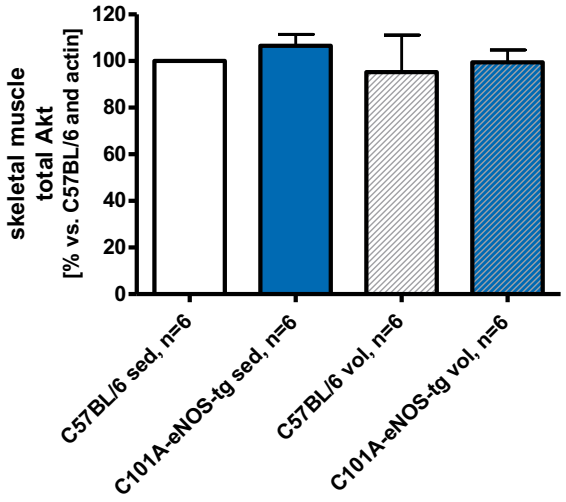

Fig. 3.111: *Evaluation of Western Blot results on skeletal muscle Akt expression in sedentary C101A-eNOS-tg (106.6 ± 4.877%, n=6, n.s.) and their transgenic negative littermates (C57BL/6) as well as after voluntary exercise (C101A-eNOS-tg: 99.46 ± 5.264%, n=6, n.s.; C57BL/6: 95.27 ± 15.84%, n=6, n.s.).*

3.5.6. PHOSPHORYLATION OF VASP AT SER239

In order to check if an activation of the NO/cGMP-pathway plays a role in this study, phosphorylated VASP at Ser239 is investigated by performing Western Blot analysis. Indeed, by voluntary exercise training an increased phosphorylation is detectable in C101A-eNOS-tg and as well in C57BL/6. In sedentary mice there is no difference between the transgenic mice and their transgenic negative littermates (see figs. 3.112-3.113), which fits to the results presented in 3.3.4.

This work was published in

Suvorava T*, Pick S*, and Kojda G. (* equal contribution)
Selective impairment of blood pressure reduction by endothelial nitric oxide synthase dimer destabilization in mice.
J Hypertens 2017;35(1):76-88. journals.lww.com/jhypertension/

word-for-word citations within the running text stand out in italic type

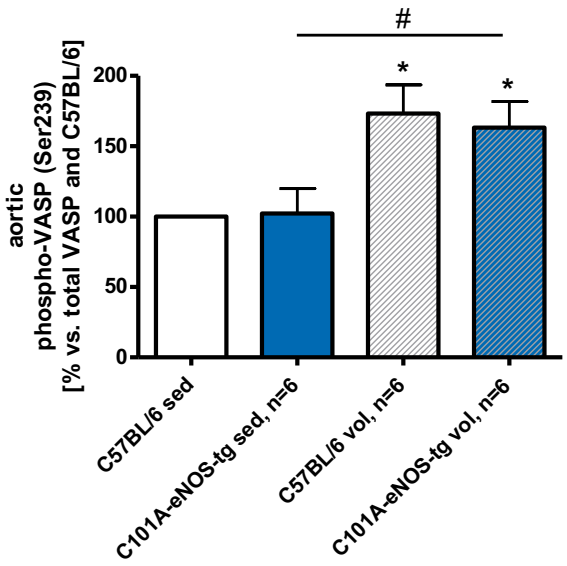

Fig. 3.112: *Evaluation of Western Blot results on aortic VASP phosphorylation at Ser239 in sedentary C101A-eNOS-tg (102.2 ± 17.69%, n=6, n.s.) and their transgenic negative littermates (C57BL/6) as well as after voluntary exercise (C101A-eNOS-tg: 163.3 ± 18.42%, n=6, p=0.0186, p<0.05 vs. C101A-eNOS-tg sed by 1-way ANOVA and Newman-Keuls post test; C57BL/6: 173.2 ± 20.44%, n=6, p=0.0159).*

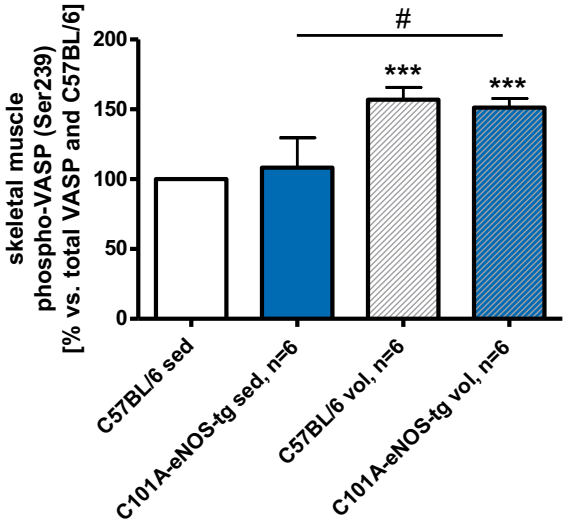

Fig. 3.113: *Evaluation of Western Blot results on skeletal muscle VASP phosphorylation at Ser239 in sedentary C101A-eNOS-tg (108.3 ± 21.34%, n=6, n.s.) and their transgenic negative littermates (C57BL/6) as well as after voluntary exercise (C101A-eNOS-tg: 151.2 ± 6.529%, n=6, p=0.0005, p<0.05 vs. C101A-eNOS-tg sed by 1-way ANOVA and Newman-Keuls post test; C57BL/6: 156.9 ± 8.778%, n=6, p=0.0013).*

This work was published in

Suvorava T*, Pick S*, and Kojda G. (* equal contribution)
Selective impairment of blood pressure reduction by endothelial nitric oxide synthase dimer destabilization in mice.
J Hypertens 2017;35(1):76-88. journals.lww.com/jhypertension/

word-for-word citations within the running text stand out in italic type

4. DISCUSSION

Essential hypertension is associated with an impairment of endothelium-dependent vasodilation, one of the characteristics of a state known as endothelial dysfunction. This is a multifactorial phenomenon in which the so-called eNOS 'uncoupling', the desensitization of sGC, the nitration, the inactivation of prostacyclin synthase (CYP8A1), the oxidative activation of endothelin-1, and the direct inactivation of NO by $O_2^{-\bullet}$ play a concomitant role [81]. In this study, the focus is on the increase in oxidative stress and, thus, the decrease in NO bioavailability – more precisely, the reaction of endogenous NO with $O_2^{-\bullet}$ by the formation of peroxynitrite within the endothelium [4,46]. This reduction of bioavailable NO further results in a lower efficacy of NO/cGMP-signal transduction pathway in smooth muscle cells, leading to an impact on vasorelaxation. Here, NO has an effect on sGC, which is further inhibited in expression and activity by $O_2^{-\bullet}$ and peroxynitrite [82]. Additionally, peroxynitrite oxidizes BH_4, which has an impact on eNOS dimer formation [83]. This 'uncoupling' leads to an increased production of ROS, like $O_2^{-\bullet}$, again scavenging proximate vasodilating NO under formation of peroxynitrite, ending up in a vicious cycle and potentiating oxidative stress. In several animal studies with experimental hypertension, for example, by angiotensin II infusion, deoxycorticosterone-acetate-salt treatment or genetic modification, a coincidence of elevated ROS was evidenced [46]. But, so far, nothing is known about the role of vascular oxidative stress in normotensive states. eNOS plays a key role in the endogenous synthesis of the radicals NO and $O_2^{-\bullet}$ within the endothelium, which is indispensable for the physiological regulation of the vascular tone and, thus, for the regulation of blood pressure [84]. But *the specific role of eNOS-dependent formation of $O_2^{-\bullet}$ and thus the impact of endothelial oxidative stress on the regulation of blood pressure* are still unclear.

The aim of this study is to investigate the influence of eNOS dimer stability on the regulation of blood pressure. In the states in which eNOS is 'uncoupled', one mechanism is that the balance between NO and $O_2^{-\bullet}$ shifts towards $O_2^{-\bullet}$ [26]. Therefore, an animal model with an endothelial-specific overexpression of a dimer-destabilized eNOS mutant

This work was published in

Suvorava T*, Pick S*, and Kojda G. (* equal contribution)
Selective impairment of blood pressure reduction by endothelial nitric oxide synthase dimer destabilization in mice.
J Hypertens 2017;35(1):76-88. journals.lww.com/jhypertension/

word-for-word citations within the running text stand out in italic type

in C57BL/6 is used to determine the generation of oxidative and nitrosative stress and their influence on blood pressure, as well as the effect of shear-dependent activation of eNOS.

In this experimental study, it is shown that *endothelial-specific 1.5-fold overexpression of a dimer-destabilized eNOS mutant in C57BL/6* (C101A-eNOS-tg), *proven by the colocalization of CD31 (PECAM-1) and eNOS* [85], *generates endothelial oxidative stress, as evidenced by an increased formation of $O_2^{-\bullet}$, as well as posttranslational protein modifications* like eNOS tyrosine-nitration and S-glutathionylation. As a result of increased oxidative stress, eNOS is hyperphosphorylated at Ser1176/9 in C101A-eNOS-tg. This presumably prevents eNOS-induced reduction of blood pressure but has no effect on endothelium-dependent relaxation *in an otherwise healthy and normotensive mouse strain*. Hyperphosphorylation is driven by an activation of AMPKα and cannot be further increased by shear-dependent forces via Akt. Treatment with the antioxidant Tempol® reveals a significant and reversible reduction of blood pressure indicating a causal role for ROS generated by dimer-destabilized eNOS here, whereas Tempol® has no effect in C57BL/6.

These data strongly suggest that the dimer-destabilization of eNOS and the resulting increase of endothelium-specific $O_2^{-\bullet}$ generation are *involved in the regulation of blood pressure in C101A-eNOS-tg.* Thus, alterations in eNOS activity, which induce the production of oxidative and nitrosative stress within the endothelium of resistance vessels, might contribute to the initiation of essential hypertension.

4.1. eNOS Mutation

The transgenic mouse model C101A-eNOS-tg is characterized by the coexistence of normal and dimer-destabilized eNOS. Active eNOS is a dimer that is coordinated via two cysteines, each binding to a central Zn-ion [19]. This study is based on a mutant eNOS in which one of the essential cysteine residues, Cys101, is replaced by alanine. As expected, this C101A-eNOS cannot form a stable dimer, and this cannot even be rescued by the

This work was published in

Suvorava T*, Pick S*, and Kojda G. (* equal contribution)
Selective impairment of blood pressure reduction by endothelial nitric oxide synthase dimer destabilization in mice.
J Hypertens 2017;35(1):76-88. journals.lww.com/jhypertension/

word-for-word citations within the running text stand out in italic type

application of supraphysiological levels of the potentially rescuing cofactor BH_4 to the isolated enzyme [58,59]. The destabilization of eNOS is further proven by native gel electrophoresis, which shows a more prominent monomer band in C101A-eNOS-tg and an equal dimer band as compared to transgenic negative littermates.

Mutations of these residues responsible for the Zn-finger coordination have been shown to inhibit dimeriziation and, thus, the generation of NO: For example, in a human eNOS mutation of cysteine 99 to alanine, *a reduction of BH_4 affinity, enzyme stability, citrulline formation and an irreversible loss of heme were* observable [45]. *The decreased stability of the human eNOS C99A mutant could be confirmed by gel filtration analysis, in which the mutant enzyme appeared as a mixture of dimer and monomer* [86]. *Another investigation on C94A, C99A and C94A plus C99A mutations of human eNOS also confirmed the destabilization of dimer formation and showed a small catalytic activity (<10 %) of the purified mutated enzymes* [87]. In contrast, it was found that *a C96S/C101S double mutant of bovine eNOS expressed* in COS-7 cells *showed about 50 % of the catalytic activity of wild-type eNOS despite strong dimer-destabilization* with no dimer appearance following low-temperature gel separation [88]. These reports are consistent with previous findings of this workgroup in stably transfected HEK 293 *in which the mutant C101A-eNOS activity was 45 % lower* than that in the wild-type enzyme [58,59]. Moreover, in this study, it was observed that $O_2^{-\bullet}$ generation by C101A-eNOS in HEK 293 as measured with electron-spin-resonance was doubled, suggesting that the idea of mutation was successfully implemented considering dimer-destabilization and a shift in ROS formation.

4.2. eNOS Protein Overexpression

The protein sequences of murine and bovine eNOS show a consistency of 90.9%. Therefore, the used antibodies could detect eNOS of both species. Total eNOS is significantly overexpressed in eNOS-tg and C101A-eNOS-tg as shown by Western Blot analysis in aortic, myocardial, lung and skeletal muscle tissue.

This work was published in

Suvorava T*, Pick S*, and Kojda G. (* equal contribution)
Selective impairment of blood pressure reduction by endothelial nitric oxide synthase dimer destabilization in mice.
J Hypertens 2017;35(1):76-88. journals.lww.com/jhypertension/

word-for-word citations within the running text stand out in italic type

Of note, the mRNA expression of native murine eNOS is decreased in eNOS-tg as well as in C101A-eNOS-tg, and additionally, there is a stronger expression of bovine eNOS-mRNA in eNOS-tg than in C101A-eNOS-tg. This suggests that murine eNOS is downregulated by the introduced bovine eNOS, presuming that the content of bovine eNOS protein, native or destabilized, is greater than the amount of detected overexpression.

4.3. eNOS and Oxidative Stress

The transgenic mouse model used in this study, C101A-eNOS-tg, *is characterized by the coexistence of normal and dimer-destabilized eNOS in the endothelium of otherwise healthy mice without any signs of cardiovascular disease. Likewise, such concomitant generation of NO by wild-type enzyme and $O_2^{-\bullet}$ by C101A-eNOS itself might resemble the situation in endothelial cells of pathologic vessels in which dysfunctional 'uncoupled' and functional coupled eNOS molecules can exist in the same cell at the same time* [89]. The *dimer-destabilization of eNOS is evidenced by an increase of eNOS monomer appearance* while *separating aortic homogenates on low-temperature gels*. Cold conditions of 4°C have to be obeyed carefully here, as proteins can denaturate on the gel. Therefore, the running speed has to be downregulated in order to prevent a temperature rise, but it should not be too slow as blurring increases due to diffusion effects. To prevent from erroneously detected increased monomer levels by accidently denaturating conditions on the gel itself, probes of C101A-eNOS-tg are compared with wildtype probes which show a more prominent dimer band. This also proves the fact, that eNOS dimers are resistant to denaturating effects of SDS [83].

Furthermore, an increase in $O_2^{-\bullet}$ formation by C101A-eNOS is evident in C101A-eNOS-tg. This can be abolished by the NOS-inhibitor *L-NAME, identifying C101A-eNOS as the underlying source. In addition, the strong increase of $O_2^{-\bullet}$-dependent protein modifications, such as* protein phosphorylation, *tyrosine-nitration, and S-glutathionylation in C101A-eNOS-tg demonstrate the biological relevance of increased*

This work was published in

Suvorava T*, Pick S*, and Kojda G. (* equal contribution)
Selective impairment of blood pressure reduction by endothelial nitric oxide synthase dimer destabilization in mice.
J Hypertens 2017;35(1):76-88. journals.lww.com/jhypertension/

word-for-word citations within the running text stand out in italic type

$O_2^{-\bullet}$. To investigate protein modifications, eNOS has to be accumulated by immunoprecipitation. This is carried out by using magnetical antibody-preloaded beads. The analysis is accomplished by incubation with specific antibodies to detect phosphorylated eNOS, S-gluthathionylated eNOS or tyrosine-nitrated eNOS. Finally, the detection is done with fluorescent dye antibodies: To ensure the specificity of the method, several negative control experiments are performed on each set. Thus, incubation with dyes, which would not give a signal, and which are used during the following procedure, is done. These controls also ensure the binding of the particular target in its step, as certain dyes might give a signal if no binding is achieved. For example, after the binding of eNOS protein from tissue lysate, no signal can be achieved after the application of anti-rabbit dye, whereas this particular dye gives a signal on the beads themselves or the bound polyclonal anti-eNOS antibody respectively. This control experiment, thus, ensures saturated binding. Additionally, the whole on-bead-construct is denaturated and applied on a Western Blot. A band at 135 kDa indicates that eNOS protein is present. Finally, to ensure the detection of eNOS-tyrosine-nitration, a costaining of 3-nitrotyrosine and total eNOS is performed after elution and running a Western Blot (see fig. 2.11B).

In contrast, the overexpression of wild-type eNOS in eNOS-tg does not increase $O_2^{-\bullet}$ formation, tyrosine nitration or S-glutathionylation, which further indicates that the impairment of eNOS dimerization is the cause of oxidative stress in C101A-eNOS-tg. Similar results, that is the absence of increased oxidative stress, were obtained by investigating another colony harboring a stronger endothelium-specific overexpression of wild-type eNOS [37]. Furthermore, S-glutathionylation does not only seem to be an outcome of increased oxidative stress but also a mechanism leading to eNOS 'uncoupling' itself as it reversibly decreases NO generation and increases $O_2^{-\bullet}$ production. In endothelial cells, eNOS S-glutathionylation comes along with impaired endothelium-dependent vasorelaxation as seen in blood vessels of hypertensive animals: Here, S-glutathionylation is increased and endothelium-dependent vasorelaxation is decreased [14].

This work was published in

Suvorava T*, Pick S*, and Kojda G. (* equal contribution)
Selective impairment of blood pressure reduction by endothelial nitric oxide synthase dimer destabilization in mice.
J Hypertens 2017;35(1):76-88. journals.lww.com/jhypertension/

word-for-word citations within the running text stand out in italic type

Superoxide dismutases are enzymes that catalyze the reaction of $O_2^{-\bullet}$ to hydrogen peroxide:

$$2\ O_2^{-\bullet} + 2\ H^+ \rightarrow H_2O_2 + O_2$$

This reaction competes with the formation of peroxynitrate from $O_2^{-\bullet}$ and NO, which is actually 5 times faster. The catalytic reaction is favorized upon increased expression levels of SOD [36].

There are three known major groups of SODs, depending on the protein fold and the metal cofactor in the reactive center: the mostly eukaryotic Cu/Zn-type, binding both copper and zinc, the prokaryotic and mitochondrial Fe- and Mn-type, binding either iron or manganese, and the prokaryotic Ni-type, binding nickel. In humans, three forms of SOD are present: The soluble SOD1 is located in the cytoplasm, SOD2 in the mitochondria, and SOD3 is extracellular and in this study referred to as ecSOD. The dimeric SOD1 and the tetrameric SOD3 contain copper and zinc, whereas the mitochondrial and also tetrameric SOD2 contains manganese. The antioxidant and SOD-mimetic Tempol® catalyzes the enzymatic reaction mentioned above.

ecSOD is expressed in the vasculature by smooth muscle cells and secreted to the interstitium subsequently [90,91]. Here, between the endothelial layer and the smooth muscle, the highest concentrations of ecSOD occur. 99% can be found tissue-bound, e.g. to polyanionic sites such as heparin sulphates at the outer membrane of endothelial cells. It is suggested to be protective for NO while it traverses from the endothelium to the layer of smooth muscle cells on the vascular wall [91,92].

Regarding the enzyme ecSOD itself, the outcome of this study is consistent with the previous findings, e.g. in eNOS overexpressing mice [91], which describe an upregulation due to the higher bioavailability of NO, as it is existent in eNOS-tg [80]. High levels of its substrate $O_2^{-\bullet}$ do not seem to have an effect on ecSOD expression levels, as seen in C101A-eNOS-tg. Thus, expression levels of ecSOD are supposedly a marker for NO bioavailability. Surprisingly, after the treatment of C101A-eNOS-tg with Tempol® and

This work was published in

Suvorava T*, Pick S*, and Kojda G. (* equal contribution)
Selective impairment of blood pressure reduction by endothelial nitric oxide synthase dimer destabilization in mice.
J Hypertens 2017;35(1):76-88. journals.lww.com/jhypertension/

word-for-word citations within the running text stand out in italic type

shifting the balance towards NO, no increase can be seen in the expression of ecSOD. Supposedly, there is a leveling effect of the SOD-mimetic Tempol®.

C101A-eNOS mutation provokes a shifted balance in the production of either NO or $O_2^{-\bullet}$. As shown by lucigenin-enhanced chemiluminescence, an increase in $O_2^{-\bullet}$ is measurable in C101A-eNOS-tg. This method is very sensitive, but the reaction conditions have to be obeyed carefully: A concentration of 5μM should not be exceeded, otherwise eNOS and its substrate NADPH can likely reduce lucigenin which in succession reduces oxygen to $O_2^{-\bullet}$ [93]. To ensure that eNOS is the source of $O_2^{-\bullet}$, the NOS-inhibitor L-NAME is applied to the reaction. This masks the generation of photons as well as the application of the antioxidant Tempol®. The former inhibits the generation of $O_2^{-\bullet}$ itself and the latter scavenges $O_2^{-\bullet}$ already generated by eNOS.

4.4. eNOS Dimer-Destabilization and Aortic Reactivity

Surprisingly, aortic endothelium-dependent relaxation by endogenous NO in response to acetylcholine is normal in C101A-eNOS-tg *despite considerable oxidative stress, whereas endothelium-dependent relaxation impairment was clearly detectable in various animal models with similar oxidative stress*: in stroke-prone spontaneously hypertensive rats [39,94], in rats with hypertension after 5-day angiotensin II-infusion [95], in arteries of interleukin 10-deficient mice after overnight angiotensin II-incubation [96], in apoE-deficient mice [97], and in mice with renovascular hypertension after renal artery clipping [98]. *Although the reasons for this somewhat contradictory finding are not known, it seems likely that concomitant disease processes, such as atherosclerosis, overt hypertension, or diabetes contributed to endothelial dysfunction in these studies. For example, pharmacological normalization of increased aortic $O_2^{-\bullet}$ generation in a rabbit model of atherosclerosis did only partially restore the aortic endothelium-dependent relaxation and the reduced sensitivity to NO-donors* [99]. In this study, *an unchanged endothelium-independent vasodilator response to exogenous NO by the NO-donor SNAP in the aortic rings of C101A-eNOS-tg* is also observed. This indicates that the signal

This work was published in

Suvorava T*, Pick S*, and Kojda G. (* equal contribution)
Selective impairment of blood pressure reduction by endothelial nitric oxide synthase dimer destabilization in mice.
J Hypertens 2017;35(1):76-88. journals.lww.com/jhypertension/

word-for-word citations within the running text stand out in italic type

transduction in response to NO via the cGMP pathway is proceeding normally. *These data confirm that increased $O_2^{-\bullet}$ formation in C101A-eNOS-tg had little impact on NO-induced vasodilation of conductance arteries in otherwise healthy adult mice.*

4.5. eNOS AND BLOOD PRESSURE

The effect of eNOS on blood pressure is undeniable. On the one hand, in mice, eNOS deficiency [50] as well as oral treatment with the NOS-inhibitor L-NAME [54] result in significant hypertension and on the other hand, as shown in eNOS-tg, eNOS overexpression leads to a decrease in blood pressure. This indicates a functional enzyme, hence, the production of NO. This increase in NO bioavailability can be inhibited with the NOS-inhibitor L-NA specifying eNOS as the source of blood pressure-reducing NO [37]. Additionally, an increase in VASP-phosphorylation can be taken as evidence for enhanced eNOS functionality and, thus, NO production. VASP is an actin regulatory protein of the group eNA/VASP-proteins, which have a prolin-rich central region and are substrates for the protein kinases A and G in vertebrates [100]. VASP is phosphorylated by various proteins at three different sites: Protein kinase A mainly phosphorylates at Ser157, whereas PKG preferably phosphorylates at Ser239, and Thr278 is phosphorylated nonspecifically [79]. In order to determine the PK G activity and, thus, the activity of the NO-cGMP-signaling pathway, phosphorylation of VASP at Ser239 can be detected by using a specific antibody [101]. This is reversible by the treatment with L-NA, giving another hint for being dependent on NOS activity [37]. As seen in this study, phosphorylation is enhanced in tissues like aorta, skeletal muscle, lung and myocardium of eNOS-tg, but not of C101A-eNOS-tg, indicating that the overexpression of eNOS does not result in an increase in NO bioavailability here.

Additionally, and notwithstanding eNOS overexpression, C101A-eNOS-tg are normotensive despite destabilization of the protein. A reduction in blood pressure *following* the *endothelial-specific overexpression of normal eNOS has been demonstrated by different groups*: The *expression levels of eNOS, ranging between a three-fold* [37,48] *and an eight-fold increase* [102], *resulted in a comparable reduction*

This work was published in

Suvorava T*, Pick S*, and Kojda G. (* equal contribution)
Selective impairment of blood pressure reduction by endothelial nitric oxide synthase dimer destabilization in mice.
J Hypertens 2017;35(1):76-88. journals.lww.com/jhypertension/

word-for-word citations within the running text stand out in italic type

in *blood pressure, suggesting that the effect of endothelial eNOS overexpression on blood pressure regulation is limited*. But in C101A-eNOS-tg *neither blood pressure nor VASP-Ser239-phosphorylation, a measure for PKG activity and a surrogate for NO bioavailability* [103], *are altered*. One may presume that in C101A-eNOS-tg, an overexpression of eNOS does not result in an increase in NO bioavailability due to the destabilization of the protein. Since *the only difference between normal eNOS and C101A-eNOS is the generation of increased endothelial* $O_2^{-\bullet}$ *and oxidative protein modifications, wild-type and C101A-eNOS-tg* are treated *with Tempol®, a low molecular superoxide dismutase mimetic with known efficacy in hypertensive animal models* [104].

Indeed, *the observed reversible blood pressure reduction of approximately 5 mmHg induced by Tempol® resembles the calculated reduction* (see fig. 3.78) *and is consistent with the* hypothesis *that oxidative stress* generated by destabilized eNOS in C101A-eNOS-tg *inhibits the hypotensive effects of NO* by eNOS overexpression.

These data extend the previous findings on impaired eNOS activity induced by dimer-destabilization in overt experimental hypertension [105-107] *to the physiological blood pressure regulation*. They *suggest that the dimer-destabilization of eNOS, for example, induced by known cardiovascular risk factors, might contribute to the pathophysiology of essential hypertension*.

4.6. eNOS and Physical Activity

eNOS phosphorylation at Ser1177/9 stimulates the electron flow within the reductase domain, increases Ca^{2+} sensitivity and, thus, activates the enzyme [108,109]. Moreover, shear stress elicits phosphorylation by the activation of protein kinase A, which is why exercise training is performed. It has been shown to increase the phosphorylation of either eNOS or AMPKα in C57BL/6 [110]. Mice undergo a voluntary treadmill training after singularization for six weeks. This training protocol is chosen because of its similarity to endurance training, as it matches individually preferred training time, speed and duration. Furthermore, the mice do not suffer from additional stress factors, such

This work was published in

Suvorava T*, Pick S*, and Kojda G. (* equal contribution)
Selective impairment of blood pressure reduction by endothelial nitric oxide synthase dimer destabilization in mice.
J Hypertens 2017;35(1):76-88. journals.lww.com/jhypertension/

word-for-word citations within the running text stand out in italic type

as undergoing the experimental procedure of forced physical activity or mice moving freely in groups due to the aggressive nature of the C57BL/6 strain [60]. The running distance does not differ between C57BL/6 and C101A-eNOS-tg and training efficacy is evidenced by the measurement of the heart weight/body weight ratio, which increases significantly after training in both strains, indicating cardiovascular adaptation. This exercise training induces no alterations in C101A-eNOS-tg blood pressure or the phosphorylation state.

4.7. POSTTRANSLATIONAL eNOS MODIFICATIONS

Although there is *no inhibition of aortic endothelium-dependent relaxation, oxidative stress induced by dimer-destabilization might impair the activation of eNOS by physical forces, including shear* stress, which has been shown not only to increase the vascular generation of reactive oxygen species [111], but also to activate endothelial NO production and to increase vascular eNOS expression [112,113]. *This activation is largely mediated by eNOS-Ser1176/9-phosphorylation and is considered to be the most important physiological stimulus for the continuous generation of vascular NO in vivo* [76,77]. *A significantly increased phosphorylation of eNOS at Ser1176/9 and of AMPKα at Thr172* is observed *in sedentary C101A-eNOS-tg,* both of which are driven by increased levels of peroxynitrite [78]. Exercise training induces increased eNOS-Ser1176/9-phosphorylation in C57BL/6, but in striking contrast no alterations in C101A-eNOS-tg blood pressure or the phosphorylation state, *suggesting that the shear-dependent activation of eNOS is diminished by either dimer-destabilization itself, or subsequently increased endothelial $O_2^{-\bullet}$, or both. Tempol® treatment completely corrects* the *hyperphosphorylation of eNOS and AMPKα, pointing at a close relationship between $O_2^{-\bullet}$, hyperphosphorylation and eNOS-mediated blood pressure reduction. In addition, a mouse model expressing a mutant phosphomimetic S1179D* (serine residue changed to aspartic acid)*-eNOS on an eNOS-KO background showed almost normal endothelium-dependent relaxation but hypertension similar to eNOS-KO, that is, no reduction in blood pressure* [114]. *These data are consistent with the observations reported here,*

This work was published in

Suvorava T*, Pick S*, and Kojda G. (* equal contribution)
Selective impairment of blood pressure reduction by endothelial nitric oxide synthase dimer destabilization in mice.
J Hypertens 2017;35(1):76-88. journals.lww.com/jhypertension/

word-for-word citations within the running text stand out in italic type

suggesting an inhibitory effect of eNOS-Ser1176/9-hyperphosphorylation on eNOS-mediated blood pressure reduction. In C101A-eNOS-tg elevated levels of S-glutathionylated eNOS are found, which is caused by the increased oxidative stress in these animals. This is consistent with reports that describe S-glutathionylation of eNOS at two cysteine residues in between the FMN- and FAD-binding site as a trigger for 'uncoupling'; eNOS activity is decreased via S-glutathionylation and this comes along with an increase in $O_2^{-\bullet}$ generation [73]. *However, a diminished eNOS activity induced by the detected tyrosine-nitration of the enzyme* due to the increased bioavailability of peroxynitrite is expected and *may play a role as well*. Tyrosine nitration occurs in states of dissociation of *trans*-peroxynitrite to nitrogen dioxide and hydroxyl radical. Tyrosine itself is oxidized to a tyrosine radical by the hydroxyl radical and finally reacts with nitrogen dioxide under the formation of 3-nitrotyrosine [74].

4.8. eNOS and the Role of Resistance Vessels

Taking all presented findings together, it seems that the conductance and the resistance vessels have to be considered separately. The aorta as a conductance artery seems to be not affected in its contribution to systolic blood pressure regulation after the introduction of mutated and dimer-destabilized C101A-eNOS. The endothelium-dependent relaxation measured here is most likely triggered by an increase of Ca^{2+}/calmodulin binding caused by mediators. Thus, at the level of conductance vessels, the insertion of dimer-destabilized eNOS causes no alterations. But, to look at blood pressure regulation more precisely, resistance vessels, substituted in this study by investigation of skeletal muscle tissue, have to be taken into consideration, too. Here, phosphorylation of eNOS at Ser1176/9 seems to play a key role. In C101A-eNOS-tg hyperphosphorylation at this site is presumably caused by increased levels of peroxynitrite, which is formed spontaneously under diffusion control if NO and $O_2^{-\bullet}$ are in proximity. In this state of high concentrations of peroxynitrite, the enzyme partially increases its formation of $O_2^{-\bullet}$ but the formation of NO is decreased due to the destabilization of the enzyme [83]. Along with dimer-destabilization and increased

This work was published in

Suvorava T*, Pick S*, and Kojda G. (* equal contribution)
Selective impairment of blood pressure reduction by endothelial nitric oxide synthase dimer destabilization in mice.
J Hypertens 2017;35(1):76-88. journals.lww.com/jhypertension/

word-for-word citations within the running text stand out in italic type

oxidative stress, C101A-eNOS-tg is an acceptable model for this condition, and the hyperphosphorylation of eNOS at Ser1176/9 falls into place. A further phosphorylation induced by physical activity and shear is not possible in C101A-eNOS-tg, and at the level of resistance arteries no reduction in systolic blood pressure can be induced. But, if oxidative stress is eliminated by Tempol®, hyperphosphorylation of eNOS and AMPKα is corrected. This indicates a close interaction of $O_2^{-\bullet}$, hyperphosphorylation and eNOS-mediated blood pressure reduction. Regarding eNOS-tg, no increase in oxidative stress is present from the outset, and thus no hyperphosphorylation occurs. Physical forces can induce the phosphorylation of eNOS at Ser1176/9 via AMPK α and lead to a reduction in systolic blood pressure (see fig. 4.2).

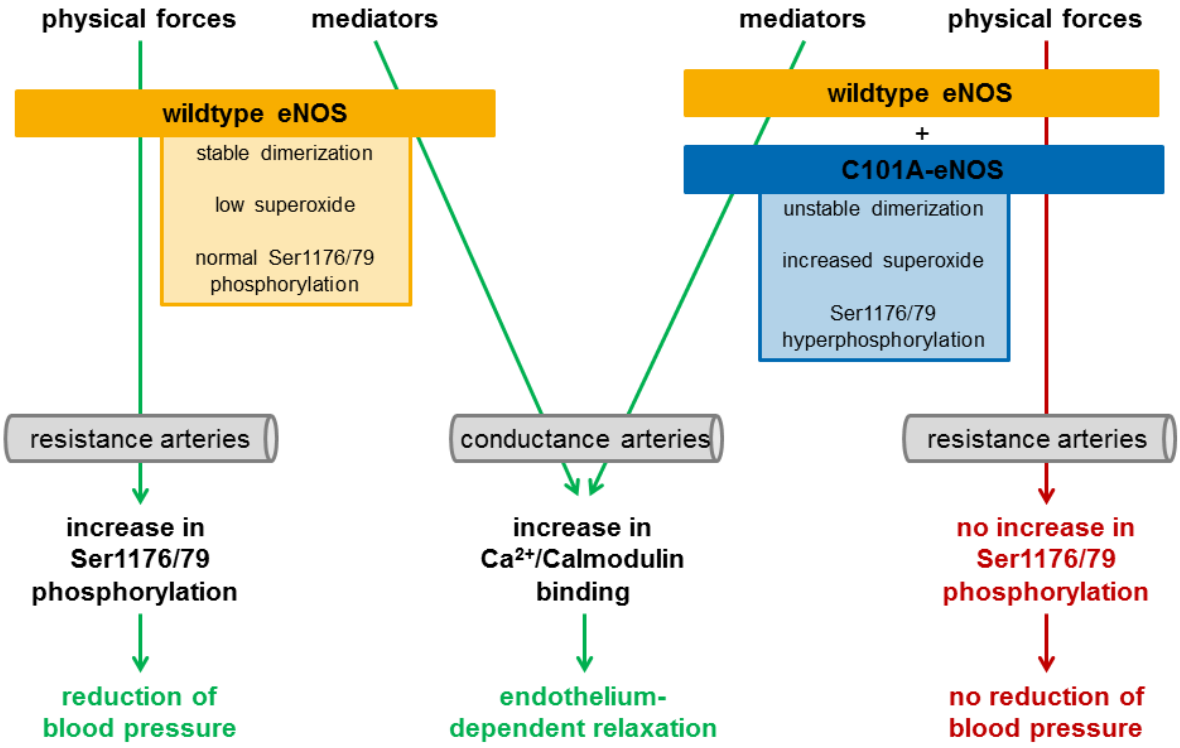

Fig. 4.2: *Hypothesis of eNOS hyperphosphorylation at Ser1176/9 after the introduction of C101A-eNOS.*

This work was published in

Suvorava T*, Pick S*, and Kojda G. (* equal contribution)
Selective impairment of blood pressure reduction by endothelial nitric oxide synthase dimer destabilization in mice.
J Hypertens 2017;35(1):76-88. journals.lww.com/jhypertension/

word-for-word citations within the running text stand out in italic type

4.9. CLINICAL ASPECTS

Endothelial dysfunction in resistance vessels was already identified in normotensive young adults with *hypertensive parents* [6]. *In addition, endothelial dysfunction in resistance vessels was demonstrated in other disease states such as in young adults with insulin-dependent diabetes mellitus despite* the *normalization of plasma glucose* [115]. Or, it might result from the *prolonged effect of passive smoking on endothelial progenitor cells* [116]. *Although there are no single-nucleotide-polymorphisms of eNOS-Zn-finger cysteines, eNOS-Ser1177-hyperphosphorylation by oxidative stress might contribute to endothelial dysfunction in resistance arteries of otherwise healthy humans, which is considered to be a risk factor for the development of overt hypertension later in life* [116]. *With respect to essential hypertension,* the *findings may provide another piece of mechanistic insight in this multifactorial disease*. In conclusion, the data presented in this work *suggest that vascular oxidative stress induced by eNOS dimer-destabilization causes nitration and* S-*glutathionylation of several proteins, as well as Ser1177-hyperphosphorylation of eNOS, which is presumably mediated by AMPK* α*. These posttranslational protein modifications are associated with the resistance of eNOS to phosphorylation at Ser1177 induced by physical forces* like *shear. Furthermore, this C101A-eNOS-dependent oxidative stress selectively prevented the blood pressure-reducing activity of vascular eNOS. These data suggest that eNOS-dependent oxidative stress in the microvascular endothelium may play a role in the development of essential hypertension.*

This work was published in

Suvorava T*, Pick S*, and Kojda G. (* equal contribution)
Selective impairment of blood pressure reduction by endothelial nitric oxide synthase dimer destabilization in mice.
J Hypertens 2017;35(1):76-88. journals.lww.com/jhypertension/

word-for-word citations within the running text stand out in italic type

5. SUMMARY

5.1. ABSTRACT

Objectives: Essential hypertension is associated with endothelial dysfunction and reactive oxygen species are considered to play a role here. *But whether endothelial superoxide anion radical ($O_2^{-\bullet}$) may play a role in the early development of hypertension remains uncertain*. The aim of this study is to investigate *whether endothelial nitric oxide synthase (eNOS)-derived endothelial oxidative stress is involved in the regulation of systolic blood pressure*.

Methods: In order to investigate whether dysfunctional vascular eNOS might contribute to the regulation of blood pressure, two different eNOS variants are overexpressed by the endothelial specific tie-2 promoter. *Wild-type eNOS [mice with endothelium-specific overexpression of bovine eNOS (eNOS-tg)] or* respectively *a novel dimer-destabilized eNOS-mutant harboring a partially disrupted zinc-finger [mice with endothelium-specific overexpression of destabilized bovine eNOS* (C101A-eNOS-tg)] was introduced in the vasculature of C57BL/6 mice. Destabilization of eNOS was induced via replacement of cysteine 101 residue by alanine, resulting in impaired eNOS dimer stability, increased $O_2^{-\bullet}$, and decreased nitric oxide (NO) bioavailability in stably transfected human embryonic kidney cells 293 (HEK 293). Mutant *mice are monitored for aortic endothelium-dependent relaxation, systolic blood pressure, levels of $O_2^{-\bullet}$, and several posttranslational modifications indicating activity and/or increased vascular oxidative stress. Some groups of mice underwent voluntary exercise training for four weeks or treatment with the superoxide dismutase mimetic Tempol®.*

Results: Western blot analysis in aortic, left ventricular myocardium, lung, and skeletal muscle tissue proves the vascular-specific overexpression of eNOS in C101A-eNOS-tg and eNOS-tg. $O_2^{-\bullet}$ levels are increased in C101A-eNOS-tg but not in eNOS-tg; and this elevation is blunted by incubation with the nitric oxide synthase (NOS) inhibitor L-nitroarginine suggesting destabilized eNOS to be a source of $O_2^{-\bullet}$. Likewise, peroxynitrite

This work was published in

Suvorava T*, Pick S*, and Kojda G. (* equal contribution)
Selective impairment of blood pressure reduction by endothelial nitric oxide synthase dimer destabilization in mice.
J Hypertens 2017;35(1):76-88. journals.lww.com/jhypertension/

word-for-word citations within the running text stand out in italic type

levels measured by protein-tyrosine-nitration and eNOS-tyrosine-nitration are increased in C101A-eNOS-tg but unchanged in eNOS-tg. Protein kinase G activity is evaluated by vasoactive stimulated protein (VASP) phosphorylation at Ser239, showing no difference in both strains vs. controls, indicating a normal NO/cGMP-pathway activation. Organ bath experiments reveal normal aortic reactivity to acetylcholine, phenylephrine, and NO-donor S-nitroso-N-acetyl-D,L-penicillamine (SNAP) in both animal strains. C101A-eNOS-tg show significantly increased *eNOS-S-glutathionylation, eNOS1176/9 phosphorylation and adenosine monophosphate activated protein kinase (AMPK)* α *phosphorylation at Thr172 in* the *aorta, skeletal muscle, left ventricular myocardium, and lung as compared* to *eNOS-tg and wild-type controls*. *Exercise training increases the phosphorylation of eNOS at Ser1176/9 and AMPK*α *in wild-types. These physiological adaptations are absent in C101A-eNOS-tg. C101A-eNOS-tg displayes normal systolic blood pressure* (measured in awake mice by tail-cuff method) *despite higher levels of eNOS, whereas eNOS-tg shows significant hypotension.* The antioxidant *Tempol® completely reverses the occurring protein modifications and significantly reduces systolic blood pressure in C101A-eNOS-tg but not in wild-types.*

Conclusion: *Oxidative stress generated by endothelial-specific expression of genetically destabilized C101A-eNOS selectively prevents the systolic blood pressure-reducing activity of vascular eNOS, while having no effect on aortic endothelium-dependent relaxation.* These data suggest that a decrease of eNOS dimer stability associated with increased vascular oxidative stress in the microvascular endothelium might directly contribute to the regulation of blood pressure and may play a role in the development of essential hypertension.

This work was published in

Suvorava T*, Pick S*, and Kojda G. (* equal contribution)
Selective impairment of blood pressure reduction by endothelial nitric oxide synthase dimer destabilization in mice.
J Hypertens 2017;35(1):76-88. journals.lww.com/jhypertension/

word-for-word citations within the running text stand out in italic type

5.2. ABSTRACT (DEUTSCH)

Hintergrund: Essentielle Hypertonie steht in Zusammenhang mit endothelialer Dysfunktion und reaktive Sauerstoffverbindungen scheinen dabei eine Rolle zu spielen. Inwiefern endotheliales Superoxid-Radikal-Anion ($O_2^{-\bullet}$) im Frühstadium der Entwicklung einer Hypertonie eine Rolle spielt, ist bisher nicht bekannt. In dieser Studie wird untersucht, ob durch endotheliale Stickstoffmonoxid Synthase (eNOS) im Endothel vermittelter oxidativer Stress an der Regulation des systolischen Blutdrucks beteiligt ist.

Methoden: Um zu untersuchen, ob dysfunktionale vaskuläre eNOS an der Regulation des Blutdrucks beteiligt sein könnte, werden zwei verschiedene eNOS Varianten endothelspezifisch mittels des Tie-2 Promotors überexprimiert. Wildtyp eNOS [Mäuse mit einer endothelspezifischen Überexpression boviner eNOS (eNOS-tg)] oder ebenso eine neue dimerdestabilisierte eNOS Mutante mit einem teilweise zerstörten Zinkfinger [Mäuse mit endothelspezifischer Überexpression destabilisierter boviner eNOS (C101A-eNOS-tg)] wird im Gefäßsystem von C57BL/6-Mäusen exprimiert. Die Destabilisierung der eNOS wird durch einen Austausch von Cystein 101 durch Alanin erreicht, was in einer verminderten eNOS Dimerstabilität, vermehrter $O_2^{-\bullet}$ und verringerten Stickstoffmonoxid (NO) Bioverfügbarkeit in stabil transfizierten humanen embryonalen Nierenzellen 293 (HEK 293) führt. Die mutierten Mäuse werden auf endothelabhängige Aortenrelaxation, systolischen Blutdruck, $O_2^{-\bullet}$ Konzentration und verschiedene posttranslationale Modifikationen, die auf Aktivität und/oder erhöhten vaskulären oxidativen Stress hindeuten, untersucht. Einige Gruppen von Mäusen werden freiwilligem körperlichen Training oder einer Behandlung mit dem Superoxiddismutasemimetikum Tempol® unterzogen.

Ergebnisse: Westernblot Untersuchungen in Aorten-, linksventrikulärem Myokard-, Lungen- und Skelettmuskelgewebe belegen die vaskulär spezifische eNOS Überexpression in C101A-eNOS-tg und eNOS-tg. $O_2^{-\bullet}$ Level sind in C101A-eNOS-tg, allerdings nicht in eNOS-tg, erhöht und dies kann durch Inkubation mit dem

This work was published in

Suvorava T*, Pick S*, and Kojda G. (* equal contribution)
Selective impairment of blood pressure reduction by endothelial nitric oxide synthase dimer destabilization in mice.
J Hypertens 2017;35(1):76-88. journals.lww.com/jhypertension/

word-for-word citations within the running text stand out in italic type

Stickstoffmonoxid Synthase (NOS)-Inhibitor Nitro-L-arginin maskiert werden, was ein Hinweis dafür ist, dass die destabilisierte eNOS als eine Quelle für $O_2^{-\bullet}$ fungiert. Ebenso sind Peroxynitritkonzentrationen, gemessen durch Protein-Tyrosin-Nitrierung und eNOS-Tyrosin-Nitrierung, in C101A-eNOS-tg erhöht, allerdings unverändert in eNOS-tg. Die Proteinkinase G Aktivität, evaluiert durch Phosphorylierung an vasoaktiv stimuliertem Protein (VASP) an Ser239, ist in beiden Linien im Vergleich zu Kontrollen unverändert, was auf eine normale Aktivierung des NO/cGMP-Signaltransduktionswegs hindeutet. Organbadexperimente zeigen eine normale Aortenreaktivität auf Acetylcholin, Phenylephrin und den NO-Donor SNAP in beiden Tierlinien. In C101A-eNOS-tg kann signifikant verstärkte eNOS-S-Glutathionylierung, eNOS-Ser1177/9-Phosphorylierung und Adenosinmonophosphatkinase (AMPK) α Phosphorylierung an Thr172 in Aorta, Skelettmuskel, linksventrikulärem Myokard und Lunge im Vergleich zu eNOS-tg und Wildtypkontrollen gezeigt werden. Körperliches Training verstärkt die Phosphorylierung der eNOS an Ser1177/9 und AMPK α in Wildtyptieren. Diese physiologischen Adaptionen können in C101A-eNOS-tg nicht beobachtet werden. C101A-eNOS-tg zeigen sich, gemessen an wachen Tieren durch die Tail-Cuff Methode, trotz einer eNOS Überexpression systolisch normoton, eNOS-tg signifikant hypoton. Das Antioxidans Tempol® kann die auftretenden Proteinmodifikationen vollständig aufheben und reduziert signifikant den systolischen Blutdruck in C101A-eNOS-tg, nicht aber in Wildtyptieren.

Schlussfolgerung: Oxidativer Stress durch endothelspezifische Überexpression genetisch destabilisierter C101A-eNOS verhindert selektiv die blutdruckvermindernde Wirkung vaskulärer eNOS, wohingegen kein Effekt auf endothelabhängige Relaxation in der Aorta besteht. Diese Daten weisen darauf hin, dass eine verringerte eNOS Dimerstabilität, die mit vaskulärem oxidativen Stress im mikrovaskulären Endothel im Zusammenhang steht, direkt an der Regulation des Blutdrucks beteiligt sein und somit bei der Entstehung der essentiellen Hypertonie eine Rolle spielen könnte.

This work was published in

Suvorava T*, Pick S*, and Kojda G. (* equal contribution)
Selective impairment of blood pressure reduction by endothelial nitric oxide synthase dimer destabilization in mice.
J Hypertens 2017;35(1):76-88. journals.lww.com/jhypertension/

word-for-word citations within the running text stand out in italic type

6. REFERENCES

1. Mancia G, Fagard R, Narkiewicz K, Redon J, Zanchetti A, Böhm M, et al. 2013 ESH/ESC guidelines for the management of arterial hypertension: the Task Force for the Management of Arterial Hypertension of the European Society of Hypertension (ESH) and of the European Society of Cardiology (ESC). Eur Heart J 2013; 34 (28):2159-2219.

2. Rossier BC, Bochud M, Devuyst O. The Hypertension Pandemic: An Evolutionary Perspective. Physiology (Bethesda) 2017; 32 (2):112-125.

3. Kojda G, Harrison D. Interactions between NO and reactive oxygen species: pathophysiological importance in atherosclerosis, hypertension, diabetes and heart failure. Cardiovasc Res 1999; 43 (3):562-571.

4. Ghiadoni L, Taddei S, Virdis A. Hypertension and endothelial dysfunction: therapeutic approach. Curr Vasc Pharmacol 2012; 10 (1):42-60.

5. Flammer AJ, Anderson T, Celermajer DS, Creager MA, Deanfield J, Ganz P, et al. The assessment of endothelial function: from research into clinical practice. Circulation 2012; 126 (6):753-767.

6. Taddei S, Virdis A, Mattei P, Ghiadoni L, Sudano I, Salvetti A. Defective L-arginine-nitric oxide pathway in offspring of essential hypertensive patients. Circulation 1996; 94 (6):1298-1303.

7. Rossi R, Chiurlia E, Nuzzo A, Cioni E, Origliani G, Modena MG. Flow-mediated vasodilation and the risk of developing hypertension in healthy postmenopausal women. J Am Coll Cardiol 2004; 44 (8):1636-1640.

8. Mordi I, Mordi N, Delles C, Tzemos N. Endothelial dysfunction in human essential hypertension. J Hypertens 2016; 34 (8):1464-1472.

9. Furchgott RF, Zawadzki JV. The obligatory role of endothelial cells in the relaxation of arterial smooth muscle by acetylcholine. Nature 1980; 288 (5789):373-376.

10. Moncada S, Higgs EA. The discovery of nitric oxide and its role in vascular biology. Br J Pharmacol 2006; 147 Suppl 1:S193-201.

11. Palmer RM, Moncada S. A novel citrulline-forming enzyme implicated in the formation of nitric oxide by vascular endothelial cells. Biochem Biophys Res Commun 1989; 158 (1):348-352.

12. Palmer RM, Ashton DS, Moncada S. Vascular endothelial cells synthesize nitric oxide from L-arginine. Nature 1988; 333 (6174):664-666.

13. Mayer B, Schmidt K, Humbert P, Böhme E. Biosynthesis of endothelium-derived relaxing factor: a cytosolic enzyme in porcine aortic endothelial cells Ca2+-dependently

converts L-arginine into an activator of soluble guanylyl cyclase. Biochem Biophys Res Commun 1989; 164 (2):678-685.

14. Forstermann U, Sessa WC. Nitric oxide synthases: regulation and function. Eur Heart J 2012; 33 (7):829-837, 837a-837d.

15. Bredt DS, Hwang PM, Glatt CE, Lowenstein C, Reed RR, Snyder SH. Cloned and expressed nitric oxide synthase structurally resembles cytochrome P-450 reductase. Nature 1991; 351 (6329):714-718.

16. Zhang M, Vogel HJ. Characterization of the calmodulin-binding domain of rat cerebellar nitric oxide synthase. J Biol Chem 1994; 269 (2):981-985.

17. Förstermann U. Janus-faced role of endothelial NO synthase in vascular disease: uncoupling of oxygen reduction from NO synthesis and its pharmacological reversal. Biol Chem 2006; 387 (12):1521-1533.

18. Förstermann U, Münzel T. Endothelial nitric oxide synthase in vascular disease: from marvel to menace. Circulation 2006; 113 (13):1708-1714.

19. Raman CS, Li H, Martasek P, Kral V, Masters BS, Poulos TL. Crystal structure of constitutive endothelial nitric oxide synthase: a paradigm for pterin function involving a novel metal center. Cell 1998; 95 (7):939-950.

20. Nathan C, Xie QW. Nitric oxide synthases: roles, tolls, and controls. Cell 1994; 78 (6):915-918.

21. Matsubara M, Titani K, Taniguchi H. Interaction of calmodulin-binding domain peptides of nitric oxide synthase with membrane phospholipids: regulation by protein phosphorylation and Ca(2+)-calmodulin. Biochemistry 1996; 35 (46):14651-14658.

22. Kraehling JR, Hao Z, Lee MY, Vinyard DJ, Velazquez H, Liu X, et al. Uncoupling Caveolae From Intracellular Signaling In Vivo. Circ Res 2016; 118 (1):48-55.

23. Miyawaki-Shimizu K, Predescu D, Shimizu J, Broman M, Predescu S, Malik AB. siRNA-induced caveolin-1 knockdown in mice increases lung vascular permeability via the junctional pathway. Am J Physiol Lung Cell Mol Physiol 2006; 290 (2):L405-413.

24. Siddiqui MR, Komarova YA, Vogel SM, Gao X, Bonini MG, Rajasingh J, et al. Caveolin-1-eNOS signaling promotes p190RhoGAP-A nitration and endothelial permeability. J Cell Biol 2011; 193 (5):841-850.

25. Saito H, Godo S, Sato S, Ito A, Ikumi Y, Tanaka S, et al. Important Role of Endothelial Caveolin-1 in the Protective Role of Endothelium-dependent Hyperpolarization Against Nitric Oxide-Mediated Nitrative Stress in Microcirculation in Mice. J Cardiovasc Pharmacol 2018; 71 (2):113-126.

26. Li H, Forstermann U. Uncoupling of endothelial NO synthase in atherosclerosis and vascular disease. Curr Opin Pharmacol 2013; 13 (2):161-167.

27. Karbach S, Wenzel P, Waisman A, Munzel T, Daiber A. eNOS uncoupling in cardiovascular diseases--the role of oxidative stress and inflammation. Curr Pharm Des 2014; 20 (22):3579-3594.

28. Searles CD. Transcriptional and posttranscriptional regulation of endothelial nitric oxide synthase expression. Am J Physiol Cell Physiol 2006; 291 (5):C803-816.

29. Siragusa M, Fleming I. The eNOS signalosome and its link to endothelial dysfunction. Pflugers Arch 2016; 468 (7):1125-1137.

30. Fisslthaler B, Loot AE, Mohamed A, Busse R, Fleming I. Inhibition of endothelial nitric oxide synthase activity by proline-rich tyrosine kinase 2 in response to fluid shear stress and insulin. Circ Res 2008; 102 (12):1520-1528.

31. Rao GH, Krishnamurthi S, Raij L, White JG. Influence of nitric oxide on agonist-mediated calcium mobilization in platelets. Biochem Med Metab Biol 1990; 43 (3):271-275.

32. Kubes P, Suzuki M, Granger DN. Nitric oxide: an endogenous modulator of leukocyte adhesion. Proc Natl Acad Sci U S A 1991; 88 (11):4651-4655.

33. Scott-Burden T, Vanhoutte PM. The endothelium as a regulator of vascular smooth muscle proliferation. Circulation 1993; 87 (Suppl. 5):V51-V55.

34. Balla G, Jacob HS, Balla J, Rosenberg M, Nath K, Apple F, et al. Ferritin: a cytoprotective antioxidant strategem of endothelium. J Biol Chem 1992; 267 (25):18148-18153.

35. Moncada S, Higgs A. The L-arginine-nitric oxide pathway. N Engl J Med 1993; 329 (27):2002-2012.

36. Gewaltig MT, Kojda G. Vasoprotection by nitric oxide: mechanisms and therapeutic potential. Cardiovasc Res 2002; 55 (2):250-260.

37. Oppermann M, Suvorava T, Freudenberger T, Dao VT, Fischer JW, Weber M, et al. Regulation of vascular guanylyl cyclase by endothelial nitric oxide-dependent posttranslational modification. Basic Res Cardiol 2011; 106 (4):539-549.

38. Bolotina VM, Najibi S, Palacino JJ, Pagano PJ, Cohen RA. Nitric oxide directly activates calcium-dependent potassium channels in vascular smooth muscle. Nature 1994; 368 (6474):850-853.

39. Morawietz H, Weber M, Rueckschloss U, Lauer N, Hacker A, Kojda G. Upregulation of vascular NAD(P)H oxidase subunit gp91phox and impairment of the nitric oxide signal

transduction pathway in hypertension. Biochem Biophys Res Commun 2001; 285 (5):1130-1135.

40. Gryglewski RJ, Palmer RM, Moncada S. Superoxide anion is involved in the breakdown of endothelium-derived vascular relaxing factor. Nature 1986; 320 (6061):454-456.

41. Lamping KG, Nuno DW, Shesely EG, Maeda N, Faraci FM. Vasodilator mechanisms in the coronary circulation of endothelial nitric oxide synthase-deficient mice. Am J Physiol Heart Circ Physiol 2000; 279 (4):H1906-1912.

42. Meng W, Ayata C, Waeber C, Huang PL, Moskowitz MA. Neuronal NOS-cGMP-dependent ACh-induced relaxation in pial arterioles of endothelial NOS knockout mice. Am J Physiol 1998; 274 (2 Pt 2):H411-415.

43. Sun D, Huang A, Smith CJ, Stackpole CJ, Connetta JA, Shesely EG, et al. Enhanced release of prostaglandins contributes to flow-induced arteriolar dilation in eNOS knockout mice. Circ Res 1999; 85 (3):288-293.

44. Waldron GJ, Ding H, Lovren F, Kubes P, Triggle CR. Acetylcholine-induced relaxation of peripheral arteries isolated from mice lacking endothelial nitric oxide synthase. Br J Pharmacol 1999; 128 (3):653-658.

45. Chen PF, Tsai AL, Wu KK. Cysteine 99 of endothelial nitric oxide synthase (NOS-III) is critical for tetrahydrobiopterin-dependent NOS-III stability and activity. Biochem Biophys Res Commun 1995; 215 (3):1119-1129.

46. Lee MY, Griendling KK. Redox signaling, vascular function, and hypertension. Antioxid Redox Signal 2008; 10 (6):1045-1059.

47. Adlam D, Bendall JK, De Bono JP, Alp NJ, Khoo J, Nicoli T, et al. Relationships between nitric oxide-mediated endothelial function, eNOS coupling and blood pressure revealed by eNOS-GTP cyclohydrolase 1 double transgenic mice. Exp Physiol 2007; 92 (1):119-126.

48. Suvorava T, Lauer N, Kumpf S, Jacob R, Meyer W, Kojda G. Endogenous vascular hydrogen peroxide regulates arteriolar tension in vivo. Circulation 2005; 112 (16):2487-2495.

49. Huang PL, Huang Z, Mashimo H, Bloch KD, Moskowitz MA, Bevan JA, et al. Hypertension in mice lacking the gene for endothelial nitric oxide synthase. Nature 1995; 377 (6546):239-242.

50. Shesely EG, Maeda N, Kim HS, Desai KM, Krege JH, Laubach VE, et al. Elevated blood pressures in mice lacking endothelial nitric oxide synthase. Proc Natl Acad Sci U S A 1996; 93 (23):13176-13181.

51. Gregg AR, Schauer A, Shi O, Liu Z, Lee CG, O'Brien WE. Limb reduction defects in endothelial nitric oxide synthase-deficient mice. Am J Physiol 1998; 275 (6 Pt 2):H2319-2324.

52. Stauss HM, Gödecke A, Mrowka R, Schrader J, Persson PB. Enhanced blood pressure variability in eNOS knockout mice. Hypertension 1999; 33 (6):1359-1363.

53. Rees DD, Palmer RM, Moncada S. Role of endothelium-derived nitric oxide in the regulation of blood pressure. Proc Natl Acad Sci U S A 1989; 86 (9):3375-3378.

54. Kojda G, Laursen JB, Ramasamy S, Kent JD, Kurz S, Burchfield J, et al. Protein expression, vascular reactivity and soluble guanylate cyclase activity in mice lacking the endothelial cell nitric oxide synthase: contributions of NOS isoforms to blood pressure and heart rate control. Cardiovasc Res 1999; 42 (1):206-213.

55. Vallance P, Collier J, Moncada S. Effects of endothelium-derived nitric oxide on peripheral arteriolar tone in man. Lancet 1989; 2 (8670):997-1000.

56. Barouch LA, Harrison RW, Skaf MW, Rosas GO, Cappola TP, Kobeissi ZA, et al. Nitric oxide regulates the heart by spatial confinement of nitric oxide synthase isoforms. Nature 2002; 416 (6878):337-339.

57. Tsutsui M, Shimokawa H, Otsuji Y, Yanagihara N. Pathophysiological relevance of NO signaling in the cardiovascular system: novel insight from mice lacking all NO synthases. Pharmacol Ther 2010; 128 (3):499-508.

58. Suvorava T, Nagy N, Pick S, Lieven O, Ruther U, Dao VT, et al. Impact of eNOS-Dependent Oxidative Stress on Endothelial Function and Neointima Formation. Antioxid Redox Signal 2015; 23 (9):711-723.

59. Weber M. Radikal-induzierte Störungen der NO-Signaltransduktion bei endothelialer Dysfunktion. Heinrich-Heine-Universität Düsseldorf; 2002.

60. Suvorava T, Kumpf S, Rauch BH, Dao VT, Adams V, Kojda G. Hydrogen peroxide inhibits exercise-induced increase of circulating stem cells with endothelial progenitor capacity. Free Radic Res 2010; 44 (2):199-207.

61. Krege JH, Hodgin JB, Hagaman JR, Smithies O. A noninvasive computerized tail-cuff system for measuring blood pressure in mice. Hypertension 1995; 25 (5):1111-1115.

62. Wilcox CS. Effects of tempol and redox-cycling nitroxides in models of oxidative stress. Pharmacol Ther 2010; 126 (2):119-145.

63. Field L, Dilts RV, Ravichandran R, Lenhert PG, Carnahan GE. An unusually stable thionitrite fron N-acetyl-D,L-penicillamine; X-ray crystal and molecular structure of 2-(acetyl amino)-2-carboxy-1,1-dimethylethyl thionitrite. Chem Commun 1978:249-250.

64. lifetechnologies.com. TaqMan ® probe based assay chemistryTaqMan ® probe based assay chemistry. 2010.

65. Schmittgen TD, Livak KJ. Analyzing real-time PCR data by the comparative C(T) method. Nat Protoc 2008; 3 (6):1101-1108.

66. Bradford MM. A rapid and sensitive method for the quantitation of microgram quantities of protein utilizing the principle of protein-dye binding. Anal Biochem 1976; 72:248-254.

67. Laemmli UK. Cleavage of structural proteins during the assembly of the head of bacteriophage T4. Nature 1970; 227 (5259):680-685.

68. Maizel JV, Summers DF, Scharff MD. SDS-acrylamide gel electrophoresis and its application to the proteins of poliovirus- and adenovirus-infected human cells. J Cell Physiol 1970; 76 (3):273-287.

69. Ohara Y, Peterson TE, Harrison DG. Hypercholesterolemia increases endothelial superoxide anion production. J Clin Invest 1993; 91 (6):2546-2551.

70. Allen RC. Phagocytic leukocyte oxygenation activities and chemiluminescence: a kinetic approach to analysis. Methods Enzymol 1986; 133:449-493.

71. Kojda G, Beck JK, Meyer W, Noack E. Nitrovasodilator-induced relaxation and tolerance development in porcine vena cordis magna: dependence on intact endothelium. Br J Pharmacol 1994; 112 (2):533-540.

72. Choi H, Tostes RC, Webb RC. Thioredoxin reductase inhibition reduces relaxation by increasing oxidative stress and s-nitrosylation in mouse aorta. J Cardiovasc Pharmacol 2011; 58 (5):522-527.

73. Chen CA, Wang TY, Varadharaj S, Reyes LA, Hemann C, Talukder MA, et al. S-glutathionylation uncouples eNOS and regulates its cellular and vascular function. Nature 2010; 468 (7327):1115-1118.

74. Hanafy KA, Krumenacker JS, Murad F. NO, nitrotyrosine, and cyclic GMP in signal transduction. Med Sci Monit 2001; 7 (4):801-819.

75. Chen ZP, Mitchelhill KI, Michell BJ, Stapleton D, Rodriguez-Crespo I, Witters LA, et al. AMP-activated protein kinase phosphorylation of endothelial NO synthase. FEBS Lett 1999; 443 (3):285-289.

76. Fulton D, Gratton JP, McCabe TJ, Fontana J, Fujio Y, Walsh K, et al. Regulation of endothelium-derived nitric oxide production by the protein kinase Akt. Nature 1999; 399 (6736):597-601.

77. Dimmeler S, Fleming I, Fisslthaler B, Hermann C, Busse R, Zeiher AM. Activation of nitric oxide synthase in endothelial cells by Akt-dependent phosphorylation. Nature 1999; 399 (6736):601-605.

78. Zou MH, Hou XY, Shi CM, Nagata D, Walsh K, Cohen RA. Modulation by peroxynitrite of Akt- and AMP-activated kinase-dependent Ser1179 phosphorylation of endothelial nitric oxide synthase. J Biol Chem 2002; 277 (36):32552-32557.

79. Smolenski A, Burkhardt AM, Eigenthaler M, Butt E, Gambaryan S, Lohmann SM, et al. Functional analysis of cGMP-dependent protein kinases I and II as mediators of NO/cGMP effects. Naunyn Schmiedebergs Arch Pharmacol 1998; 358 (1):134-139.

80. Fukai T, Siegfried MR, Ushio-Fukai M, Cheng Y, Kojda G, Harrison DG. Regulation of the vascular extracellular superoxide dismutase by nitric oxide and exercise training. J Clin Invest 2000; 105 (11):1631-1639.

81. Daiber A, Steven S, Weber A, Shuvaev VV, Muzykantov VR, Laher I, et al. Targeting vascular (endothelial) dysfunction. Br J Pharmacol 2017; 174 (12):1591-1619.

82. Munzel T, Daiber A, Ullrich V, Mulsch A. Vascular consequences of endothelial nitric oxide synthase uncoupling for the activity and expression of the soluble guanylyl cyclase and the cGMP-dependent protein kinase. Arterioscler Thromb Vasc Biol 2005; 25 (8):1551-1557.

83. Zou MH, Shi C, Cohen RA. Oxidation of the zinc-thiolate complex and uncoupling of endothelial nitric oxide synthase by peroxynitrite. J Clin Invest 2002; 109 (6):817-826.

84. Feletou M, Tang EH, Vanhoutte PM. Nitric oxide the gatekeeper of endothelial vasomotor control. Front Biosci 2008; 13:4198-4217.

85. Suvorava T, Pick S, Kojda G. Selective impairment of blood pressure reduction by endothelial nitric oxide synthase dimer destabilization in mice. J Hypertens 2017; 35 (1):76-88.

86. Ravi K, Brennan LA, Levic S, Ross PA, Black SM. S-nitrosylation of endothelial nitric oxide synthase is associated with monomerization and decreased enzyme activity. Proc Natl Acad Sci U S A 2004; 101 (8):2619-2624.

87. Rafikov R, Fonseca FV, Kumar S, Pardo D, Darragh C, Elms S, et al. eNOS activation and NO function: structural motifs responsible for the posttranslational control of endothelial nitric oxide synthase activity. J Endocrinol 2011; 210 (3):271-284.

88. Erwin PA, Lin AJ, Golan DE, Michel T. Receptor-regulated dynamic S-nitrosylation of endothelial nitric-oxide synthase in vascular endothelial cells. J Biol Chem 2005; 280 (20):19888-19894.

89. Li H, Horke S, Forstermann U. Vascular oxidative stress, nitric oxide and atherosclerosis. Atherosclerosis 2014; 237 (1):208-219.

90. Strålin P, Karlsson K, Johansson BO, Marklund SL. The interstitium of the human arterial wall contains very large amounts of extracellular superoxide dismutase. Arterioscler Thromb Vasc Biol 1995; 15 (11):2032-2036.

91. Oppermann M, Balz V, Adams V, Dao VT, Bas M, Suvorava T, et al. Pharmacological induction of vascular extracellular superoxide dismutase expression in vivo. J Cell Mol Med 2009; 13 (7):1271-1278.

92. Jung O, Marklund SL, Geiger H, Pedrazzini T, Busse R, Brandes RP. Extracellular superoxide dismutase is a major determinant of nitric oxide bioavailability: in vivo and ex vivo evidence from ecSOD-deficient mice. Circ Res 2003; 93 (7):622-629.

93. Vásquez-Vivar J, Hogg N, Pritchard KA, Martasek P, Kalyanaraman B. Superoxide anion formation from lucigenin: an electron spin resonance spin-trapping study. FEBS Lett 1997; 403 (2):127-130.

94. Grunfeld S, Hamilton CA, Mesaros S, McClain SW, Dominiczak AF, Bohr DF, et al. Role of superoxide in the depressed nitric oxide production by the endothelium of genetically hypertensive rats. Hypertension 1995; 26 (6 Pt 1):854-857.

95. Laursen JB, Rajagopalan S, Galis Z, Tarpey M, Freeman BA, Harrison DG. Role of superoxide in angiotensin II-induced but not catecholamine-induced hypertension. Circulation 1997; 95 (3):588-593.

96. Didion SP, Kinzenbaw DA, Schrader LI, Chu Y, Faraci FM. Endogenous interleukin-10 inhibits angiotensin II-induced vascular dysfunction. Hypertension 2009; 54 (3):619-624.

97. Laursen JB, Somers M, Kurz S, McCann L, Warnholtz A, Freeman BA, et al. Endothelial regulation of vasomotion in apoE-deficient mice: implications for interactions between peroxynitrite and tetrahydrobiopterin. Circulation 2001; 103 (9):1282-1288.

98. Jung O, Schreiber JG, Geiger H, Pedrazzini T, Busse R, Brandes RP. gp91phox-containing NADPH oxidase mediates endothelial dysfunction in renovascular hypertension. Circulation 2004; 109 (14):1795-1801.

99. Muller S, Konig I, Meyer W, Kojda G. Inhibition of vascular oxidative stress in hypercholesterolemia by eccentric isosorbide mononitrate. J Am Coll Cardiol 2004; 44 (3):624-631.

100. Krause M, Dent EW, Bear JE, Loureiro JJ, Gertler FB. Ena/VASP proteins: regulators of the actin cytoskeleton and cell migration. Annu Rev Cell Dev Biol 2003; 19:541-564.

101. Smolenski A, Bachmann C, Reinhard K, Honig-Liedl P, Jarchau T, Hoschuetzky H, et al. Analysis and regulation of vasodilator-stimulated phosphoprotein serine 239

phosphorylation in vitro and in intact cells using a phosphospecific monoclonal antibody. J Biol Chem 1998; 273 (32):20029-20035.

102. Ohashi Y, Kawashima S, Hirata K, Yamashita T, Ishida T, Inoue N, et al. Hypotension and reduced nitric oxide-elicited vasorelaxation in transgenic mice overexpressing endothelial nitric oxide synthase. J Clin Invest 1998; 102 (12):2061-2071.

103. Lohmann SM, Walter U. Tracking functions of cGMP-dependent protein kinases (cGK). Front Biosci 2005; 10:1313-1328.

104. Wilcox CS, Pearlman A. Chemistry and antihypertensive effects of tempol and other nitroxides. Pharmacol Rev 2008; 60 (4):418-469.

105. Mollnau H, Wendt M, Szocs K, Lassegue B, Schulz E, Oelze M, et al. Effects of angiotensin II infusion on the expression and function of NAD(P)H oxidase and components of nitric oxide/cGMP signaling. Circ Res 2002; 90 (4):E58-65.

106. Landmesser U, Dikalov S, Price SR, McCann L, Fukai T, Holland SM, et al. Oxidation of tetrahydrobiopterin leads to uncoupling of endothelial cell nitric oxide synthase in hypertension. J Clin Invest 2003; 111 (8):1201-1209.

107. Zheng JS, Yang XQ, Lookingland KJ, Fink GD, Hesslinger C, Kapatos G, et al. Gene transfer of human guanosine 5'-triphosphate cyclohydrolase I restores vascular tetrahydrobiopterin level and endothelial function in low renin hypertension. Circulation 2003; 108 (10):1238-1245.

108. Fleming I, Busse R. Molecular mechanisms involved in the regulation of the endothelial nitric oxide synthase. Am J Physiol Regul Integr Comp Physiol 2003; 284 (1):R1-12.

109. McCabe TJ, Fulton D, Roman LJ, Sessa WC. Enhanced electron flux and reduced calmodulin dissociation may explain "calcium-independent" eNOS activation by phosphorylation. J Biol Chem 2000; 275 (9):6123-6128.

110. Kojda G, Hambrecht R. Molecular mechanisms of vascular adaptations to exercise. Physical activity as an effective antioxidant therapy? Cardiovasc Res 2005; 67 (2):187-197.

111. Laurindo FR, Pedro MeA, Barbeiro HV, Pileggi F, Carvalho MH, Augusto O, et al. Vascular free radical release. Ex vivo and in vivo evidence for a flow-dependent endothelial mechanism. Circ Res 1994; 74 (4):700-709.

112. Busse R, Fleming I. Pulsatile stretch and shear stress: physical stimuli determining the production of endothelium-derived relaxing factors. J Vasc Res 1998; 35 (2):73-84.

113. Uematsu M, Ohara Y, Navas JP, Nishida K, Murphy TJ, Alexander RW, et al. Regulation of endothelial cell nitric oxide synthase mRNA expression by shear stress. Am J Physiol 1995; 269 (6 Pt 1):C1371-1378.

114. Atochin DN, Wang A, Liu VW, Critchlow JD, Dantas AP, Looft-Wilson R, et al. The phosphorylation state of eNOS modulates vascular reactivity and outcome of cerebral ischemia in vivo. J Clin Invest 2007; 117 (7):1961-1967.

115. Makimattila S, Virkamaki A, Groop PH, Cockcroft J, Utriainen T, Fagerudd J, et al. Chronic hyperglycemia impairs endothelial function and insulin sensitivity via different mechanisms in insulin-dependent diabetes mellitus. Circulation 1996; 94 (6):1276-1282.

116. Heiss C, Amabile N, Lee AC, Real WM, Schick SF, Lao D, et al. Brief secondhand smoke exposure depresses endothelial progenitor cells activity and endothelial function: sustained vascular injury and blunted nitric oxide production. J Am Coll Cardiol 2008; 51 (18):1760-1771.

PUBLICATIONS

ARTICLES

Suvorava T*, **Pick S***, Kojda G. Selective impairment of blood pressure reduction by endothelial nitric oxide synthase dimer destabilization in mice. J Hypertens 2017;35:76-88.

Impact Factor (2017): 4.085

(equal contribution)*

Detailed contribution of Pick S to the manuscript:

Methods *Western blot analysis, Real-time PCR, Lucigenin-enhanced chemiluminescence, On-bead immunoprecipitation and fluorescence detection, Blood pressure and heart rate measurements, Antioxidative treatment, Voluntary exercise training*

Results *Expression of eNOS in eNOS-Tg and C101A-eNOS-Tg, Oxidative Stress, Functional Studies, Tempol treatment, Hyperphosphorylation of eNOS at Ser1176/9, Exercise*

Supplementary Material

Suvorava T, Nagy N, **Pick S**, Lieven O, Ruther U, Dao VT, Fischer JW, Weber M, Kojda G. Impact of eNOS-Dependent Oxidative Stress on Endothelial Function and Neointima Formation. Antioxid Redox Signal 2015;23:711-23.

Impact Factor (2017): 6.337

Suvorava T, Stegbauer J, Thieme M, **Pick S**, Friedrich S, Rump LC, Hohlfeld T, Kojda G. Sustained hypertension despite endothelial-specific eNOS rescue in eNOS-deficient mice. Biochem Biophys Res Commun 2015;458:576-83.

Impact Factor (2017): 2.466

Dao VT, Floeren M, **Kumpf S**, Both C, Peter B, Balz V, Suvorava T, Kojda G. Catalase activity prevents exercise-induced up-regulation of vasoprotective proteins in venous tissue. J Cell Mol Med 2011;15:2326-34.

Impact Factor (2017): 4.499

Suvorava T, **Kumpf S**, Rauch BH, Dao VT, Adams V, Kojda G. Hydrogen peroxide inhibits exercise-induced increase of circulating stem cells with endothelial progenitor capacity. Free Radic Res 2010;44:199-207.

Impact Factor (2017): 3.188

Bas M, Kirchhartz N, Hochfeld J, Tullmann C, **Kumpf S**, Suvorava T, Oppermann M, Hafner D, Bier H, Hoffmann TK, Balz V, Kojda G. Potential role of vasomotor effects of fibrinogen in bradykinin-induced angioedema. J Allergy Clin Immunol 2008;121:969-75 e2.

Impact Factor (2017): 13.081

Suvorava T, Lauer N, **Kumpf S**, Jacob R, Meyer W, Kojda G. Endogenous vascular hydrogen peroxide regulates arteriolar tension in vivo. Circulation 2005;112:2487-95.

Impact Factor (2017): 19.309

PUBLISHED ABSTRACTS / CONGRESS PARTICIPATIONS

Suvorava T*, **Pick S***, Kojda, G.Selective impairment of blood pressure reduction by endothelial eNOS dimer-destabilization in mice. Journal of ISANH Archive (2016) 3:1 (P133).

Suvorava T*, **Pick S***, Kojda G. Genetically engineered eNOS dimer destabilization impairs blood pressure reducing activity of eNOS in mice. Circulation (2015) 132 (A15259).

Suvorava T, Nagy N, **Pick S**, Lieven O, Rüther U, Dao VT, Fischer JW, Weber M, Kojda G. Impact of eNOS-dependent Oxidative Stress on Endothelial Function and Neointima Formation. Journal of ISANH Archive (2015) 1 (221).

Suvorava T, Stegbauer J, Thieme M, **Pick S**, Rump C, Hohlfeld T, Kojda G. Deficiency of non-endothelial eNOS causes hypertension in mice. Cardiovascular Research (2014) 103 SUPPL.1 (S33–S34).

Pick S, Suvorava T, Oppermann M, Weber M, Kojda G. A role of eNOS dimer stability for essential hypertension? European Heart Journal (2013) 34 SUPPL. 1 (109).

Pick S, Suvorava T, Oppermann M, Weber M, Kojda G. A role of eNOS dimer stability for essential hypertension? FEBS Journal 280 (Suppl. 1) (2013) 122 (SW02.S7–36).

Kumpf S, Suvorava T, Oppermann M, Weber M, Kojda G. Effect of Endothelial Specific Overexpression of a Destabilized Endothelial Nitric Oxide Synthase Variant on Blood Pressure and Vascular Endothelial Function. Circulation (2012) 126 (A14020).

Suvorava T, Nagy N, **Kumpf S**, Dao VT, Fischer JW, Kojda G. Endothelial NO-Synthase-Induced Vascular Oxidative Stress Does Not Impair Endothelial Function and Vascular Remodelling. Circulation (2012) 126 (A11918).

Kocgirli O, Valcaccia S, Dao VT, Suvorava T, **Kumpf S**, Floeren M, Oppermann M, Kojda G.Vascular bradykinin type-2 receptor overexpression in eNOS knockout mice. European Heart Journal (2010) 31 SUPPL. 1 (81).

Kocgirli O, Valcaccia S, Dao VT, Suvorava T, **Kumpf S**, Floeren M, Oppermann M, Kojda G. Effects of NO on vascular bradykinin type-2 receptor expression. Cardiovascular Research (2010) 87 SUPPL. 1 (S54-S55).

Dao VT, Floeren M, **Kumpf S**, Suvorava T, Kojda G. Effect of physical activity on the expression of vasoprotective proteins in venous tissue: Role of vascular catalase. Cardiovascular Research (2010) 87 SUPPL. 1 (S55).

Suvorava T, **Kumpf S**, Kojda G. Hydrogen peroxide inhibits exercise-induced increase of circulating stem cells with endothelial progenitor capacity. FEBS Journal (2009) 276 SUPPL. 1 (392).

Kumpf S, Kocgirli O, Suvorava T, Bas M, Kojda G. Vessel-specific vasodilation by fibrinogen: Role of the (alpha)(v)(beta)(3) integrin v. Amino Acids (2009) 37 SUPPL. 1 (S73).

Suvorava T, **Kumpf S**, Adams V, Kojda G. Hydrogen peroxide inhibits exercise-induced increase of circulating stem cells with endothelial progenitor capacity. IUBMB Life (2009) 61:3 (381).

Suvorava T, **Kumpf S**, Adams V, Kojda G. Vascular oxidative stress inhibits mobilization of circulating stem cells with endothelial progenitor capacity in mice. European Heart Journal (2008) 29 Abstract Supplement (260).

Suvorava T, **Kumpf S**, Adams V, Kojda G. Vascular oxidative stress inhibits mobilisation of circulating stem cells with endothelial progenitor capacity. European Journal of Cardiovascular Prevention and Rehabilitation (2008) SUPPL. 1 (S41).

Kumpf S, Oppermann M, Suvorava T, Kojda G. Impairment of proteinkinase G stimulation by vascular specific overexpression of endothelial nitric oxide synthase. Naunyn Schmiedebergs Arch Pharmacol (2007) 375 SUPPL. 1 (30).

Suvorava T, **Kumpf S**, Adams V., Hambrecht R, Kojda G. Role of Endogenous Hydrogen Peroxide in Exercise-Induced Mobilization of Endothelial Progenitor Cells. European Journal of Cardiovascular Prevention and Rehabilitation (2007) 14 SUPPL. 1 (S10,439).

CURRICULUM VITAE

Name	**Stephanie** Han-Whei **Pick**, geb. Kumpf
Geburtsdatum	02. Februar 1981
Geburtsort	Essen

2000	Abitur Immanuel-Kant-Gymnasium Heiligenhaus
2000 - 2001	Studium der chinesischen Sprache und Kultur National Taiwan Normal University, Taipei, Taiwan (R.o.C.)
2001 - 2003	Grundstudium der Chemie Heinrich-Heine-Universität Düsseldorf
2003 - 2005	Hauptstudium der Biomedizinischen Chemie Johannes-Gutenberg-Universität Mainz
2005 - 2010	Studium der Pharmazie Heinrich-Heine-Universität Düsseldorf
10 2002 – 04 2010	Studentische Hilfskraft Institut für Pharmakologie und Klinische Pharmakologie Heinrich-Heine-Universität Düsseldorf
05 2010 – 10 2010	Pharmazeutin im Praktikum, Grünewald-Apotheke Solingen
11 2010 – 04 2011	Pharmazeutin im Praktikum, Grünenthal GmbH Aachen
06 2011	Approbation als Apothekerin
06 2011 – 11 2013	Promotion unter der Leitung von Prof. Dr. G. Kojda Institut für Pharmakologie und Klinische Pharmakologie Heinrich-Heine-Universität Düsseldorf

ACKNOWLEDGEMENTS / DANKSAGUNG

Ich sage „Herzlichen Dank“…

… Herrn Prof. Dr. Georg Kojda für die Idee dieser Arbeit und die Überlassung des Themas. Sein bereits früh in mich gesetztes Vertrauen hat mein wissenschaftliches Interesse schon als Studentin und später als Doktorandin stets gefördert und gefordert, und dabei meinen eigenen Ideen Raum gegeben. Damit hat er entscheidend meine berufliche und auch persönliche Entwicklung geprägt. Dank ihm habe ich diese und weitere Arbeiten auf verschiedenen nationalen und internationalen Kongressen vorstellen dürfen.

… Herrn Prof. Dr. Matthias Kassack für seine freundliche Unterstützung und die Vertretung dieser Arbeit vor der Mathematisch-Naturwissenschaftlichen Fakultät der Heinrich-Heine-Universität Düsseldorf.

… Frau Dr. Tatsiana Suvorava für die exzellente Betreuung, ihre fachliche Kompetenz, unzählige Diskussionsstunden und nicht zuletzt ihre gute Freundschaft.

… meinen Kollegen (Ilse Alonso-Martinez, Marion Bisha, Dr. Charlotte Both, Dr. Thao-Vi Dao, Dr. Sawsan El-Agouri, Dr. Pegah Erfanian-Trudung, Farbod Khosravani, Oktay Kocgirli), die die Zeit haben unvergesslich werden lassen.

… Herrn Prof. Dr. Thomas Hohlfeld und Frau Kirsten Bartkowski für die fachliche Unterstützung bei den Lucigenin-Messungen sowie viele konstruktive Gespräche.

… dem Team des kardiologischen Labors (Prof. Dr. Miriam Cortese-Krott, Dr. Thomas Krenz, Sivatharsini Thasian-Sivarajah) für ihre Unterstützung bei den realtime-PCR Versuchen.

… Herrn Prof. Dr. Jens W. Fischer und allen Mitarbeitern des Instituts für Pharmakologie und Klinische Pharmakologie für die kollegiale Zusammenarbeit.

… meiner Freundin Julia Sielaff für unzählige mittägliche Oasen und ihren kritischen Blick auf die Form dieser Arbeit.

… meinem Mann Tobias Pick für seine Liebe, seine Geduld und seinen steten Glauben an mich. Ohne seine bedingungslose Unterstützung gäbe es die vorliegende Arbeit nicht.

… meinen Eltern Yung-Mei und Heinrich Kumpf dafür, dass sie mich zu der Person gemacht haben, die ich heute bin.

… allen lieben Verwandten, Freunden und Bekannten für so manches offene Ohr und für ihren Zuspruch.

Ohne den Tod von Versuchstieren hätte diese Forschungsarbeit nicht entstehen können. Sie sind es wert, dass wir uns an sie erinnern.

Diese Arbeit wurde unterstützt aus Mitteln der Forschungskommission der Heinrich-Heine-Universität Düsseldorf, Nr. 9772446 (Dr. Tatsiana Suvorava).

VERSICHERUNG AN EIDES STATT

Ich versichere an Eides Statt, dass die Dissertation von mir selbstständig und ohne unzulässige Hilfe unter Beachtung der „Grundsätze zur Sicherung guter wissenschaftlicher Praxis an der Heinrich-Heine-Universität Düsseldorf“ erstellt worden ist.

Düsseldorf, 09.04.2018 Stephanie Pick